Master's Thesis

MSc Environomical Pathways for Sustainable Energy Systems

Techno-economic analysis of solar PV and wind power plants with hydrogen energy storage systems as a frequency regulation provider

July 2023

Author:
Catarina Isabel Novais da Luz Sousa de Almeida

Supervisors:
Eduardo Prieto Araujo (Universitat Politècnica de Catalunya)
Jenny Hedblom (FLOWER TECH)

Escola Tècnica Superior
d'Enginyeria Industrial de Barcelona

Acknowledgements

I would like to take this opportunity to express my deepest gratitude and appreciation to the people who have played a significant role in the completion of my thesis.

First and foremost, I extend my heartfelt thanks to my two supervisors who have worked closely with me throughout this research. I am truly grateful to Jenny Hedblom for her unwavering support at Flower. Her expertise and dedication were very important in shaping the trajectory and success of my thesis. Additionally, I extend my sincere appreciation to Eduardo Prieto Araujo for his role as my academic supervisor. His insightful feedback, academic expertise, and mentorship were instrumental in the success of this work. I would also like to express my sincere gratitude to Bart Olsthoorn from Flower for his invaluable technical insights throughout the development of this master's thesis.

Next, I would like to thank all other individuals who, although not directly involved in this thesis, have provided support and encouragement that has been essential to its successful completion. Your presence has been truly crucial.

I would like to start by expressing my profound gratitude to my parents, whose constant support and encouragement have been vital to my academic journey. Their belief in me, constant guidance, and sacrifices have been the driving force behind my accomplishments.

I would also like to acknowledge my grandparents, uncles and aunt for supporting me and giving me continuous encouragement to pursue my passions and embrace new challenges.

Furthermore, I would like to extend my gratitude to my friends who have provided intangible emotional support throughout the different stages of my life. From the early years, I am grateful to have Ana Marta, Rita, and Roxo by my side. A special thank you to Rodrigo and Zé for being so present in my life during my latest adventure and for always supporting my decisions. Additionally, during my bachelor's degree, I would like to express my appreciation to Bernardo, Lourenço, Miguel and my plenário colleagues for their friendship and support. Finally, I want to express my thanks to my friends who have been by my side during the two years of my master's journey: Ari, Madalena, Mariana, Vicente and my two groups - sessões de petit gateau and l'ovellas.

To all those mentioned above, I extend my deepest gratitude for being an integral part of my journey. Your support, encouragement, and friendship have made this achievement possible, and I am truly fortunate to have had your presence in my life.

Abstract

Renewable energy has emerged as a crucial component in the transition towards decarbonizing the power sector, offering a clean and sustainable alternative to fossil fuels. However, the integration of these variable renewable electricity sources diminishes system inertia and creates frequency regulation challenges [1]. To address these operational and technical difficulties, energy storage devices are critical in supporting grid stability. In particular, hydrogen storage can act as an intermediary for intermittent electricity production and thus contribute to a more balanced energy system in the coming years [2].

Therefore, this thesis presents a comprehensive techno-economic analysis of integrating solar and wind power plants with a hydrogen storage system to provide frequency regulation services. The study focuses on the profitability of participating in the Day-ahead Spot Market and explores the impact of frequency regulation provision on project profitability, over the project's lifetime of 20 years. A case study in Sweden is used to evaluate the results obtained from an optimization model developed using the *Gurobi* solver.

The findings demonstrate the significance of revenue from frequency regulation services in achieving overall profitability. Wind scenarios outperform solar scenarios due to higher renewable energy availability. In the wind scenario, the analysis revealed a payback period of 16 years and a total hydrogen (H_2) production of 582 tonnes. Notably, approximately 62% of the total revenue was attributed to participation in the Down-regulation frequency market, with the wind power plant emerging as the primary revenue-generating component. On the other hand, in the solar scenario, the payback period was extended to 19 years, accompanied by a total hydrogen production of 584 tonnes. In this case, the solar power plant accounted for the majority of revenue, and 51% of the total revenue of the project was attained through participation in the Down-regulation market. The future scenarios indicate that market landscapes and technological advancements will enhance economic indicators and make renewable power plants integrated with hydrogen energy storage systems projects more attractive.

Additionally, a sensitivity analysis reveals the key factors influencing the Levelized Cost of Electricity, Net Present Value, and Payback Period in different scenarios.

Finally, these research outcomes provide valuable insights for decision-making, emphasizing the importance of considering various factors, such as market prices, system size, system costs, and discount rates, in the techno-economic analysis of renewable energy projects. This study contributes to the existing knowledge in the field and offers guidance for stakeholders involved in renewable energy system planning and implementation.

Contents

List of Figures

List of Tables

Nomenclature

aFRR Automatic Frequency Restoration Reserve

ASYM Asymmetrical

BRP Balancing Responsible Party

BSP Balancing Service Provider

CAPEX Capital Expenditures

EAP Energy Activation Payment

EU European Union

FC Fuel cell

FCR-D Frequency Containment Reserve - Disturbance

FCR-N Frequency Containment Reserve - Normal

FFR Fast Frequency Reserve

IEA International Energy Agency

IRENA International Renewable Energy Agency

LVH Lower Heating Value

mFRR Manual Frequency Restoration Reserve

MILP Mixed-Integer Linear Programming

NZE Net Zero Emissions

OPEX Operational Expenditures

P2P Power-to-Power

PaB Pay-as-Bid

PaC Pay-as-Cleared

PEM polymer Electrolyte Membrane

PV Solar Photovoltaic

REPEX Replacement Expenditure

SM Spot Market

SoC State of Charge

SYM Symetrical

SvK Svenska Kraftnät

TAC Total Annual Cost

TSO Transmission System Operator

VAT Value Added Tax

VRES Variable renewable electricity sources

1 Introduction

Renewable energy has been playing a significant role in the energy transition toward the decarbonization of the power sector [19]. Renewable energy sources such as solar and wind offer a clean, sustainable alternative to fossil fuels, which can help reduce greenhouse gas emissions and mitigate the effects of climate change [20]. The rapid growth of renewable energy over the past decade, driven by technological advances and policy incentives, has led to significant cost reductions and increased deployment, making renewable energy a cost-effective and viable option for meeting our energy needs [21]. In 2021, 28.7 % of the world's electricity came from renewable sources [22], which is especially relevant as we face the challenges of climate change, environmental degradation, and energy access, the transition to renewable energy is more important than ever to achieve net zero emissions (NZE) [19].

NZE refers to balancing the amount of greenhouse gas emissions produced and the amount removed from the atmosphere. This can be achieved by reducing emissions through various measures, such as energy efficiency and renewable energy, and by removing emissions through processes such as carbon capture and storage, afforestation, and reforestation [19].

One of the steps towards NZE is the large-scale implementation of hydrogen production technologies complemented with other decarbonization technologies, such as renewable power[23]. According to the EU's strategy for hydrogen, there are areas of application for renewable hydrogen in the industrial, transport, power generation, and construction sectors, where hydrogen can replace fossil fuels [2]. Therefore, renewable hydrogen has been identified as one of the solutions to achieve the EU's commitment to achieve NZE by 2050 [2].

For this reason, the hydrogen demand will have almost doubled to 530 Mt, making hydrogen-based fuels 13% of the global final energy demand in 2050 [19]. The utilization of hydrogen as an energy carrier is a topic of great interest since 1990 [24], due to its numerous distinctive properties, including the fact that it is the most abundant element in the universe and its specific energy is 120 MJ/Kg, which is up to three times higher energy per mass than hydrocarbon-based fuel [25]. However, there are still some significant challenges regarding hydrogen, therefore, if its production rises to successfully achieve NZE by 2050, new and different production techniques would need to be deployed [19].

According to the International Energy Agency, about 17 % of the total hydrogen production in 2050 will be used as fuel in gas-fired power plants, which will be needed to balance the intermittency created by the increasing electricity generation from solar and wind power plants [19]. In general, the requirement for balancing services is anticipated to rise because the decarbonization of the power sector implies an increase in the share of solar and wind in the electricity generation mix. In 2021, the total installed capacity of solar and wind was 849 GW and 825 GW [26], respectively, and these numbers are expected to quadruple until 2030 to achieve NZE [19]. The emergence of these variable renewable electricity sources (VERS) creates instability in the grid due to their intermittent and seasonal characteristics [27]. Additionally, the growing penetration of VRES reduces the system inertia, which causes frequency regulation problems [1].

To solve the mentioned operational and technical difficulties caused by VRES, the Frequency Regulation Markets are responsible to prevent frequency deviations from 50 Hz (in Europe) or 60 Hz (in the United States) [28]. To fulfill these requirements, market participants must inject or withdraw active power in response to a dispatch signal emitted typically by the local transmission system operator (TSO) [28]. The specifications and requirements of each Frequency Regulation Market depend on the electricity market designs, policy frameworks, and market regulations across countries [29].

As a result of the VRES high penetration in the power system, frequency issues that occur almost instantaneously must be resolved [30]. Therefore, there has been a significant increase in demand for energy sources with faster ramp capability. The lower ramping capability of traditional units causes a slower response in this regulation provision [30]. Hence, renewable energy sources can be key in delivering these services given their capability of fast response [30]. Moreover, energy storage devices also play a critical role in supporting the stability of the grid, mitigating the impact of VRES on the grid frequency

[24]. The participation of storage systems in the Frequency Regulation Market brings new sources of value for resource owners and new options for system operators to manage grid reliability [31].

In addition, VRES can be coupled with energy storage systems to reduce energy curtailment and improve their participation in frequency regulation [32, 33]. In particular, the literature supports that hydrogen storage can act as an intermediary for intermittent electricity production and thus contribute to a more balanced energy system in the coming years [2]. Besides this, hydrogen storage systems can offer flexible operation and provide frequency regulation to improve the power system reliability [34].

1.1 Objectives and Scope

The current study analyses a system that combines a hydrogen-based Power-to-Power (P2P) system (coupling an electrolyzer, compressor, a hydrogen storage unit, and a fuel cell system) and VRES power plants (PV or wind power plants) to exchange electricity with the grid in both directions. Firstly, a system design and size are chosen based on previous studies [35, 36]. Thereafter, to determine the best plant operation to maximize profits, an optimization algorithm is developed that simulates the system's ideal operation in the Day-ahead Spot Market (SM) and Frequency Regulation Markets in Sweden, during a period of 20 years. Additionally, the participation in the Frequency Regulation Markets and inclusion of renewable power plant's impact on the economic indicators of the project. Furthermore, a sensitivity analysis evaluates the effects of the variations in the investment costs and size of the hydrogen energy system and the market prices. Finally, Future Scenarios are analyzed to assess the impact of market adaptations and technology developments on the final results.

The present work was developed in partnership with Flower, a Swedish start-up located in Stockholm. Considering the study's potential significance in the energy transition and its use in Flower's operations, the approach adopted is mainly focused on the Swedish electricity markets and its network specificity and needs. Nonetheless, it is possible to adapt the model to future research and take advantage of the line of reasoning followed in this research.

Sweden is a global leader in decarbonization and has the target to achieve a net-zero carbon economy by 2045 [37]. As a consequence, 68 % of the electricity generated in 2020 was produced by renewable sources [37], and a significant wind and solar capacity have been installed in the country, reaching a total of 1 577 MW and 12 080 MW for solar and wind capacity, respectively, in 2021 [26]. Besides this, according to the Swedish Energy Agency, hydrogen will play an important role in supporting the drive to NZE in Sweden [38], as a flexibility provider to balance a high VRE share in the power system, for the production of biofuels and as a reductant in the steel industry [39]. Thereby, Sweden has the prerequisites necessary to be selected as the case study for this thesis.

Although other studies have analyzed similar hydrogen-based energy storage systems [35, 36], there has been relatively little research on how hydrogen can participate in Frequency Regulation Markets specifically. Therefore, this thesis aims to fill this gap in the literature by exploring the technical and economic challenges associated with integrating hydrogen into Frequency Regulation Markets. This work analyses the hydrogen energy storage system size and cost impact on the economic indicators, the differences between having a solar PV power plant or a wind power plant charging the hydrogen storage system, and how future market and technology changes will affect the results.

2 State-of-art

The state-of-the-art in this thesis covers the following topics:

1. Hydrogen energy technologies (production, storage, and fuel cells).
2. Existing literature on the integration of solar PV and wind power plants with hydrogen energy storage systems, and its participation in the electricity market as a frequency regulation provider, including case studies and comparative analyses.
3. Fundamentals of Day-ahead SM and Frequency Regulation Markets, including existing policies, regulations, and market mechanisms related to the deployment of renewable energy technologies and energy storage systems in Sweden.
4. Future scenarios of hydrogen deployment and Frequency Regulation Market adaptation with a particular interest in the Swedish markets.

2.1 Hydrogen Technologies

Hydrogen has a wide range of applications in various industries and sectors due to its unique properties. One of the most important applications of hydrogen is in energy production. Hydrogen fuel cells are used to generate electricity by converting the chemical energy of hydrogen into electrical energy [40]. Besides this, hydrogen has potential applications in energy storage, where excess electricity from renewable sources, such as wind and solar, can be converted into hydrogen and stored for later use in fuel cells [2].

Another important application of hydrogen is in the transportation sector. Hydrogen-powered vehicles have the potential to produce zero emissions, making them a promising solution to reduce air pollution and combat climate change [41]. Hydrogen is also used as a feedstock for the production of a range of chemicals, such as ammonia, methanol, and other organic compounds [34].

Overall, the potential hydrogen usage is diverse and significant. This thesis explores particularly the power-to-power(P2P) hydrogen application, which refers to the use of hydrogen as an energy carrier for power generation applications. In this case, the process involves using renewable electricity from wind and solar or from the grid to generate hydrogen through electrolysis. The produced hydrogen can then be stored and used in fuel cells to generate electricity on demand. Hence, the production of hydrogen via electrolysis, fuel cells, and hydrogen storage processes are the main topics of this Section of the state-of-art analysis.

2.1.1 Hydrogen Production

Water electrolysis is the process of using an electrical current to split water molecules into their component parts, hydrogen, and oxygen. This process is carried out in an electrolysis cell, which consists of an anode (positively charged) and a cathode (negatively charged) separated by an electrolyte [3].

When an electric current is applied to the electrolysis cell, water molecules are split at the cathode and anode [42]. The overall reaction for water electrolysis is described in (1) [43]. Oxygen (O_2) is also produced as a byproduct.

$$2H_2O + electricity \rightarrow 2H_2 + O_2 \tag{1}$$

According to the literature [44], proton-exchange membrane (PEM) and alkaline electrolysis are the two electrolyzer technologies that are commercially available on a large scale. Both are operable at low temperatures [44]. Alkaline electrolyzers operate between $40\,^{\circ}\mathrm{C}$ and $90\,^{\circ}\mathrm{C}$, and in the case of PEM elec-

trolyzers, between 20 °C and 100 °C[3]. Some companies intend to advance and commercialize high-temperature electrolysis, however, this technology has cost and durability issues [44].

A PEM electrolyzer uses a solid polymer electrolyte membrane to separate the anode and cathode [3]. The membrane is made of a special polymer material that allows only positively charged ions, such as protons, to pass through [3]. An alkaline electrolyzer, on the other hand, uses an alkaline electrolyte solution, typically potassium or sodium hydroxide, instead of a solid polymer electrolyte membrane [3] (Table 1). The efficiency of water electrolysis depends on several factors, including the type of electrolyte used. A PEM electrolyzer can have an efficiency between 65 % and 80 %, while an alkaline electrolyzer has an efficiency between 70 % and 80 % [45], as mentioned in Table 1.

The charge carriers and the specific cathode and anode reactions differ between the types of electrolyzers. For example, in a PEM electrolyzer, the cathode reaction involves the reduction of protons (H^+) and electrons (e^-) to form hydrogen gas (H_2) [43]. In contrast, the anode reaction involves the oxidation of water molecules (H_2O) to form oxygen gas (O_2) and positively charged hydrogen ions (H^+), as described in Table 1 [43].

In an alkaline electrolyzer, the cathode reaction involves the reduction of water molecules to form hydroxide ions (OH^-) and hydrogen gas (H_2), while the anode reaction involves the oxidation of water molecules to form oxygen gas (O_2) and hydroxide ions (OH^-) [43], as described in Table 1.

As shown in Table 1, both types of electrolyzers were operated at an output pressure of 3 MPa. The stack lifetime, representing the operational durability of the electrolyzers, varied for each type. The alkaline electrolyzer exhibited a stack lifetime ranging from 60 000 to 90 000 hours, as reported in the study by Schmidt et al. [46]. On the other hand, the PEM electrolyzer demonstrated a stack lifetime of 50 000 to 80 000 hours [47].

Table 1: PEM and alkaline electrolyzers technical characteristics.

	Alkaline Electrolyzer	**PEM Electrolyzer**	**Source**
Anode reaction	$2OH^- \rightarrow \frac{1}{2}O_2 + H_2O + 2e^-$	$H_2O \rightarrow \frac{1}{2}O_2 + 2H^+ + 2e^-$	[43]
Cathode reaction	$2H_2O + 2e^- \rightarrow H_2 + 2OH^-$	$2H^+ + 2e^- \rightarrow H_2$	[43]
Charge carrier	OH^-	H^+	[43]
Electrical efficiency [%]	70 - 80	65 - 80	[45]
Cell temperature [°C]	40 - 90	20 - 100	[43]
Output pressure [MPa]	3	3	[48, 49]
Stack Lifetime [h]	60 000 - 90 000	50 000 - 80 000	[46, 47]

A common practice to increase the hydrogen production rate and cell's efficiency is by using an electrolytes stack, which means connecting the anode of one cell to the cathode of the next cell, and so on, forming a series of interconnected cells [50].

The overview of each cell operation is described in Fig. 1.

The major differences between these two types are summarized in Table 2. The main advantages of PEM electrolyzers are the rapid start-up time, dynamic operation, and capability of the partial load operation, which makes them suitable for intermittent applications [3]. Besides this, PEM fuel cells have a compact design and produce higher gas purity [3]. Currently, manufacturers offer PEM stack in the MW power

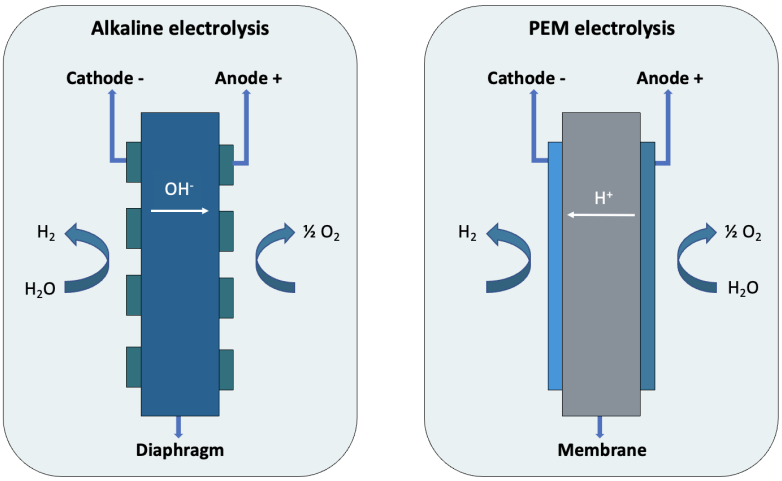

Figure 1: Operating principle of PEM and alkaline electrolysis [3]

range [51]. However, PEM electrolyzers use relatively less mature technology, have higher costs, lower lifetime, and operate in a corrosive environment [3].

On the other hand, alkaline electrolyzers are less expensive (due to the use of non-noble catalysts), have high durability, are relatively mature, and have a higher power range [3]. However, alkaline electrolyzers have longer response times and worse partial and dynamic operation [3]. Finally, alkaline electrolyzers have a corrosive electrolyte and produce hydrogen gas less pure [3].

Table 2: Comparison between PEM and alkaline electrolyzers [3].

	Advantages	**Challenges**
PEM	- Rapid response time - Partial operation performance - Higher gas purity - Compact system design - Dynamic operation	- Relatively higher costs - Less mature technology - Lower lifetime of the stack. - Corrosive environment
Alkaline	- Relatively lower cost - Mature technology - Longer lifetime of stack - Cost-effective	- Longer response time . - Low partial operation range - Lower purity - Lower dynamic operation - Corrosive electrolyte

2.1.2 Hydrogen Storage

Hydrogen can be stored via material-based or physical-based methods, some technologies can be found in Fig. 2 [4].

Physical-based hydrogen storage involves containing hydrogen as a gas or a liquid through the utilization of structural vessels to store the hydrogen while adjusting the density through pressure and temperature changes [42]. This method is based on two main principles: cooling and compression [42]. Hydrogen storage densities increase by raising hydrogen pressure and decreasing its temperature. However, safety issues arise with higher pressures [42].

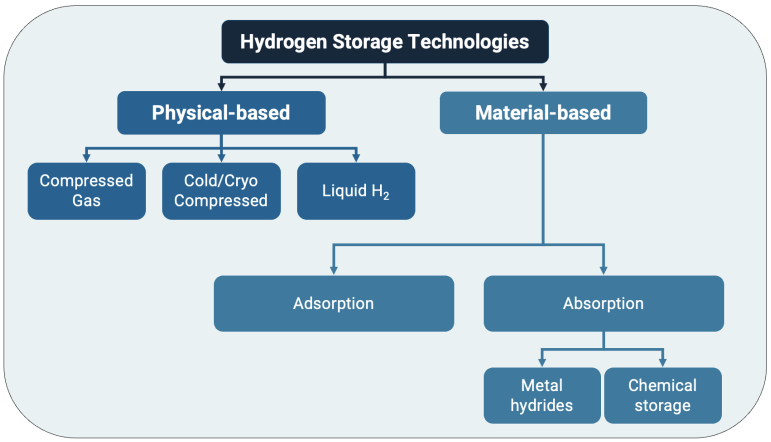

Figure 2: Hydrogen storage technologies [4]

There are three main physical-based technologies: compressed gas hydrogen storage, liquid hydrogen storage, and cold/cryo-compressed hydrogen storage.

In compressed hydrogen gas storage, vessels operate at high pressures, as high as 70 MPa, and near ambient temperature [42]. As pressure increases from 0.1 MPa to 70 MPa, the hydrogen density increases from 0.1 kg/m^3 to 40 kg/m^3 [4]. Besides this, the theoretical energy consumption to compress hydrogen isothermally from 2 MPa to 35 MPa is 3.8 MJ/kg$_{H2}$ and 4.9 MJ/kg$_{H2}$ for 70 MPa [52]. There are four pressure vessels available to store the hydrogen compressed gas [53, 54]. Type I vessel is an all-metal construction and is typically the lowest cost but also has the greatest mass option, therefore used for lower pressures (around 30 MPa) and stationary applications [54]. Type II vessels are usually more expensive but allow better hydrogen densities. Type III and IV are used for vehicle applications and their costs are significantly higher than the other two types [53].

In liquid hydrogen storage, hydrogen is cooled to very low temperatures (near the normal boiling point of H_2, $-253.15\,^{\circ}\mathrm{C}$) to liquefy it and stored in insulated tanks. These vessels operate at low pressures (below 0.6 MPa) [42]. With a large storage density of 70.9 kg/m^3, this technology also offers safety benefits because of the storing pressure [4]. However, hydrogen liquefaction is an energy-intensive process, consuming almost one-third of the energy contained in hydrogen [55].

In cryo-compressed hydrogen storage, temperature and pressure are optimized to obtain the highest storage density possible [4]. According to the literature [4], the optimal temperature is between $-238\,^{\circ}\mathrm{C}$ and $-163\,^{\circ}\mathrm{C}$ and pressure between 5 MPa and 70 MPa, which corresponds to hydrogen densities between 60 kg/m^3 and 71.5 kg/m^3. At 20 MPa and $-193\,^{\circ}\mathrm{C}$ the energy consumption to cryo-compress the hydrogen is around 10 MJ/kg$_{H2}$, which is a noteworthy advantage, compared to liquid hydrogen [42]. Despite the big advantage of density improvement, this method has the disadvantages of heat leakage and higher power consumption than the other options [4]. Moreover, the vessel might suffer from the hydrogen embitterment effect (a phenomenon where the mechanical properties of a metal are degraded due to the presence of hydrogen) which could lead to the deterioration of the pressure vessel [4]. Therefore, to overcome these drawbacks cold-compressed hydrogen can be used instead, even though it decreases the hydrogen density [42]. This technology uses higher pressures (around 50 MPa) and temperatures above $-123.15\,^{\circ}\mathrm{C}$ and below $0\,^{\circ}\mathrm{C}$ [42].

The main technical differences between the physical-based hydrogen storage technologies are summarized in Table 3.

Material-based hydrogen storage involves storing hydrogen in a chemical compound or a solid-state material, which has the capacity to reversibly store hydrogen [4]. Moreover, these materials must have a large storage capacity at tolerable operating temperatures and pressures, fast kinetics, and reasonably

Table 3: Physical-based hydrogen storage technologies technical characteristics.

	Compressed gas	**Liquid**	**Cryo-compressed**
Pressure [MPa]	< 70 [42]	< 0.6 [42]	5 to 70 [4]
Temperature [°C]	*ambient temperature* [42]	-253 [42]	-238 to -163 [4]
Density [Kg/m^3]	< 40 [4]	70.9 [4]	60 to 71.5 [4]
Energy consumption [MJ/Kg_{H_2}]	< 4.9 [52]	40 [55]	10 [1] [42]

low cost [4]. Material-based technologies can be divided into two main technologies: adsorption and absorption.

Adsorption is a surface process that involves the transfer of a molecule from a gas or liquid to a solid surface and is typically reversible [4]. These materials can be, for example, carbon-based, metal-organic frameworks, and zeolites [4]. Although this technology can achieve higher storage capacity for hydrogen compared to other storage methods such as compressed gas storage [56]. This feature minimizes the capital and operating costs for compression and may also ease some of the high-pressure storage's technical issues [56].

Regarding absorption, there are two main technologies worth mentioning, which are metal hydrides and chemical storage.

Metal hydrides are metallic-based materials that absorb hydrogen. This process is done under moderate pressure and low temperatures. Additionally, because of its relatively low working temperatures, this technology is one of the safest methods to store hydrogen. However, metal hydrides have slow kinetics, low reversibility, and high dehydrogenation temperatures [4].

Chemical storage refers to covalently bound solid or liquid hydrogen with compounds that generally have a higher density [42]. This technology has great potential to be used as a liquid organic hydrogen carrier, but it is hardly regenerated so these materials are utilized as a single-use fuel [4].

To conclude, according to the literature, compressed gas storage and metal hydride storage are the most relevant technologies for stationary applications [57]. Additionally, storing hydrogen as compressed gas is currently the most common method and the most used in the literature for grid integration purposes [57].

2.1.3 Fuel Cells

A hydrogen fuel cell is a device that converts the chemical energy stored in hydrogen fuel directly into electrical energy through an electrochemical reaction [5]. The fuel cell consists of three main components: the anode, the cathode, and the electrolyte [58]. The anode, which serves as the negative electrode, is where hydrogen gas is fed into the fuel cell. The cathode, the positive electrode, receives oxygen from the air [58]. The electrolyte separates the anode and cathode. Depending on the type of electrolyte, either protons (H^+) or oxide ions (OH^-) through it, while electrons travel through an external circuit to deliver electric power [58].

During this process, heat is generated as a byproduct. The overall reaction is expressed in (2) [58].

[1] at 20 MPa and $-193\,°C$

$$2H_2 + O_2 \rightarrow 2H_2O + electricity + heat \tag{2}$$

Fuel cells are divided into six main groups according to the fuel and electrolyte they use [5]. These are alkaline, phosphoric acid, solid oxide, molten carbonate, proton exchange membrane (PEM), and direct methanol fuel cells. From these six categories, only alkaline and PEM fuel cells have quick start-up capability [5]. For this reason, only PEM and alkaline fuel cells are further analyzed, considering that the fuel cell's fast response is essential for the purpose of this thesis.

In Fig. 3 the operating principles of PEM and alkaline fuel cells are described.

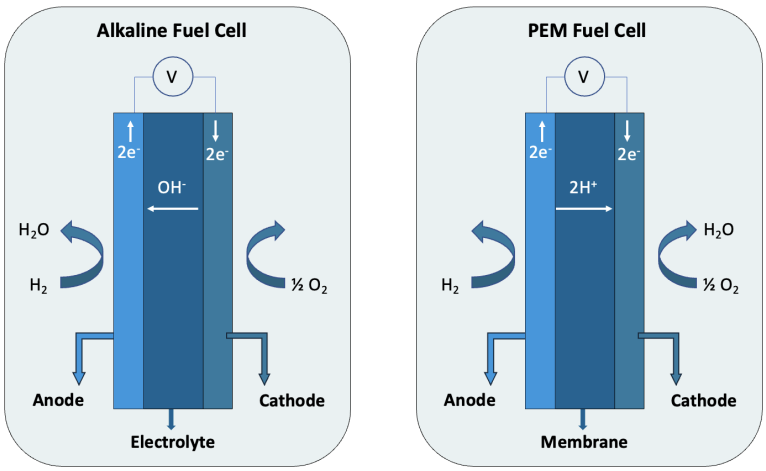

Figure 3: Operating principle of alkaline and PEM fuel cells [5]

In a PEM fuel cell, hydrogen (H_2) fuel is fed into the anode compartment, while oxygen (O_2) from the air is fed into the cathode [5]. The electrolyte allows only protons (H^+) to pass through to the cathode, while the electrons (e^-) are forced to flow through an external circuit to reach the cathode [5]. At the cathode, the protons combine with oxygen (O_2) and electrons (e^-) to form water (H_2O) [5]. The equations that describe this process are in Table 4.

In an alkaline fuel cell, hydrogen (H_2) is fed into the anode, and oxygen (O_2) is fed into the cathode [5]. At the anode, hydrogen gas reacts with hydroxide ions (OH^-), producing water (H_2O) and electrons (e^-) [5]. The electrons (e^-) flow through an external circuit to the cathode, where they react with oxygen (O_2) and water (H_2O) to form hydroxide ions (OH^-) [5]. The hydroxide ions (OH^-) produced at the cathode migrate to the anode through the electrolyte [5]. As for PEM fuel cells, the chemical reactions are described in Table 4.

These two fuel cell technologies have relatively high electrical efficiencies compared to the other technologies [5]. Alkaline fuel cells have an electrical efficiency of around 60 % and PEM fuel cells between 53 % and 58 % [5]. Furthermore, both fuel cell technologies operate at low temperatures (between 90 °C and 100 °C), in the case of alkaline fuel cells, and PEM fuel cells operate from 50 °C to 100 °C) [5]. This specification gives these two types of fuel cells the capability of a quick start-up, due to a lower warm-up time [13].

As shown in Table 4, the operating pressure for alkaline fuel cells is set at 0.4 MPa. On the other hand, PEM fuel cells typically operate within a range of 0.3 to 0.4 MPa [59, 60].

Regarding the stack lifetime, alkaline fuel cells exhibit a lifespan ranging from 4 800 to 8 600 hours [61]. On the other hand, PEM fuel cells demonstrate a longer stack lifetime, with values ranging from 9 700 to 29 700 hours.

Table 4: PEM and alkaline fuel cells technical characteristics.

Specifications	Alkaline Fuel Cell	PEM Fuel Cell	Source
Anode reaction	$2H_2 + 4OH^- \rightarrow 4H_2O + 4e^-$	$H_2 \rightarrow 2H^+ + 2e^-$	[5]
Cathode reaction	$O_2 + 2H_2O + 4e^- \rightarrow 4OH^-$	$\frac{1}{2}O_2 + 2H^+ + 2e^- \rightarrow H_2O + H^+$	[5]
Charge carrier	OH^-	H^+	[5]
Electrical efficiency [%]	60	53 - 58	[5]
Cell temperature [ºC]	90-100	50 - 100	[5]
Operating pressure [MPa]	0.4	0.3 - 0.4	[59, 60]
Stack Lifetime [h]	4 800 - 8 600	9 700 - 40 000	[61, 62]

Regarding PEM fuel cells, corrosion, and electrolyte management issues are mitigated by the use of a solid electrolyte [13], which improves the lifetime of the cell [63]. However, the price of the system is increased due to the use of a noble-metal catalyst (usually platinum) to separate the electrons and protons in the hydrogen. The platinum catalyst is also particularly sensitive to fuel contamination [13]. On the other hand, alkaline fuel cells have lower costs since their configuration does not include precious metals [13]. Nevertheless, alkaline fuel cells are highly sensitive to carbon dioxide (CO_2) in the air, which can affect cell performance because the pore system is filled by carbonate [64].

The main differences between these two types of fuel cells are summarized in Table 5.

Table 5: Comparison between PEM and alkaline fuel cells [13].

	Advantages	Challenges
PEM	- Reduced corrosion - Low temperature - Quick start-up and load following - Reduced electrolyte management problems	- Expensive catalysts - Fuel impurities sensitivity
Alkaline	- Lower cost - Low temperature - Quick start-up	- CO_2 sensitivity

2.2 Hydrogen Technologies Integrated with Solar PV and Wind Power Plants

PV power plants have the necessary characteristics to be economically competitive and commercially viable to produce hydrogen [65]. PV power plants are usually connected via a DC/DC converter to a PEM or alkaline electrolyzers due to the quick-start capability of these technologies, crucial to cope with the intermittency of this renewable source [66].

Furthermore, combining wind energy and electrolyzer improves the performance of wind turbines by mitigating the effects of the unpredictability of the wind [67]. The selection of an electrolyzer for a

wind power plant follows the same reasoning as for PV power plants, however, in this case, an AC/DC converter is used instead of DC/DC [66].

Compressed hydrogen gas was the technology utilized to store hydrogen before it was used in its next application in the vast majority of the studies analyzed [35, 36, 67, 68, 69, 70, 71, 72]. This occurs as a result of the relatively simple and low-cost advantages of storing hydrogen as a compressed gas, compared to other storage technologies such as liquid hydrogen or solid-state hydrogen storage [4].

Regarding the fuel cell selection, due to the faster dynamics of PEM fuel cells, they were used in the majority of the papers analyzed [70, 35, 36]. Besides the appealing features of these fuel cells, it is predicted that by 2030 PEM technology will be the industry standard [70].

The literature has shown better results for hydrogen storage systems integrated with PV power plants, compared to wind power plants [67, 66]. However, the system performance is dependent on the site specifications, and considering the relevance of wind power plants in the electrical system, this thesis will compare the results obtained from a PV/H_2 and a wind/H_2 system. An important conclusion from the integration of electrolyzers with renewable sources is the impact of intermittent operation [73, 74]. Due to the variable nature of solar and wind, the electrolyzer might be forced to shut down, which can increase the degradation rate, thus the stack lifetime [74]. To mitigate the negative effects of the intermittent operation on the performance of the electrolyzer several strategies can be employed to avoid the shutdowns an improve its operation [73].

The current economic characteristics of the electricity market and the investment costs of hydrogen technologies are not sufficiently attractive in some case studies [35, 75, 76]. Nevertheless, the provision of ancillary, such as frequency regulation, improves the profitability of the power plant and adds a new revenue stream [35, 71, 70, 77].

In Table 6, a summary of the hydrogen systems specifications, gathered from the literature, is presented. This Table highlights the hydrogen technologies used if the system is participating in the Frequency Regulation Markets and the main conclusions of each study.

Table 6: Hydrogen systems specifications and performance.

Source	**Energy source**	**Electrolyzer**	**H_2 storage**	**Fuel cell**	**Frequency regulation**	**Conclusions**
[77]	Wind Grid	Generic	Compressed gas	Generic	yes	PEM fuel cell technology is promising as it is expected to provide frequency balancing services.
[76]	Wind Grid	PEM	Compresed gas	Generic	yes	The different scenarios analysed had negative profits due to high wind and hydrogen technology CAPEX.
[78]	PV	Alkaline	X	X	X	The CAPEX associated with larger electrolyzers are not offset by a rise in hydrogen output.

Table 6 (continued)

Source	Energy source	Electrolyzer	H_2 storage	Fuel cell	Frequency regulation	Conclusions
[70]	Wind Grid	PEM	Compressed gas	PEM	yes	Participation in balancing markets is a feasible option and provides an extra revenue source.
[35]	PV Grid	PEM	Compressed gas	PEM	yes	A P2P CAPEX reduction of 80% to 95% is required to ensure profits. Frequency regulation provision decreases the cost of electricity by 15%.
[36]	PV Grid	PEM	Compressed gas	PEM	X	When the system is almost independent from grid import and seasonal energy storage is necessary, P2P is less expensive than BESS.
[67]	PV Wind	Alkaline	Compressed gas	X	X	The overall system efficiency was between 7.69% and 9.37% for PV/H_2 systems and 5–14% for wind/H_2.
[68]	PV Wind	Alkaline	Compressed gas	X	X	In this case study, the best scenario was when 100% of PV is used (0% wind).
[75]	Grid	PEM	X	X	yes	The current economic characteristics of the market are not sufficiently attractive for a hydrogen power plant.
[69]	Wind Grid	Alkaline	Compressed gas	Generic	yes	The fuel cell is used only when there are significant variations in the price of power and significant balancing expenses.
[72]	PV Grid	Generic	X	X	X	Future improvements might include providing ancillary services.
[79]	PV Grid	Generic	Compressed gas	Generic	yes	The highest profits come from providing balancing capacity.
[71]	Grid	Generic	Compressed gas	X	yes	Participation in ancillary markets and the hydrogen markets improves the economic viability of the plant.

2.3 Fundamentals of Day-ahead SM and Frequency Regulation Markets

Frequency regulation is an essential service that helps maintain the balance between electricity supply and demand on the grid [80]. As electricity cannot be stored in large quantities, the supply must match demand in real-time to maintain system stability [80].

The increasing penetration of renewable energy sources poses unique challenges to the stability and reliability of the power system [81]. One of the major challenges is the reduction of system inertia due to the fact that most renewable sources are connected to the grid through a converter [81]. Inertia is a crucial property of the power system that refers to its ability to maintain a stable frequency in response to sudden changes in power demand or supply [82]. In traditional power systems, the rotating machinery provides resistance to the change in rotational speed, which is expressed by the moment of inertia that can act as a buffer against sudden changes in frequency [82]. Therefore, as renewable share increases, the overall level of inertia in the system decreases, which can lead to greater frequency fluctuations and instability [81]. To address this issue, additional frequency regulation measures are required to maintain the stability and reliability of the power system [81]. Frequency regulation ensures that the frequency of the electricity grid remains constant by adjusting the power output of generators to match the changing demand for electricity [80].

Frequency regulation markets are designed to incentivize power generators and other market participants to provide this service to the grid [83]. Two types of frequency regulation can be distinguished: Up-regulation and Down-regulation [83]. Up-regulation refers to the process of increasing the amount of power being generated or decreasing the power consumed in response to a frequency deviation below the set point (50 Hz in Sweden) [83]. Down-regulation, on the other hand, refers to the process of reducing the amount of power being generated or increasing the consumed power, when the frequency is above the set point [83]. Moreover, there are symmetric and asymmetric markets. In a symmetric market, participants have to place both up and Down-regulation bids. On the contrary, in an asymmetric market (ASYM), participants can decide between up, down, or provide both types of regulation [83].

These markets operate differently in different regions and countries but typically involve the following elements: market design, market participants, payment mechanism, and regulation frameworks [83].

Regarding market design, Frequency Regulation Markets can be organized as centralized markets or decentralized bilateral contracts [84]. Centralized markets involve a system operator (TSO) that purchases frequency regulation services from market participants [84]. Decentralized bilateral contracts, on the other hand, allow market participants to negotiate frequency regulation contracts with each other directly [84].

Additionally, market participants can be power generators, energy storage providers, demand response providers, and aggregators [83]. In some markets, participants are required to meet certain technical performance standards to ensure that the frequency regulation service is provided reliably and efficiently [83].

Furthermore, the market participants can bid on capacity or energy, meaning that they can sell their power availability, which, is called a capacity market, or, on the other hand, their available energy in a certain period of time [84]. Particularly, in the capacity markets, remuneration can be done through capacity payments, energy activation payments (EAP), or both [84]. Capacity payments are made to ensure that market participants are available to provide the service when needed, while energy payments are made when the actual amount of frequency regulation service is provided [84]. Besides this, the price, in both energy or capacity markets, can be set as pay-as-bid (PaB) or as pay-as-cleared (PaC), which refers to the marginal price [84].

Finally, Frequency Regulation Markets are subject to regulation by government agencies or regulatory bodies, such as the TSOs, to ensure that they operate reasonably and efficiently [28]. Regulatory frameworks vary widely and can impact market design, payment mechanisms, and other aspects of the market [28].

To conclude, Frequency Regulation Markets are an important part of the electricity grid, and can play a critical role in enabling the integration of VRES and other distributed energy resources [85]. In the next Section, the Frequency Regulation Markets in Sweden will be described.

2.3.1 Swedish Day-ahead SM and Frequency Regulation Markets

In Sweden, the TSO is called *Svenska kraftnät* (SvK), and one of its main responsibilities is to keep the balance between production and consumption at all times, which is executed by running balancing markets [83]. SvK must have access to different reserves and ancillary services in order to balance and manage disturbances in the power system. This is mainly done by procuring different types of ancillary services from participants in the electricity market [7].

Sweden's electrical system is divided into four bidding areas (SE1, SE2 SE3 and SE4), as described in Fig. 4 [6]. Since more electricity is produced in northern Sweden than in the south, a significant amount of electricity is transmitted from the north to the south [86]. In Sweden, the power distribution system for hydroelectric and nuclear power sources is organized in a separate manner. The northern regions of SE1 and SE2 primarily produce hydroelectric power, whereas the southern region of SE3 predominantly generates nuclear power[87].

The transmission grids of Sweden, Finland, Norway, and eastern Denmark are all included in the synchronized Nordic system [88]. This means that they operate at the same frequency, which allows for the free flow of electricity across national borders [88]. Besides this, transmission lines (DC or AC) connect the Nordic system to other countries, as it is described as black dashed lines in Fig. 4 [6].

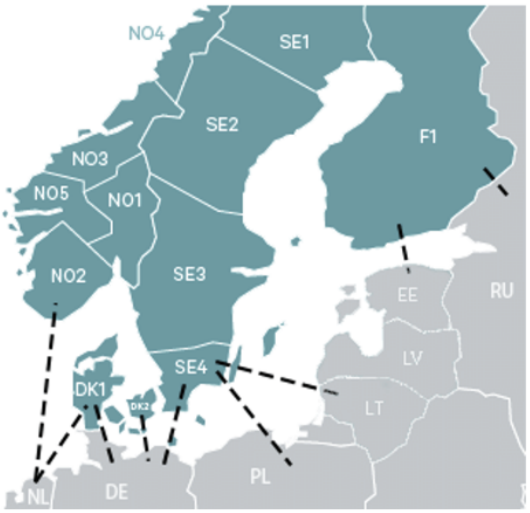

Figure 4: Nordic synchronous grid and transmission lines (black dashed lines) [6]

The Swedish day-ahead spot market (SM) is a marketplace where the price for each hour of the next day is set through a competitive auction. Participants in the market submit their offers for either producing or consuming electricity in their specific price area [83]. The bids in the Swedish day-ahead spot market are subject to a minimum size requirement of 0.1MW and must be submitted prior to the gate closure time, which is at 12:00 CET on the day preceding the actual operation [89]. Furthermore, the clearing prices for each hour and the acceptance of bids are generally disclosed at 12:45 CET, also on the day prior to the operation [89].

The marketplace for the trading of electricity is the Nordic power market Nord Pool, which has a spot market for trading electricity per hour for delivery the next day. Most of the trade per hour takes place

on Nord Pool, while a smaller portion is made directly between electricity generators and electricity suppliers [90].

Furthermore, there are two different types of market participants in the Frequency Regulation Markets in Sweden: Balancing Service Providers (BSPs) and Balancing Responsible Parties (BRPs) [83]. BSPs are responsible for providing frequency regulation services to the TSO, which involves adjusting their electricity production or consumption in response to changes in the frequency of the electricity grid, they can be generators, demand response, and storage operators [83]. BRPs, on the other hand, are responsible for ensuring that the energy consumption in their operation area matches the energy production, and they must balance their energy supply and demand in real-time to avoid imbalances and ensure the stability of the electricity grid [83].

There are six different Frequency Regulation Markets in Sweden [7]. The market time unit is one hour in every market, which means the bids are placed for each hour of the day [7].

Firstly, Fast Frequency Reserve (FFR) is automatically activated when frequency changes and the level of rotational energy in the system is low [7]. Additionally, there are three Frequency Containment Reserve (FCR) products, also known as the primary reserve, which are Upward Frequency Containment Reserve Disturbance (FCR-D Up), Downward Frequency Containment Reserve Disturbance(FCR-D Down), and Frequency Containment Reserve Normal (FCR-N) [7]. FCR-N is linearly activated when the frequency is between 49.9 Hz and 50.1 Hz [7]. Additionally, FCR-D Up is activated when the frequency is below 49.9 Hz and above 49.5 Hz [7]. FCR-D Down, on the other hand, is activated when the frequency is between 50.1 Hz and 50.5 Hz [7]. Besides this, there are two frequency restoration reserve markets: Automatic Frequency Restoration Reserve (aFRR) and Manual Frequency Restoration Reserve (mFRR) [7]. The aFRR product, also known as the secondary reserve, is automatically activated for frequency deviations from 50 Hz [7]. The tertiary reserve (mFRR) is manually activated when requested by SvK when the frequency is not 50 HZ [7]. The frequency activation ranges for the 6 different markets are described in Fig. 5.

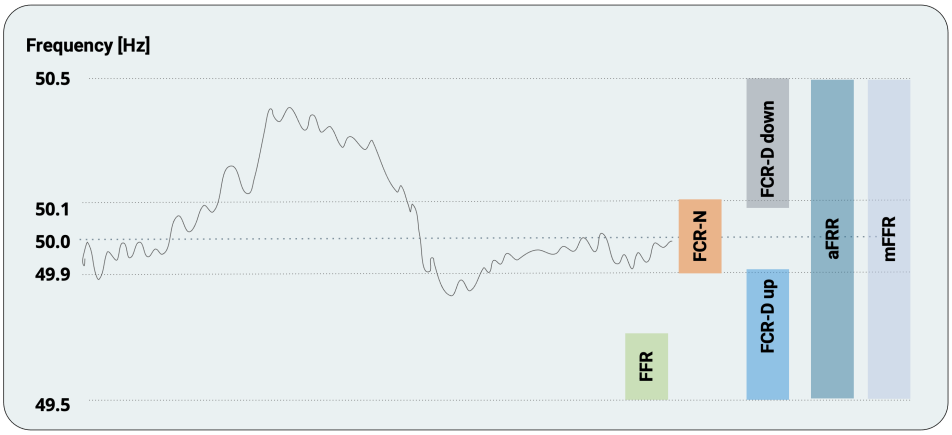

Figure 5: Frequency regulation markets frequency activation ranges [7]

In Table 7, the main requirements of each Frequency Regulation Markets are summarized.

The majority of the Frequency Regulation Markets in Sweden are capacity markets, except for mFRR, which is an energy market [7]. The minimum bid size is 0.1 MW for all markets except aFRR and mFRR, which only allow larger units to participate [7]. In the case of aFRR, the minimum bid is 1 MW, and 10 MW for mFRR (in SE4 zone the minimum mFRR bid size is 5 MW) [7].

Regarding the activation time, in FFR the units providing this service need to be fully activated within seconds (0.7 seconds if the frequency is at 49.5 Hz, 1 s if the frequency is at 49.6 Hz, and 1.3 seconds if the frequency is at 49.7 Hz) [7]. FCR-N requires a full activation in 3 minutes, but 63 % of the total

capacity needs to be provided in 60 seconds [7]. For both FCR-D Up and down, the unit needs to be fully activated in 30 seconds, but 50 % of the total capacity has to be activated in 5 seconds [7]. The secondary and tertiary reserves allow longer activation times, compared with the other reserves, 5 minutes and 15 minutes, respectively, for aFRR and mFRR [7].

Furthermore, the endurance requirement refers to how long a unit providing frequency regulation must be continuously activated [7]. In the case of FCR-N, aFRR and mFRR one hour is the minimum endurance time [7]. For FCR-D Up and down the unit must be activated for at least 20 minutes [7]. Lastly, FFR units can be activated for 5 seconds or 30 seconds depending on the market participant preference [7].

Moreover, FFR only procures Up-regulation and the capacity is remunerated as PaC [7]. On the other hand, FCR-N is symmetric, the capacity is remunerated as PaB and there is EAP, meaning that the market participant is not only paid for its availability but for the activation [7]. FCR-D Down and up only procure down and Up-regulation, respectively, and the capacity is remunerated as PaB [7]. The aFRR market is asymmetric and remunerates capacity as PaC and there is EAP [7]. Finally, mFRR is also asymmetric and remunerates the energy as PaC [7].

Table 7: Overview of Frequency Regulation Markets requirements in Sweden. Source: [7]

	FFR	**FCR-N**	**FCR-D Up**	**FCR-D Down**	**aFRR**	**mFRR**
Market type	Capacity market	Capacity market	Capacity market	Capacity market	Capacity market	Energy market
Minimum bid size	0.1 MW	0.1 MW	0.1 MW	0.1 MW	1 MW	10 MW[2]
Activation time	0.7 s at 49.5 Hz 1 s at 49.6 Hz 1.3 s at 49.7 Hz	3 min 63% in 60 s	30 s 50% in 5 s	30 s 50% in 5 s	5 min	15 min
Endurance	30 s or 5 s	1 h	20 min	20 min	1 h	1 h
Symmetry	Up	SYM	Up	Down	ASYM	ASYM
Remuneration	PaC	PaB EAP	PaB	PaB	PaC EAP	PaC

Moreover, Sweden is a member of the Nordic Balancing Model, which means that, together with other Nordic countries (Denmark, Finland and Norway), Sweden procures aFRR capacity and mFRR energy from the common Nordic market [91].

Table 8 presents the average capacity price and volume procured, in Sweden, per hour. The mFRR mar-

[2] In SE4 is 5MW

ket was not included since it is an energy market. There are four main factors that influence FCR prices [92]. Firstly, given that hydroelectric generators provide the majority of FCR, anything influencing these resources are expected to have an impact on FCR prices [92]. Secondly, the day-ahead wholesale electricity price relates to the opportunity cost for a hydro producer to deviate from its normally optimal output level in order to deliver FCR [92]. Thirdly, the amount of water in their reservoirs influences the hydroelectric producers' ability to generate electricity, and consequently, their capacity and willingness to provide FCR [92]. Finally, the demand for other balancing services can also impact the prices of FCR, for example, aFRR can compete for the same resources that would otherwise be supplied by FCR [92].

Table 8: Average capacity price in 2022 and maximum volume procured in Sweden [7].

Market	Average capacity price 2022 [EUR/MW/hour]	Maximum volume procured [MW]
FFR	37	100
FCR-N	65	558
FCR-D Up	63	538
FCR-D Down	32	231
aFRR	81 (up) and 57 (down)	111

Besides this, the Nordic TSOs will introduce new FRR and FCR requirements to promote harmonization and to keep up with the changes in the power system [93]. One of these changes is the increase of renewable share, which will lead to low inertia situations [93]. The TSOs foresee that FCR-D will not be sufficient in these situations, therefore upgraded FRR requirements are needed [93]. Regarding FCR, the current full activation time requirement will be replaced by the new power and energy-provided assessments. These requirements aim to achieve a better correlation between the system's actual performance from the power system point of view [93]. Additionally, although there is currently no stability requirement in place, there is a need to ensure the system's reliable operation by preventing undamped oscillations in frequency, which becomes increasingly crucial as the system's inertia decreases [93].

2.4 Future Scenarios

In recent years, there has been a significant increase in the use of renewable energy sources and hydrogen as a means of reducing greenhouse gas emissions and moving towards a more sustainable energy system [8]. According to the IEA [8], to achieve NET ZERO globally by 2050, solar PV and wind will lead the electricity sector, as seen in Fig. 6. By 2030, solar a wind together will represent 40% of the electricity production market, and 70 % by 2050 [8].

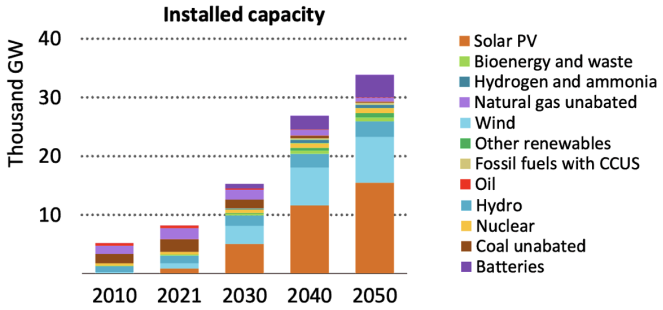

Figure 6: Electricity generation from 2010 to 2050 [8]

Furthermore, hydrogen production is expected to rise nearly five times from today to 2050. From the low-emissions hydrogen produced in 2050, almost three-quarters use water electrolysis [8]. The installed

capacity of electrolyzers is expected to reach 720 gigawatts GW in 2030 and 3 670 GW in 2050 [8]. As a consequence, in 2050, more than 14 800 TWh of electricity generation will be used to produce low-emissions hydrogen, which is equivalent to more than 50 % of the global electricity production in 2021 [8].

Particularly in Sweden, SvK and the Swedish Energy Agency (*Energimyndighetens* in Swedish) have projected four scenarios to achieve NET ZERO by 2045, each scenario considers different energy mixes and hydrogen production rates [15].

Firstly, in the *small-scale renewable scenario* (SF), electricity usage increases, but not to the same extent as the other scenarios [2]. This scenario is characterized by a strong expansion of solar power production [2]. Secondly, in the *mixed roadmap scenario* (FM), wind and solar installed capacity is expanded [2]. Besides this, in Sweden, two nuclear power plants are continued after a 60-year lifespan [2]. However, the hydrogen economy is not fully developed [2]. Thirdly, in the *electrification plannable scenario* (EP), there is a sharp increase in electricity usage [2]. Renewable production is being expanded together with plannable production (nuclear and hydro) [2]. Finally, in the *electrification renewable scenario* (EF) renewable power plants are built to large extent [2]. Hydrogen is a source of flexibility and a crucial component of the energy transition, combined with short-term storage batteries [2].

Table 9 presents the installed capacity of renewable and nuclear power plants and the share of renewables in the total capacity installed, in Sweden, for the year 2021 and the future values for each scenario in 2035 and 2045. Besides this, hydrogen production, in Sweden, is included for the same years and scenarios.

Table 9: Installed capacity, hydrogen production and renewable share in 2021 and for each scenario in 2035 and 2045 [14, 2, 15].

	2021	**2035**				**2045**			
		SF	FM	EP	EF	SF	FM	EP	EF
Hydropower capacity [GW]	16.1	16.3	16.3	16.3	16.3	16.3	16.3	16.3	16.3
Nuclear capacity [GW]	6.9	5.9	5.9	6.9	6.9	0	2.6	8.4	0
Wind capacity [GW]	12.0	17.1	19.3	23.6	28.8	22.6	31.5	33.8	55.3
Solar capacity [GW]	1.7	15.9	7.1	7.9	11.5	29.1	8.9	11.0	19.1
Renewable share [%]	76	90	89	88	90	100	96	89	100
Hydrogen Production [TWh]	0	5	8	24	34	11	16	64	84

2.4.1 Energy Technologies

Currently, the production of electricity using hydrogen is still more expensive compared with other traditional power plants powered by fossil fuels [94]. Nonetheless, taking into account the European hydrogen strategy, it is expected that the price of hydrogen production decreases [94]. According to the IEA, the price of producing hydrogen from renewable electricity could decrease by 30 % by the year 2030 as a result of the increased hydrogen production, technological developments and economy of scale [34]. Considering the implementation of stricter climate laws and a better market regulations structure, electricity production from hydrogen appears to be economically competitive in the 2040 forecast [94].

The costs of each hydrogen technology vary depending on several factors, including the project specifications. Therefore, it is challenging to predict these costs' exact value in the future [34]. Nonetheless, the IEA states that the CAPEX of PEM electrolyzer is supposed to be 828 EUR/kW_e in 2050 [34]. Besides this, due to the scaling benefits, PEM fuel cells are predicted to have an investment cost of 523 EUR/kW_e [95].

Regarding the provision of balancing services, according to the literature, electrolyzers have the technological and financial ability to take part in the balancing services currently and in the future [94].

Furthermore, the technical specifications of electrolyzers and fuel cells are also expected to improve. According to IRENA [34], until 2050, the efficiency of the electrolyzer will improve to 76 % and the lifetime

will increase to 100 000 hours. Regarding fuel cells, the European Commission wants to develop an economical viability of PEM fuel cell power for stationary applications with a lifetime of over 40 000 hours [62]. The theoretical efficiency of a PEM fuel cell is established at 83% [96]. Nevertheless, in practical applications, this ideal efficiency cannot be attained due to inherent system losses. However, according to the manufacturers, advancements in fuel cell technology are anticipated to elevate the efficiency levels to 70 % and potentially higher during the latter part of this decade [97].

Finally, regarding VRES technologies, it is anticipated that the CAPEX costs associated with solar PV power plants will decline significantly, with commercial PV expected to decrease 50 % by 2050 [98]. Additionally, for onshore wind energy, it is projected that the CAPEX costs associated will experience a substantial decline ranging between 37 % and 49 % by the year 2050 [99].

2.4.2 Short-term Forecast of Electricity Markets in Sweden

The Swedish TSO has forecast the average annual price of electricity in the country (SE) and for every bidding zone (SE1, SE2, SE3 and SE4), in Sweden, until 2026, as described in Fig. 7. In all the Swedish bidding zones, the average annual price decreases sharply between 2023 and 2024, which is explained by the current significantly higher fuel prices, which are expected to gradually return to a lower level after 2023 [9]. Additionally, since SE1 imports electricity from SE2 and Finland, the increase in demand in SE1 causes a rise in the average annual prices in the north of Sweden [9]. In the other zones, the price stabilizes or increases again, depending on the changes in electricity demand [9].

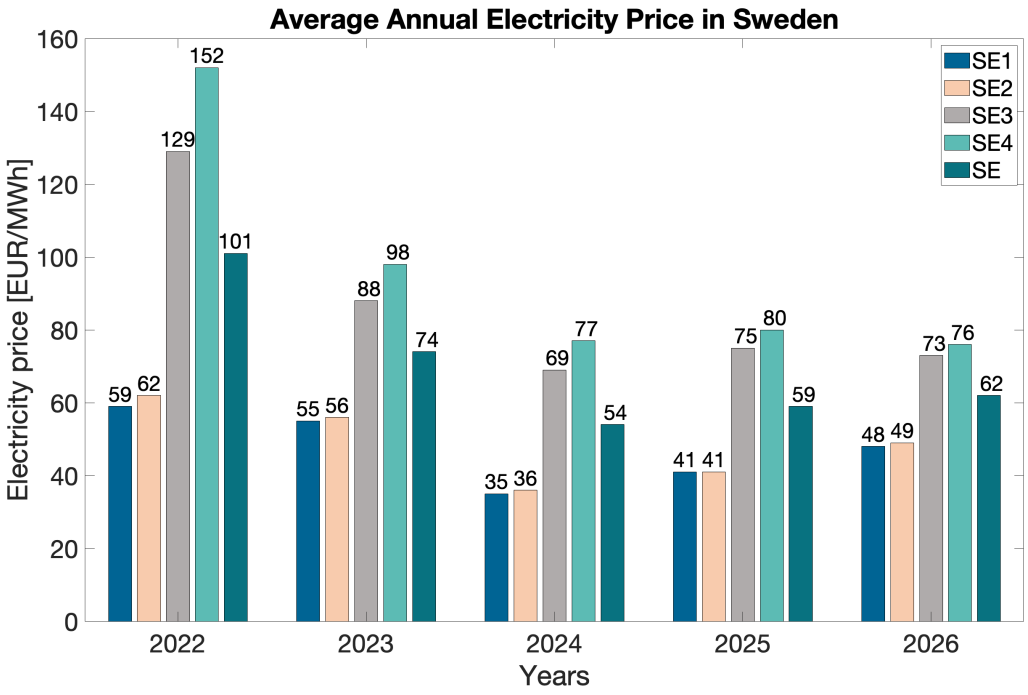

Figure 7: Average annual price of electricity for each bidding zones, from 2023 to 2027 [9]

Furthermore, according to the Swedish Energy Agency [15], the Frequency Regulation Market prices are difficult to predict and can have a major impact on any income from using hydrogen production for this purpose, for this reason, SvK has done a short-term prediction of the frequency regulation costs until 2025, as shown in Fig. 8 [9].

The need for frequency regulation services has increased and thus also the prices, which is expected to continue until 2025 according to SvK [15]. The prices could eventually stagnate in the future if more participants enter the market, which could increase competition and pressure the prices [15].

The cost of the frequency containment reserve for FCR-N and FCR-D Up are expected to decrease over the analysis period [9]. Since FCR-D Down was only implemented on January 2022, there are no historical market prices to base a cost estimate, which makes the cost estimate more uncertain compared to other ancillary services [9]. The annual cost for FCR-D Down is expected to rise continuously, as the procured volume increases [9]. The cost of the aFRR is expected to rise continuously during 2021-2024 as more volume is procured [9]. A common Nordic capacity market was integrated in the last quarter of 2022, which, together with the participation in the European aFRR market in 2024, is expected to lead to lower costs for aFRR, as will be further explained in the next Section [9].

In addition to the mFRR energy market, a capacity market will be implemented in the Nordics, which is expected to start towards the end of 2023. The mFRR costs in Fig. 8 only include the capacity procurement and not the energy activation market [9].

.

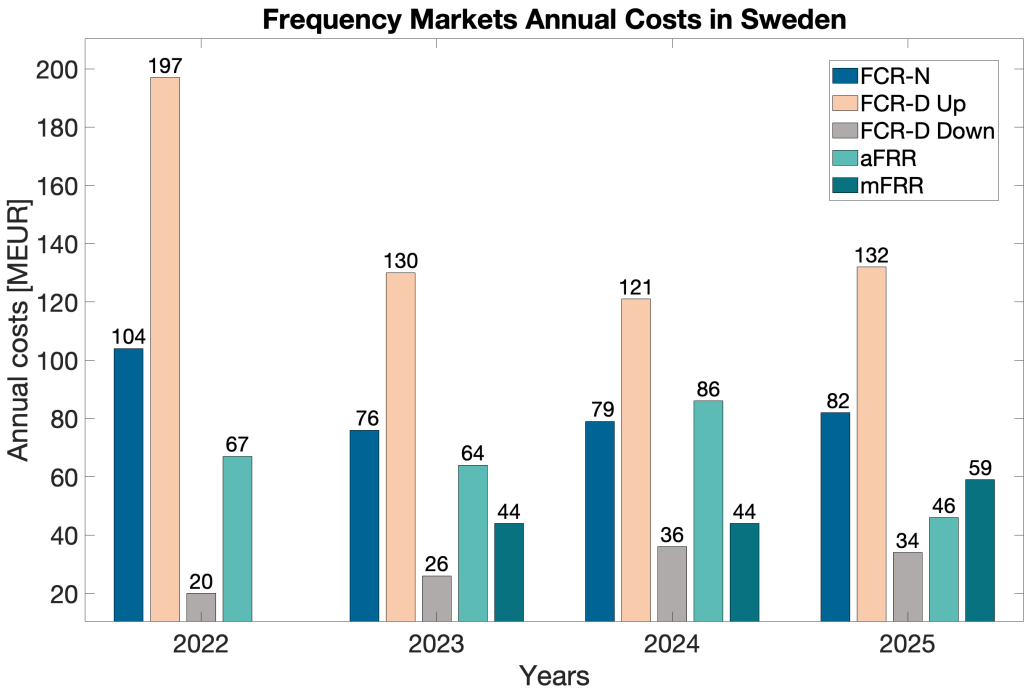

Figure 8: Annual costs for several Frequency Regulation Markets, in Sweden, 2022 to 2025 [9]

2.4.3 European Markets

On March 2023, the European Commission published a proposal for electricity market design reform [100]. This proposal promotes the participation of non-fossil flexibility, such as demand side response and storage, by introducing additional requirements or features in the design of the capacity mechanism that facilitate these types of asset participation [100]. Besides this, the EU Commission proposal also encourages the deployment of more stable long-term contracts such as Power Purchase Agreements [100].

Besides this, Sweden will join in 2024 two European Cooperations: the Platform for the International Coordination of Automated Frequency Restoration and Stable System Operation (PICASSO) and the Manually Activated Reserves Initiative (MARI) [91].

The Picasso project is a European common aFRR energy market, which seeks to enhance economic and technical efficiency [16]. The Picasso project has 26 TSOs as members [16].

On the other hand, the MARI project is a European common mFRR energy market, with the purpose to secure economically efficient purchases by ensuring the financial neutrality of the TSOs [17]. The MARI project already has 29 countries[17].

The requirements of Picasso and MARI projects are described in Table 10. Both markets are PaC, asymmetric and the minimum bid size is 1 MW. The full activation time is 5 minutes in the Picasso project and 12.5 minutes in the MARI project [16, 17]. The aFRR and mFRR markets in Sweden will have to change accordingly to ensure their compatibility with the European projects [91].

Table 10: Overview of European Frequency Regulation Markets [16, 17].

	Picasso	**MARI**
Market type	Energy market	Energy market
Minimum bid size	1 MW	1 MW
Activation time	5 min	12.5 min
Symmetry	ASYM	ASYM
Remuneration	PaC	PaC

3 Methodology

In this Chapter, the methodology followed during this thesis to obtain the desired results is explained in detail. As mentioned previously, the main objective of this work is to assess the technical and economic feasibility of providing frequency regulation services with hydrogen energy storage systems coupled with solar PV and wind power plants.

Therefore, firstly, the methodology describes the analyzed system, including the description of the components and their interactions with the grid. Secondly, the Day-ahead SM and Frequency Regulation Markets operation section focuses on understanding the market dynamics and exploring market participation and operation strategies. Finally, the optimization model developed is described, which includes the variables, constraints, and objective function definition.

3.1 System Description

In the examined system configuration illustrated in Fig. 9, the energy system involves a localized renewable power plant, specifically an onshore wind or solar PV installation, which supplies electrical energy to both the electric grid and the electrolyzer-compressor system. Alternatively, the electrolyzer-compressor system can also draw electricity from the electric grid as a source. The electrolyzer operates to produce hydrogen gas, which is subsequently compressed and stored within a gas tank. Lastly, the generated hydrogen gas can be utilized by a fuel cell to convert it back into electrical energy, which is subsequently fed into the electric grid.

The objective of the P2P hydrogen system in this configuration is to enhance flexibility and mitigate the variable profile of renewable power plants. By capitalizing on the price volatility within the Day-ahead SM and offering ancillary services, the system aims to optimize the utilization of renewable energy resources while ensuring a reliable power supply.

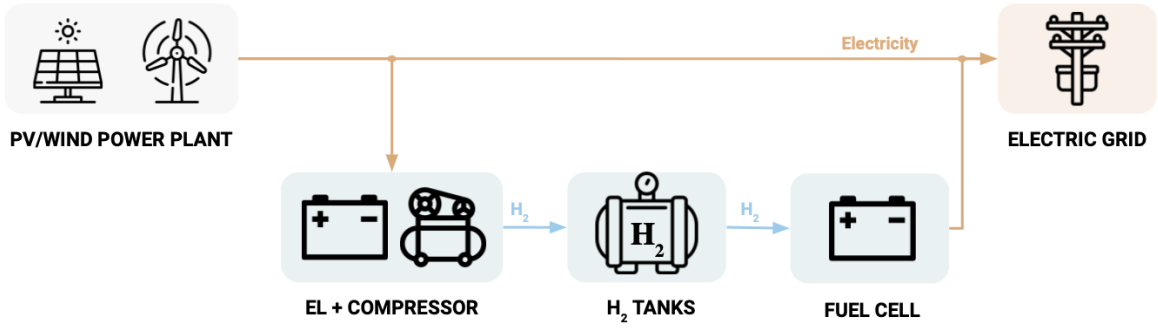

Figure 9: Energy system components and energy flows including renewable energy source

Furthermore, an analysis of the same configuration without the inclusion of a renewable energy source (Fig. 10) is conducted to facilitate a comparative evaluation of the advantages and disadvantages associated with its incorporation.

Detailed descriptions of the design parameters and associated costs for each component of the system can be found in Chapter 4 of this thesis.

3.2 Electricity and Frequency Markets Operation

The formulated optimization model incorporates the prices and characteristics specific to the Swedish markets as a baseline input. However, it possesses the flexibility to be adapted and tailored to suit alternative market settings and conditions.

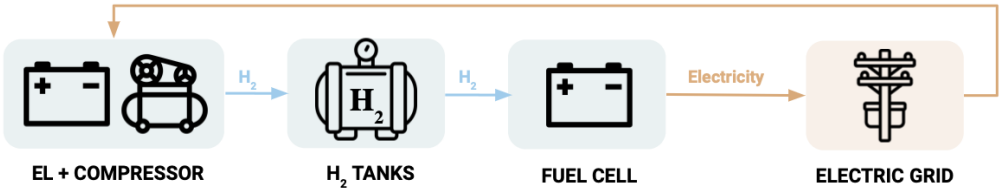

Figure 10: Energy system components and energy flows excluding renewable energy source

The model is designed to optimize the operational aspects of the system in order to maximize profitability within the analyzed time period. To achieve this objective, the model evaluates and selects among various market participation options, namely the Day-ahead SM, Up-regulation frequency market, and Down-regulation frequency market. The only frequency markets included in the optimization were the FCR-D Down and FCR-D Up markets, due to Flower Tech's special interest in analyzing these markets. Besides this, as outlined in Section 2.3.1, the technical specifications of the system align with the requirements of these markets, and the alluring market prices and volumes further justify this decision.

With regard to the bid strategy, the hourly bid prices in the three markets are established as a parameter input, derived from historical data. In this context, the provision of frequency regulation services occurs only when they yield higher profitability compared to trading the same energy on the Day-ahead SM. Consequently, assuming perfect foresight of future prices and quantities enables an ideal optimization of energy flows. However, in a more realistic scenario, market participants lack such perfect foresight, which forces them to rely on forecast techniques to anticipate market prices and activated volumes [35].

As illustrated in Fig. 11, for generation assets such as fuel cells and renewable energy sources, the maximum power that can be offered in the Up-regulation market is determined by subtracting the accepted bid in the Day-ahead market from the total capacity. Similarly, the available power for Down-regulation corresponds to the accepted amount in the Day-ahead spot market. Conversely, for consumption assets like electrolyzers, the bidding capacity in the Down-regulation market is limited to the same amount as in the Day-ahead spot market. As for Up-regulation, the available power is calculated by deducting the accepted power in the Day-ahead spot market from the total capacity of the electrolyzer.

As previously elucidated, the FCR-D markets in Sweden operate as capacity markets wherein market participants are remunerated for maintaining a specified capacity, without receiving compensation for actual activations. Upon examining the frequency events data within the Nordic synchronized grid, it was observed that FCR-D Down and up events transpired at a mere 0.40% and 0.89% respectively in the year 2022 [18], as described in Table 11. Consequently, it was deemed reasonable to disregard activations by assuming that assets are never activated for FCR-D Up nor FCR-D Down-regulation.

Table 11: FCR-D events in 2022 in the Nordic synchronized grid. Source: [18]

Total number of frequency events	FCR-D Down events	FCR-D Up events
181 577	720 (0.40 %)	1 613 (0.89 %)

3.3 Optimization model

This study entails a techno-economic optimization approach, incorporating the technical constraints of the energy system alongside market requirements and characteristics. The objective is to examine the impact of energy arbitrage and ancillary service provision on the optimal revenue, achieved through the optimization of energy flows among system components, the purchase and sale of electricity to the electric grid, and the provision of frequency regulation services. Notably, the described model is adaptable, allowing for the inclusion or exclusion of specific, as well as different bid strategies that do not necessitate perfect foresight of market prices.

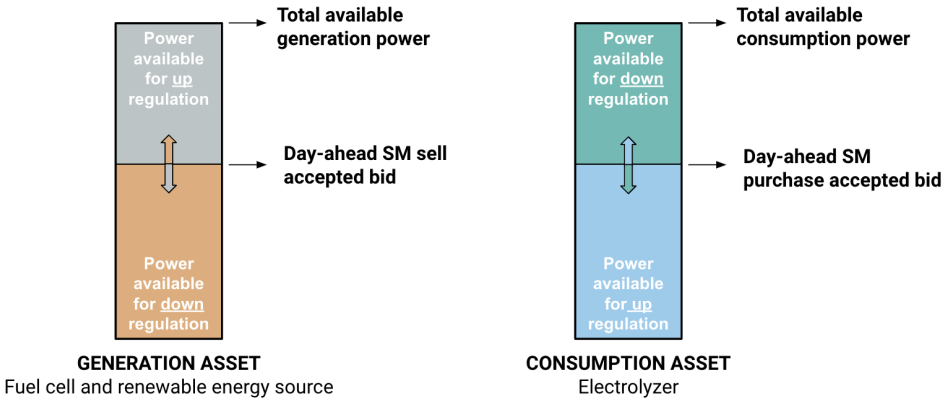

Figure 11: Bid structure of generation and consumption assets

The model simulates the actual energy flows within the system and employs mixed-integer linear programming (MILP) techniques to solve the optimization problem. Implemented as a cost optimization algorithm, the model is coded in Python and utilizes the Gurobi solver for solution computation. The Python code of each optimization model can be accessed in Appendix A. The selection of this approach was driven by the inherent complexity of the system, however, it is important to acknowledge that the adoption of a linear approach entails a simplification, as not all components of the system adhere strictly to linearity in their behavior. Besides this, EXCEL is used to manage and analyze the input data, and the optimization results were analyzed using MatLab and EXCEL, as described in Fig. 12. The model simulates the operation of the system over a time period of at least one year, with hourly temporal resolution, providing a comprehensive view of the system's operation and maximizing profitability.

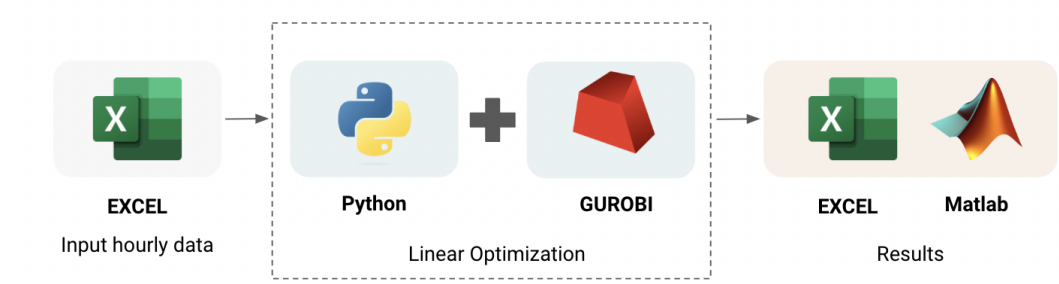

Figure 12: Schematic illustration of the optimization model methodology

3.3.1 Input Parameters

This section provides a description of the input parameters used in the report. The input parameters can be categorized as either constant values throughout the optimization process or as hourly data. These parameters can be adjusted and modified based on the specific time period and market conditions under analysis. The specific value of each input parameter used in the case study of this master's thesis is described in Section 4.

The renewable energy sources considered in this context are wind onshore and solar PV. Consequently, the input parameters that refer to renewable energy need to be specified in the model for either solar PV or wind, based on the type of analysis desired.

Table 12 presents the renewable energy available and the concept of renewable energy availability, which represents the proportion of the overall capacity of renewable energy sources that is accessible during each hour. It is pertinent to highlight that the availability factor input includes the system loss of the renewable energy source, as specified in Section 4 of the study. Besides this, Table 12 also includes the

respective hourly degradation factor that influences the power output of the renewable energy source.

Table 12: Renewable energy input parameters.

Parameter	Type	Symbol	Unit
Renewable energy availability factor	hourly data	av_{rene}	MW/MW_e
Renewable energy available	hourly data	E_{rene}	MW
Degradation of renewable energy source	hourly data	Deg_{rene}	% power output/h

Moreover, Table 13 includes the hourly market prices associated with the Day-ahead SM as well as the up and down Frequency Regulation Markets. In addition, it should be noted that the acceptance of bids for both up and Down-regulation is included as an input parameter, representing the proportion of accepted bids relative to the total number of bids made in each market. Whether a bid is accepted or not depends on factors such as the market type and the specific details of the bid [101]. These acceptance parameters are included to make the scenario more realistic by acknowledging that not all bids are accepted.

Table 13: Market prices and minimum bid parameters.

Parameter	Type	Symbol	Unit
Up-regulation prices	hourly data	P_{up}	EUR/MW
Up-regulation minimum bid	constant	B_{upMin}	EUR/MW
Down-regulation prices	hourly data	P_{down}	EUR/MW
Down-regulation minimum bid	constant	$B_{downMin}$	EUR/MW
Day-ahead SM purchase prices	hourly data	$P_{SM_{purchase}}$	EUR/MWh
Day-ahead SM sell prices	hourly data	$P_{SM_{sell}}$	EUR/MWh
Day-ahead SM minimum bid	constant	B_{SMMin}	EUR/MWh
Up-regulation acceptance	constant	$accep_{up}$	%
Down-regulation acceptance	constant	$accep_{down}$	%

Furthermore, Table 14 includes the installed capacity for each component of the energy system analyzed.

Table 14: Installed capacity input parameters.

Parameter	Type	Symbol	Unit
Renewable source capacity	constant	Q_{rene}	MW
Electrolyzer capacity	constant	Q_{EL}	MW
Fuel cell capacity	constant	Q_{FC}	MW
Tank capacity	constant	Q_{tank}	$MWh_{LHV_{H2}}$
Compressor capacity	constant	Q_{comp}	MW

Additionally, Tables 15 and 16 present the CAPEX and OPEX costs, respectively, associated with each component within the system.

Furthermore, Table 17 incorporates the REPEX costs for both the electrolyzer and fuel cell. This inclusion holds significance due to the comparatively shorter operational lifetimes of these components, as elaborated upon in Chapter 4 since the REPEX of a component is only relevant if the component lifetime is shorter than the project period.

Finally, Table 18 presents the technical parameters associated with the hydrogen system. These parameters encompass the lifetime, efficiency, minimum load, and capacity factor of the electrolyzer and fuel cell. Additionally, the Table provides the compressor consumption, LHV of hydrogen (which is $120MJ/kg_{H2}$ [102]), and the discharge rate of the hydrogen tank. The discharge rate of the hydrogen tank indicates the hourly percentage of hydrogen lost from the tank.

Table 15: CAPEX input parameters.

Parameter	Type	Symbol	Unit
Renewable source CAPEX	constant	$CAPEX_{rene}$	EUR/MW_e
Electrolyzer CAPEX	constant	$CAPEX_{EL}$	EUR/MW_e
Fuel cell CAPEX	constant	$CAPEX_{FC}$	EUR/MW_e
Tank CAPEX	constant	$CAPEX_{tank}$	EUR/$KWh_{LHV_{H2}}$
Compressor CAPEX	constant	$CAPEX_{comp}$	EUR/MW_e

Table 16: OPEX input parameters.

Parameter	Type	Symbol	Unit
Renewable source OPEX	constant	$OPEX_{rene}$	% of CAPEX
Electrolyzer OPEX	constant	$OPEX_{EL}$	% of CAPEX
Fuel cell OPEX	constant	$OPEX_{FC}$	% of CAPEX
Tank OPEX	constant	$OPEX_{tank}$	% of CAPEX
Compressor OPEX	constant	$OPEX_{comp}$	% of CAPEX

Table 17: REPEX input parameters.

Parameter	Type	Symbol	Unit
Electrolyzer REPEX	constant	$REPEX_{EL}$	EUR/MW_e
Fuel cell REPEX	constant	$REPEX_{FC}$	EUR/MW_e

Table 18: Technical input parameters of the hydrogen system.

Parameter	Type	Symbol	Unit
Electrolyzer efficiency	constant	η_{EL}	%
Fuel cell efficiency	constant	η_{FC}	%
Electrolyzer capacity factor	constant	γ_{EL}	% of capacity
Fuel cell capacity factor	constant	γ_{FC}	% of capacity
Compressor capacity factor	constant	γ_{comp}	% of capacity
Electrolyzer minimum load	constant	ζ_{EL}	% of capacity
Fuel cell minimum load	constant	ζ_{FC}	% of capacity
Electrolyzer stack lifetime	constant	τ_{EL}	hours
Fuel cell stack lifetime	constant	τ_{FC}	hours
Compressor consumption	constant	ω_{EL}	MJ/Kg_{H2}
H_2 LVH	constant	LVH_{H_2}	MJ/Kg_{H2}
Discharge rate of H_2 tank	constant	ϵ_{FC}	%

3.3.2 Optimization Variables

This section outlines the optimization variables utilized in the study. These variables can assume either continuous or binary values, depending on the specific context of the model. Notably, the optimization process is performed on an hourly basis, meaning that the variables are optimized independently for each hour.

Table 19 provides a description of the electricity flow among the individual components of the energy system, including the energy consumption specifically associated with the compression of hydrogen.

Table 19: Electricy flows optimization variables

Parameter	Type	Symbol	Unit
Energy flow from renewable source to electrolyzer	continuous	$E_{renetoEL}$	MWh
Energy flow from renewable source to grid	continuous	$E_{renetogrid}$	MWh
Energy flow from grid to electrolyzer	continuous	$E_{gridtoEL}$	MWh
Energy flow from fuel cell to grid	continuous	$E_{FCtogrid}$	MWh
Compressor energy consumption	continuous	E_{comp}	MWh

Moreover, Table 20 encompasses the variables related to hydrogen flows, including the consumption of hydrogen, the production, as well as the storage of hydrogen within the tank.

Table 20: Hydrogen flow optimization variables

Parameter	Type	Symbol	Unit
Hydrogen production	continuous	E_{ProdH2}	MWh
Hydrogen consumption	continuous	E_{ConsH2}	MWh
Hydrogen tank content	continuous	E_{tank}	MWh

Additionally, within Table 21, the binary variables define the activation status of both the electrolyzer and the fuel cell.

Table 21: Optimization variables for the activation of the electrolyzer and fuel cell

Parameter	Type	Symbol	Unit
Electrolyzer activation	binary	A_{EL}	-
Fuel cell activation	binary	A_{FC}	-

Furthermore, Table 22 includes the parameters that represent optimization variables for market bids in each market (day-ahead SM, Up-regulation, and Down-regulation). These variables are associated with either the renewable energy source, fuel cell, or electrolyzer.

Finally, the degradation of the fuel cell and electrolyzer are also considered and included in Table 23.

3.3.3 Optimization Constraints

This section provides a description of the constraints included in the optimization model, which are valid for every hour (the time interval Δt is set to 1 hour) of the analyzed period, represented by the superscript t.

The energy flows between the system components are described in Equations (3) to (9). The electricity generated by the renewable energy source in each time step is determined based on its availability and the hourly degradation, as expressed in (3). The electricity generated by the renewable energy source can be allocated either to the grid or to the electrolyzer, as indicated in (4). The electrolyzer utilizes electricity from either the renewable energy source or the electric grid to produce hydrogen, as described in (5), considering the electricity consumption of the compressor (5). Subsequently, the fuel cell employs the

Table 22: Optimization variables for market bids

Parameter	Type	Symbol	Unit
Electrolyzer purchase bid in Day-ahead SM	continuous	B_{ELSM}	EUR/MWh
Fuel cell sell bid in Day-ahead SM	continuous	B_{FCSM}	EUR/MWh
Renewable energy source sell bid in Day-ahead SM	continuous	B_{reneSM}	EUR/MW
Electrolyzer bid in Up-regulation market	continuous	B_{ELup}	EUR/MW
Fuel cell bid in Up-regulation market SM	continuous	B_{FCup}	EUR/MW
Renewable energy source bid in Up-regulation market	continuous	B_{reneup}	EUR/MW
Electrolyzer bid in Down-regulation market	continuous	B_{ELdown}	EUR/MW
Fuel cell bid in Down-regulation market	continuous	B_{FCdown}	EUR/MW
Renewable energy source bid in Down-regulation market	continuous	$B_{renedown}$	EUR/MW

Table 23: Optimization variables for electrolyzer and fuel cell degradation

Parameter	Type	Symbol	Unit
Electrolyzer degradation	continuous	Deg_{EL}	% of power output/h
Fuel cell degradation	continuous	Deg_{FC}	% of of power output/h

stored hydrogen to generate electricity injected into the electric grid, as represented in (6). To maintain linearity and restrict the complexity of the model, the electrolyzer and the fuel cell are assumed to possess constant efficiency values [35], as depicted in Equations (5) to (6). The compressor-specific energy consumption is described in (7). Equation (8) states that the hydrogen consumption must be constrained to be lower than the quantity stored in the hydrogen tank. The amount of hydrogen stored in H2 tanks is measured based on its stored energy, as indicated in (9). This equation considers the production and consumption of hydrogen while taking into account the possibility of self-discharge processes.

$$E^t_{rene} = av^t_{rene} \cdot Q_{rene} \cdot Deg^t_{rene} \quad \forall t \tag{3}$$

$$E^t_{rene} = E^t_{renetogrid} + E^t_{renetoEL} \quad \forall t \tag{4}$$

$$E^t_{ProdH2} = (E^t_{renetoEL} + E^t_{gridtoEL} - E^t_{comp}) \cdot \eta_{EL} \quad \forall t \tag{5}$$

$$E^t_{ConsH2} = E^t_{FCtogrid} \cdot \eta_{FC} \quad \forall t \tag{6}$$

$$E^t_{comp} = \left(\frac{E^t_{ProdH2}}{LHV_{H_2}} \right) \cdot \omega_{comp} \quad \forall t \tag{7}$$

$$E^t_{ConsH2} \leq E^t_{tank} \quad \forall t \tag{8}$$

$$E^{t+1}_{tank} = E^t_{tank} \cdot (1 - \epsilon tank) + E^t_{ProdH2} - E^t_{ConsH2} \quad \forall t \tag{9}$$

The inter-component energy exchanges within the system are subject to limitations imposed by the capacities of each component, as outlined in Equations (10) to (13). These component capacities are predetermined inputs of the model and are described in detail in Chapter 4. Both the electrolyzer and the

fuel cell are subject to additional constraints, including minimum load requirements, capacity factors, and degradation factors. These constraints are represented in (10) and (11), where A_{EL} and A_{FC} are binary variables indicating the operational state of the components (1 when the component is on, 0 when the component is off), enabling the monitoring of component start-up and shut-down events. Moreover, the tank and compressor must also comply with their respective capacity constraints to ensure proper system operation ((12) and (13)).

$$A^t_{EL} \cdot \zeta_{EL} \cdot Q_{EL} \leq \frac{E^t_{gridtoEL} + E^t_{renetoEL} - E^t_{comp}}{\Delta t} \leq A^t_{EL} \cdot Q_{EL} \cdot CF_{EL} \cdot Deg^t_{EL} \quad \forall t \tag{10}$$

$$A^t_{FC} \cdot \zeta_{FC} \cdot Q_{FC} \leq \frac{E^t_{FCtogrid}}{\Delta t} \leq A^t_{FC} \cdot Q_{FC} \cdot CF_{FC} \cdot Deg^t_{FC} \quad \forall t \tag{11}$$

$$E^t_{tank} \leq Q^t_{tank} \qquad \forall t \tag{12}$$

$$E^t_{comp} \leq Q^t_{comp} \qquad \forall t \tag{13}$$

As highlighted in Section 3.3, the consideration of up and Down-regulation activations is omitted in the analysis, resulting in solely the energy flows from the components (specifically, the electrolyzer, fuel cell, and renewable energy source) to the grid through accepted day-ahead SM energy bids. This specific modeling approach is described mathematically in Equations (14) to (16).

$$E^t_{FCtogrid} = B^t_{FCSM} \qquad \forall t \tag{14}$$

$$E^t_{gridtoEL} = B^t_{ELSM} \qquad \forall t \tag{15}$$

$$E^t_{renetogrid} = B^t_{reneSM} \qquad \forall t \tag{16}$$

Furthermore, in the day-ahead SM as well as the Up and Down-regulation markets, each bid has to satisfy the minimum bid size criteria specific to each market. Equations (17) to (25) outline this concept, specifying that a bid can either be 0, indicating non-participation in the corresponding market at that particular time, or it must be higher than the minimum bid size requirement.

$$B^t_{FCSM} = 0 \vee B^t_{FCSM} \geq B_{SMMin} \qquad \forall t \tag{17}$$

$$B^t_{FCup} = 0 \vee B^t_{FCup} \geq B_{upMin} \qquad \forall t \tag{18}$$

$$B^t_{FCdown} = 0 \vee B^t_{FCdown} \geq B_{downMin} \qquad \forall t \tag{19}$$

$$B^t_{ELSM} = 0 \vee B^t_{ELSM} \geq B_{SMMin} \qquad \forall t \tag{20}$$

$$B^t_{ELup} = 0 \vee B^t_{EL} \geq B_{upMin} \qquad \forall t \tag{21}$$

$$B^t_{ELdown} = 0 \vee B^t_{ELdown} \geq B_{downMin} \qquad \forall t \tag{22}$$

$$B^t_{reneSM} = 0 \vee B^t_{reneSM} \geq B_{SMMin} \qquad \forall t \tag{23}$$

$$B^t_{reneup} = 0 \vee B^t_{reneup} \geq B_{upMin} \qquad \forall t \tag{24}$$

$$B^t_{renedown} = 0 \vee B^t_{renedown} \geq B_{downMin} \qquad \forall t \tag{25}$$

As shown in Fig. 11, Equations (26) to (31) explain the limitations on power availability for each bid. When it comes to generation assets like the fuel cell and renewable energy source, the bids for Down-regulation (capacity to generate less electricity) must be higher than the accepted bid in the day-ahead SM (as stated in Equations (26) and (30)). On the other hand, Up-regulation bids (capacity of generating more electricity) can only be considered if the accepted power in the day-ahead SM is lower than the total available capacity of the asset ((27) and (31)). For consumption assets like the electrolyzer, it's the opposite. Up-regulation bids (capacity of consuming less electricity) should be lower than the accepted bid in the day-ahead SM (28). However, Down-regulation bids (capacity of consuming more electricity) can be accepted if the accepted bid in the day-ahead SM is lower than the total available capacity of the electrolyzer (29).

$$B^t_{FCdown} \leq B^t_{FCSM} \qquad \forall t \tag{26}$$

$$B^t_{FCup} \leq Q_{FC} \cdot CF_{FC} \cdot Deg^t_{FC} - B^t_{FCSM} \qquad \forall t \tag{27}$$

$$B^t_{ELup} \leq B^t_{ELSM} \qquad \forall t \tag{28}$$

$$B^t_{ELdown} \leq Q_{EL} \cdot CF_{EL} \cdot Deg^t_{EL} - B^t_{ELSM} \qquad \forall t \tag{29}$$

$$B^t_{renedown} \leq B^t_{reneSM} \qquad \forall t \tag{30}$$

$$B^t_{reneup} \leq E^t_{rene} - E^t_{renetoEL} - E^t_{renetogrid} \qquad \forall t \tag{31}$$

Several studies have addressed the degradation of fuel cells and electrolyzers, characterizing it as a linear increase expressed as a percentage of power per hour [103, 104, 61, 105]. However, the literature also acknowledges that the degradation process is influenced by the operational conditions. Shutdown/start-up events, transient loading, and operation above or below rated power [106, 107, 108] have been identified as factors exacerbating degradation. To reduce the computational requirements and make the optimization process more efficient, the present thesis adopts the linear degradation approach. In this approach,

both the electrolyzer and fuel cell are subjected to degradation factors (Deg_{EL} and Deg_{FC}), these factors multiply the power of the fuel cell and electrolyzer, therefore they decrease when the degradation increases. Whereby degradation increases linearly until a predefined minimum limit of the degradation factors is reached (as denoted in (32) and (33)). Once the limit is reached, REPEX costs are factored in, and the degradation factors (Deg_{EL} and Deg_{FC}) are reset to 1.

$$Deg_{EL}^{t+1} = Deg_{EL}^{t} - \frac{1}{\tau_{EL}} \qquad \forall t \tag{32}$$

$$Deg_{FC}^{t+1} = Deg_{FC}^{t} - \frac{1}{\tau_{FC}} \qquad \forall t \tag{33}$$

3.3.4 Optimization Objective Function

The optimization algorithm employed aims to maximize the cumulative revenue generated over the specified time period, as outlined in (34). This Equation includes the various cash flows associated with the energy system's participation in the day-ahead spot market and Frequency Regulation Markets. Additionally, the algorithm takes into account the bid acceptance parameters specific to the Frequency Regulation Markets.

$$\begin{aligned} \text{Revenue} = \sum_{t} & \, accep\_up \cdot P_{up}^{t} \cdot (B_{reneup}^{t} + B_{ELup}^{t} + B_{FCup}^{t}) \\ & + accep\_down \cdot P_{down}^{t} \cdot (B_{renedown}^{t} + B_{ELdown}^{t} + B_{FCdown}^{t}) \\ & + P_{SM_{sell}}^{t} \cdot (B_{reneSM}^{t} + B_{FCSM}^{t}) - P_{SM_{purchase}}^{t} \cdot B_{ELSM}^{t} \end{aligned} \tag{34}$$

3.4 Techno-economic analysis equations

3.4.1 Technical Calculations

Table 24: Technical parameters description.

Parameter	Symbol	Unit
Electrolyzer shutdowns	S_{EL}	-
Fuel cell shutdowns	S_{FC}	-
Electrolyzer operating hours	H_{EL}	hours
Total H_2 produced	$Prod_{H2}$	Kg
Fuel cell operating hours	H_{FC}	hours
Share renewable energy injected in the grid	$GINJ_{rene}$	%
Total energy delivered to the grid	E_{toGrid}	MWh
Overall system efficiency	η_{sys}	%
System losses	E_{loss}	MWh

Equation (35) represents the computation used to derive the proportion of renewable power that is injected into the grid.

$$GINJ_{rene} = \frac{\sum_{t} E_{renetogrid}^{t}}{\sum_{t} E_{rene}^{t}} \tag{35}$$

Furthermore, Equation (36) describes the calculation utilized to determine the total energy delivered to the grid. According to (36), the energy supplied to the grid is the summation of the energy derived from

renewable sources and the energy generated by the fuel cell system, both of which are supplied to the grid.

$$E_{toGrid} = \sum_{t} E^{t}_{renetogrid} + \sum_{t} E^{t}_{FCtogrid} \tag{36}$$

Equation (37), characterizes the overall efficiency of the system. It quantifies the ratio between the energy delivered to the grid and the energy injected into the system from the grid and renewable sources while accounting for variations in the energy content of the tank.

$$\eta_{sys} = \frac{\sum_{t} E^{t}_{renetogrid} + \sum_{t} E^{t}_{FCtogrid}}{E^{t=final}_{tank} - E^{t=0}_{tank} + \sum_{t} E^{t}_{rene} + \sum_{t} E^{t}_{gridtoEL}} \tag{37}$$

Finally, Equation (38), provides a measure of the losses incurred by the system. These losses are determined by calculating the difference between the total energy injected into the system and the energy injected into the grid.

$$E_{loss} = E^{t=final}_{tank} - E^{t=0}_{tank} + \sum_{t} E^{t}_{rene} + \sum_{t} E^{t}_{gridtoEL} - \sum_{t} E^{t}_{renetogrid} - \sum_{t} E^{t}_{FCtogrid} \tag{38}$$

3.4.2 Economic Calculations

Table presents an overview of the parameters utilized in the computation of economic indicators, which will form a crucial part of this thesis analysis. Equations (39) to (48) describe the mathematical formulations employed for calculating each economic indicator. These Equations provide insights that contribute to the assessment of the project's financial viability and profitability.

Table 25: Economic parameters description.

Parameter	Symbol	Unit
Year	n	-
Discount rate	d	%
Total discounted costs	C	EUR
Total discounted revenue	R	EUR
Annual cash flow	CFLOW	EUR
Net present value	NPV	EUR
Return on investment	ROI	%
Internal rate of return	IRR	%
Payback Perdiod	PBP	years
Levelized cost of electricity	LCOE	EUR/MWh

Equation (39) represents the initial investment cost (C_0) of the project, calculated by summing the CAPEX of the different components. With regard to the REPEX costs, it is important to note that they are incurred exclusively in the years when the fuel cell or the electrolyzer reaches their respective operational limits, necessitating replacements. In terms of the OPEX, it is worth mentioning that the values employed are represented as a percentage of the CAPEX. To estimate the total opex costs, the aggregate opex value was calculated and evenly distributed across each year of the project analysis, as described in (40). The total discounted costs, taking into account the CAPEX, REPEX, and OPEX costs is calculated according to (41).

$$\begin{aligned} C_0 =& Q_{rene} \cdot CAPEX_{rene} + Q_{FC} \cdot CAPEX_{FC} \\ &+ Q_{EL} \cdot CAPEX_{EL} + Q_{comp} \cdot CAPEX_{comp} + Q_{tank} \cdot CAPEX_{tank} \end{aligned} \tag{39}$$

$$\begin{aligned} n \cdot C_{opex_n} =& Q_{rene} \cdot CAPEX_{rene} \cdot OPEX_{rene} + Q_{FC} \cdot CAPEX_{FC} \cdot OPEX_{FC} \\ &+ Q_{EL} \cdot CAPEX_{EL} \cdot OPEX_{EL} + Q_{comp} \cdot CAPEX_{comp} \cdot OPEX_{comp} \\ &+ Q_{tank} \cdot CAPEX_{tank} \cdot OPEX_{tank} \end{aligned} \tag{40}$$

$$C = \sum_n \frac{C_{capex_n} + C_{opex_n} + C_{repex_n}}{(1+d)^n} \tag{41}$$

Equation (42) represents the calculation of the total discounted revenues. The *Revenue* parameter in this Equation refers to the output generated by the optimization mode for each year of the analysis period.

$$R = \sum_n \frac{Revenue_n}{(1+d)^n} \tag{42}$$

Equation (43) defines the cash flow (CF_n) in each year (n) as the difference between the revenue (R_n) and the costs (C_n) incurred in that year.

$$CFLOW_n = R_n - C_n \tag{43}$$

The NPV of a project is calculated according to (44). This indicator provides a measure of the project's profitability by assessing whether the present value of the expected cash flows is positive or negative. A positive NPV suggests that the project is expected to generate more value than the initial investment, indicating its potential profitability. Conversely, a negative NPV indicates that the project may not generate sufficient returns to cover the costs and may not be financially viable.

$$NPV = \sum_n CFLOW_n \tag{44}$$

Furthermore, (45) represents the calculation of the ROI for a project. The ROI provides an assessment of the profitability and efficiency of the investment. It measures the return generated by the project relative to the initial investment made. A higher ROI indicates a higher return on the investment, suggesting that the project is generating more value compared to its initial cost. Conversely, a lower ROI suggests that the project's returns may be relatively lower compared to the initial investment.

$$ROI = \frac{NPV}{C_0} \cdot 100 \tag{45}$$

Additionally, by setting the NPV equal to zero, Equation (46) allows us to calculate the IRR. The IRR represents the discount rate at which the present value of the project's cash flows equals the initial investment. It indicates the rate of return that the project is expected to generate.

$$NPV = 0 = \sum_n \frac{cashflow_n}{(1+IRR)^n} \tag{46}$$

Moreover, (47), the payback period is determined by assessing the number of years it takes for the cumulative cash flows to reach or surpass the initial investment amount.

$$PBP = Number\ of\ years\ before\ cumulative\ cash\ flows \geq C_0 \tag{47}$$

Finally, (48) calculates the LCOE of the project, by quantifying the the average cost of generating electricity over the project's lifespan. In the context of this project, the LCOE calculation takes into account the energy generated and supplied to the grid.

$$LCOE = \frac{C}{\sum_n \frac{E_{renetogrid_n} + E_{FCtogrid_n}}{(1+d)^n}} \tag{48}$$

4 Case Study

4.1 Renewable energy resources

In this Section, the hourly availability VRES is described, along with an examination of the generation characteristics specific to solar PV and onshore wind power plants chosen to be part of this thesis case study. The solar PV power plant and the onshore power plant selected for this study exhibit an identical installed capacity. This deliberate choice ensures that this particular technical specification remains consistent and impartial, thus minimizing its influence on the subsequent analysis and performance comparison.

4.1.1 Solar Electricity Generation

This thesis considers Swedbank Solar PV Park as a case study, focusing on its distinctive attributes. The Swedbank Solar PV Park has a peak power capacity of 12 MW and is situated in Ostergotland, Sweden [109].

To investigate the hourly solar availability at the specified location, this study used the Photovoltaic Geographical Information System (PVGIS) online tool. Apart from assessing solar availability, this tool also facilitates the optimization of slope and azimuth angles [110]. PVGIS employs SARAH2 solar irradiation data from the year 2020 [110]. The input parameters for PVGIS are PV technology, system loss, and mounting type, as summarized in Table 26.

Table 26 presents the key parameters and assumptions related to the solar PV system used in this study. The first row specifies the solar PV capacity, which was assigned the value of 12 MW, as in the Swedbank Solar PV Park [109]. The subsequent rows highlight the assumptions made for the solar PV technology, where crystalline silicon is considered as the technology choice since this is the most commonly used technology [111], and for the mounting type, which is fixed. The azimuth and slope angle were obtained using the PVGIS optimization tool. The literature suggests that in the context of the northern hemisphere, the optimal azimuth angle for solar collectors is determined by ensuring their alignment towards the south [112] (represented by 0 degrees in this thesis). However, the PVGIS tool was employed to optimize the azimuth angle, obtaining a value of -11 degrees, which is closely aligned with a southern orientation. Moreover, the PVGIS tool also provided the optimal slope angle for the solar panels, resulting in a tilt angle of 47 degrees.

The next rows focus on the economic aspects of the solar PV system. The solar PV CAPEX is stated as 800 EUR/KW_e, according to [113]. The solar PV OPEX is estimated to be 0.3% of the CAPEX [113]. The solar PV system is assumed to have a lifetime of 25 years [113], and the annual degradation rate is assumed to be 0.36 % [113]. Additionally, a system loss of 14 % of the system's capacity is considered an assumption.

Table 26: Solar PV parameters and assumptions.

Parameter	Value	Unit	Source
Solar PV capacity	12	MW	[109]
Solar PV technology	Crystalline silicon	-	*assumption*
Solar PV mounting type	fixed	-	*assumption*
Azimuth	-11	º	[109]
Slope	47	º	[109]
Solar PV CAPEX	800	EUR/KW_e	[113]
Solar PV OPEX	0.1	% of CAPEX	[114]
Solar PV lifetime	25	years	[113]
Solar PV degradation	0.36	%/year	[113]
Solar PV system loss	14	% power output	*assumption*

Based on the parameters described before, the solar availability in the selected location in 2020 is presented in Fig. 13. The aforementioned yearly profile was consistently replicated over a span of 20 years,

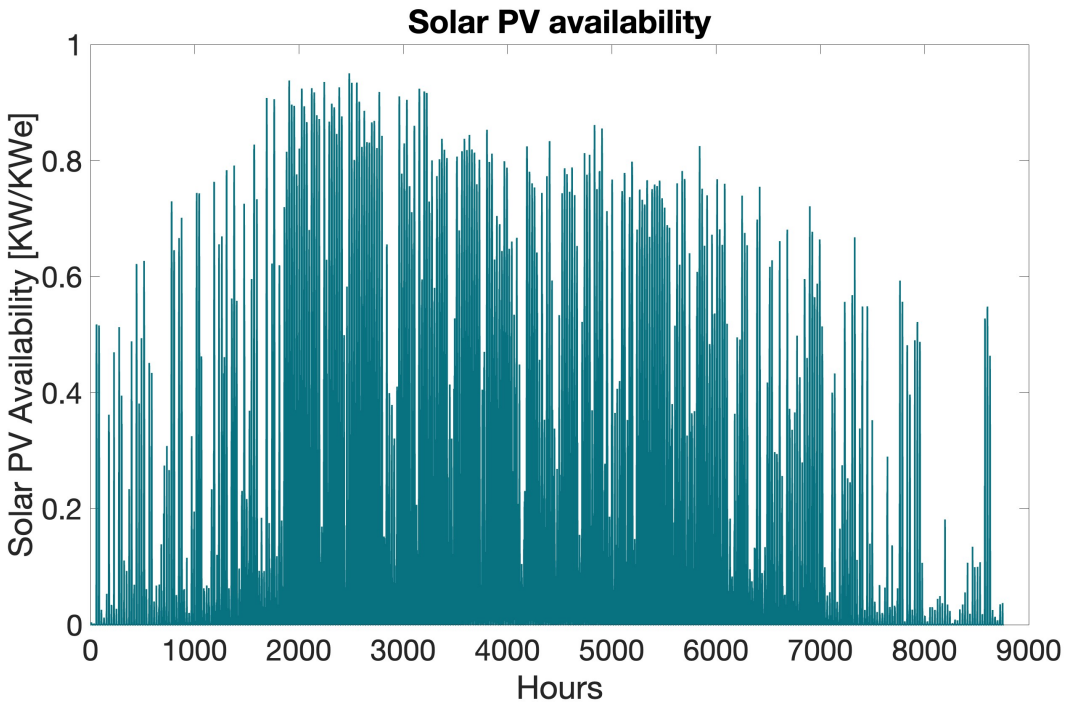

Figure 13: Solar availability in 2020 in the selected location

with the assumption that its characteristics remained unchanged in each successive year.

4.1.2 Onshore Wind Electricity Generation

This Section provides a comprehensive description of the onshore wind parameters utilized in this study, with a specific focus on the selected case study: the Hedbodberget Wind Farm located in Dalarna, Sweden[115]. The wind farm under consideration has a total installed power capacity of 12 MW [115].

To accurately assess wind availability, the Modern-Era Retrospective analysis for Research and Applications, Version 2, database (MERRA-2) from NASA was used [116]. Hourly data from the year 2019 was gathered from this database for further analysis [116]. In terms of turbine specifications, the power curve of a *Vestas V90 2000* wind turbine [117] was used for calculating the power output availability, in the specific location of this analysis, since this is the wind turbine used specifically in the Hedbodberget Wind Farm [115]. A performance factor of 90 % was considered in these calculations, while the turbine hub height was set at 100 meters.

To determine the surface roughness, an esteemed resource known as the *Global Wind Atlas* was consulted [118]. This tool was developed through a collaborative partnership between the Department of Wind Energy at the Technical University of Denmark (DTU Wind Energy) and the World Bank Group, the *Global Wind Atlas* indicated a surface roughness value of 0.05 meters [118].

These relevant onshore wind technical and cost parameters and described in Table 27.

Based on the parameters described before, the wind availability in the selected location in 2019 is presented in Fig. 14. The aforementioned yearly profile was consistently replicated over a span of 20 years, with the assumption that its characteristics remained unchanged in each successive year.

Table 27: Onshore wind parameters and assumptions.

Parameter	Value	Unit	Source
Onshore wind capacity	12	MW	[109]
Wind onshore CAPEX	1 235	EUR/KW_e	[21]
Wind onshore OPEX	3	% of CAPEX	[119]
Onshore wind performance factor	90	% of power output	*assumption*
Turbine hub height	100	m	*assumption*
Surface roughness	0.05	º	[109]
Onshore wind lifetime	25	years	[120]
Onshore wind turbine degradation	1.6	%/year	[121]

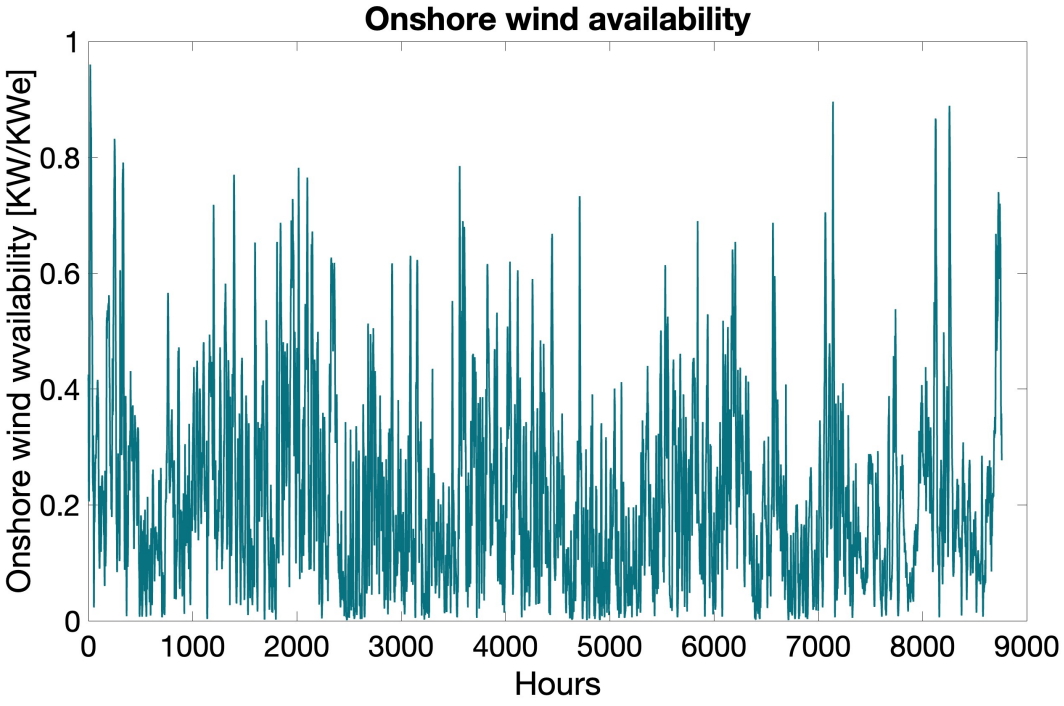

Figure 14: Wind availability in 2019 in the selected location

4.2 Market-related Inputs

As stated in Section 3.2, the optimization process focused solely on incorporating two specific frequency markets, namely the FCR-D Down and FCR-D Up markets. The pricing data utilized for both markets corresponds to the year 2022 and was sourced from the Mimer platform [10]. Since the Mimer platform provides average prices, and given that the remuneration strategy for both markets follows a pay-as-bid approach, it is assumed that the acceptance rates for Up-regulation ($accep_{up}$) and Down-regulation ($accep_{down}$) are set at 90 % within the optimization model. The graphics presented in Fig. 15 and Fig. 16 describe the prices associated with the up and Down-regulation of FCR-D, respectively, that were used as an input in the optimization model. These figures utilize a cumulative frequency graph and a year-long profile to illustrate the price differentials. Based on the analysis of these Figures, it can be concluded that the prices for Up-regulation exhibit relatively higher values compared to the prices for Down-regulation.

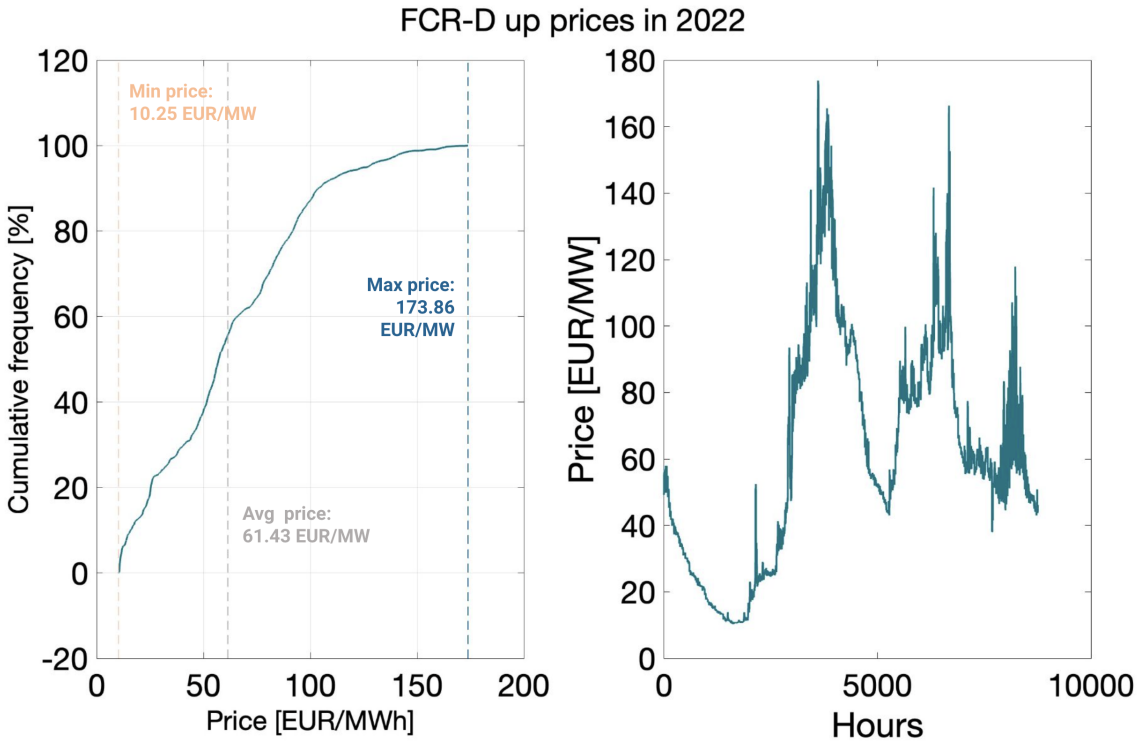

Figure 15: FCR-D Up average prices in Sweden in 2022[10]. Cumulative frequency (left) and year-long profile (right)[10].

Within the scope of the 20-year analysis, the hourly prices for FCR-D Up and Down-regulation between 2023 and 2025 exhibit a proportional deviation from the corresponding values observed in 2022, mirroring the annual cost trends outlined in Fig. 8. From 2025 onwards, the prices were assumed to remain constant, aligning with the premise discussed in Section 2.4.2 that the Swedish TSO anticipates market saturation and consequent price stagnation.

With respect to the Day-ahead SM prices, the corresponding values for the year 2022 were obtained from the NordPool platform [11]. In terms of the prevailing tax rates, given the nature of this analysis, the ordinary tax income was disregarded. However, the value-added tax (VAT) in Sweden for the year 2022 was accounted for, standing at a rate of 25% [122]. This VAT rate was incorporated into the final price for both purchases and sales made in the Day-ahead SM. The graphics presented in Fig. 17 describe the average hourly prices in all the bidding zones, associated with Day-ahead SM in 2022, that were used as input in the optimization model.

The pricing of the Day-ahead SM during a 20-year operational period was determined based on the information presented in Fig. 7. Specifically, the hourly prices between 2023 and 2026 will deviate from

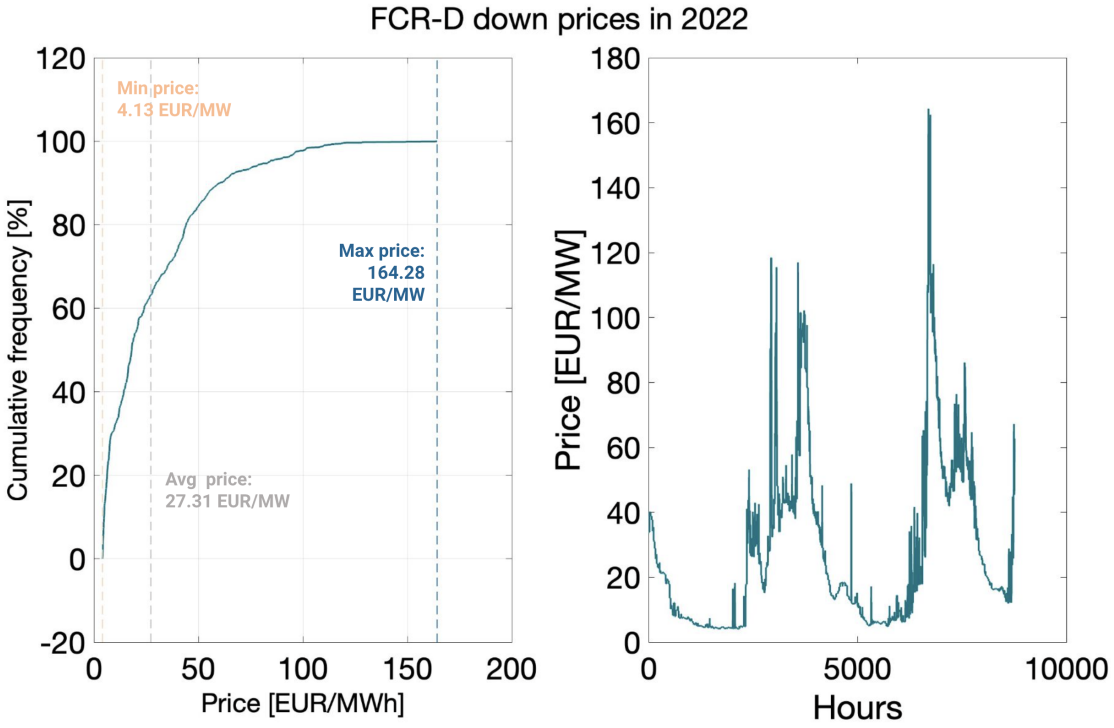

Figure 16: FCR-D Down average prices in Sweden in 2022[10]. Cumulative frequency (left) and year-long profile (right)[10].

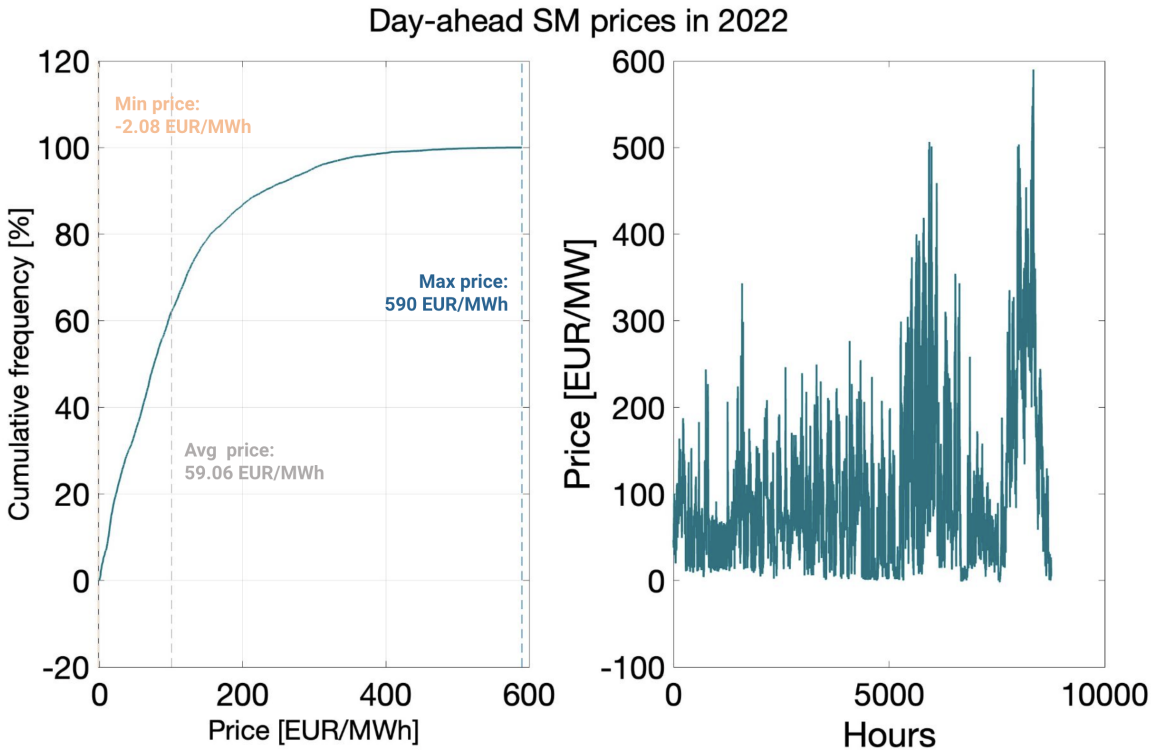

Figure 17: Day-ahead SM clearing prices in the Swedish market in 2022 [11]. Cumulative frequency (left) and year-long profile (right) [11].

the values observed in 2022 in proportion to the average annual price change depicted in Fig. 7. Subsequently, starting from 2026, a constant increase was assumed, matching the rate of increase observed between 2025 and 2026, which is 3.8 %. This assumption is substantiated by the literature [123], which supports the adoption of an annual growth rate of 3-4 % up until 2050.

4.3 Hydrogen Energy System Design and Costs

This Section of the thesis describes the system size and cost parameters specific to the chosen case study. These parameters are essential for evaluating the feasibility and economic implications of the proposed system within the context of the case study.

To simplify the model and improve computational efficiency, the system size was set according to the methodology described in [35]. This approach aimed to reduce the complexity and running times of the analysis. However, in Chapter 5.3, a sensitivity analysis is conducted to evaluate the effects of the system size on the obtained results. This investigation aims to provide a comprehensive assessment of how varying system sizes impact the outcomes, thereby enhancing the overall comprehensiveness of the study.

Furthermore, PEM electrolyzer and fuel cell stacks were selected for this particular system because of several factors. As mentioned in Section 2.1, despite their relatively higher costs compared to alternative technologies, the decision to opt for PEM-based components was driven by the imperative need for rapid response, enhanced dynamic performance, and the ability to operate under partial load conditions, which are critical requirements for the intended system operation. In addition, the selection of a type I compressed hydrogen gas storage tank was motivated by two primary considerations: its relatively lower cost compared to other types of storage tanks and its suitability for stationary applications. Given the intended use of the tank within the system, the choice of a type I storage tank was considered adequate. For the compression step, the most suitable technology is, according to the literature [35], a three-stage intercooled compressor, with a constant compression ratio on each stage and constant efficiency.

4.3.1 Electrolyzer

The CAPEX of the electrolyzer considers electrolyzer stack costs, installation labor, and other costs related to the installation.

Table 28 presents the parameters and assumptions PEM electrolyzer, which is considered in the analysis of this master thesis. The Table provides key information regarding the electrolyzer's capacity, CAPEX, REPEX, OPEX, stack lifetime, minimum load, capacity factor, efficiency, and maximum degradation.

The electrolyzer capacity is assumed to be 3 MW, representing the desired power output of the system. The electrolyzer CAPEX is estimated to be 1 352 EUR/KW_e, as reported in [124], which considers the electrolyzer stacks costs, installation labor, and other electrolyzer's balance of service costs. The REPEX is considered to be 40 % of the CAPEX, based on the findings presented in [36]. Furthermore, the OPEX is assumed to be 1 % of the CAPEX, as indicated by [124].

The electrolyzer stack lifetime is expected to be 40 000 hours, as reported in [47]. This parameter represents the operational lifetime of the electrolyzer stack before replacement or refurbishment is required. The electrolyzer's minimum load is determined to be 10% of its capacity, as discussed in [125].

To assess the electrolyzer's performance, two additional factors are considered. The electrolyzer capacity factor is assumed to be 90 % of its capacity. The electrolyzer efficiency is estimated at 70 % of its capacity, as reported in [45].

Finally, a minimum degradation factor of 0.1 is assumed, representing a 90% decrease in the performance of the electrolyzer. This factor represents the maximum allowable degradation of the electrolyzer's performance over its operational lifetime before replacement or refurbishment is required.

Table 28: PEM electrolyzer parameters and assumptions.

Parameter	Value	Unit	Source
Electrolyzer capacity	3	MW	*assumption*
Electrolyzer CAPEX	1 352	EUR/KW_e	[124]
Electrolyzer REPEX	40	% of CAPEX	[36]
Electrolyzer OPEX	1	% of CAPEX	[124]
Electrolyzer stack lifetime	40 000	hours	[47]
Electrolyzer minimum load	10	% of capacity	[125]
Electrolyzer capacity factor	90	% of capacity	*assumption*
Electrolyzer efficiency	70	% of capacity	[45]
Electrolyzer pressure output	3	MPa	[48]
Minimum degradation factor	10	% of capacity	*assumption*

Fig. 18 illustrates the progressive degradation of the electrolyzer over a period of 20 years, as analyzed in this study. Upon reaching the maximum degradation factor, the degradation process is reset to its initial state, denoted as 1. Moreover, the model incorporates replacement costs, referred to as REPEX costs, which account for the expenses associated with replacing the fuel cell system. Examining Fig. , it becomes evident that the electrolyzer system will incur replacement costs at specific time intervals throughout the 20-year duration of the analysis. Specifically, these replacement costs occur in the following years: 5, 9, 13 and 17.

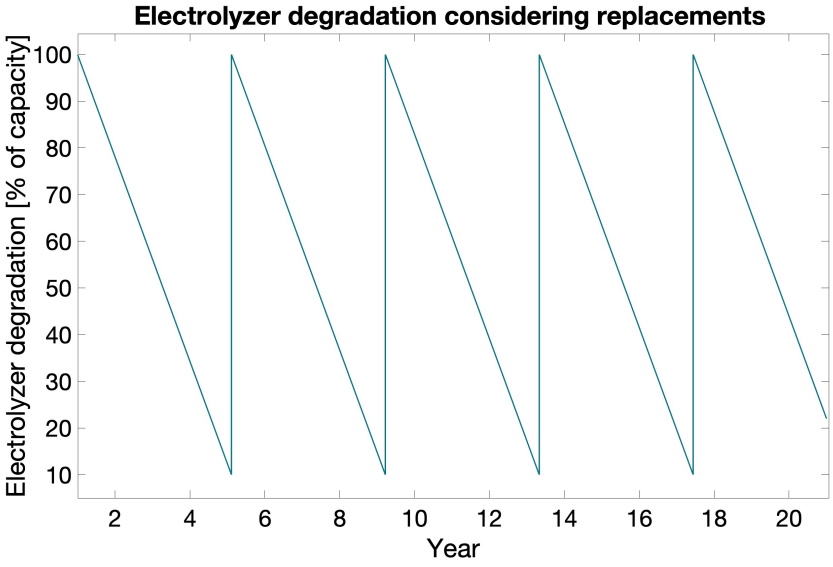

Figure 18: Electrolyzer linear degradation, considering replacements and minimum degradation factor

4.3.2 Hydrogen Compressor

Table 29 presents the parameters and assumptions related to the compressor, which are of significance in the analysis conducted in this study.

To determine the minimum capacity of the electrolyzer, an initial step involves calculating the maximum hydrogen production. This involves replacing the variable E_{comp} with the equation given in Eq. 7, as outlined in Eq. 5. In this calculation, it is assumed that the sum of energy from the grid to the electrolyzer ($E_{gridtoEL}$) and the VRES to the electrolyzer ($E_{renetoEL}$) correspond to the electrolyzer capacity (Q_{EL}), multiplied by the duration of one hour. This approach yields a maximum hydrogen production of 2.05 MWh. Subsequently, by substituting this value into Eq. 7, a minimum compressor capacity of 65 kW

is obtained. However, due to the consideration of a capacity factor (CF_{comp}) assumption of 90%, the compressor capacity for this specific case study is assumed to be 75 kW. The calculations pertaining to the minimum compressor capacity, dependent on the electrolyzer capacity, are succinctly summarized in Eq. 49.

$$CF_{comp} \cdot Q_{comp} \geq \frac{Q_{EL} \cdot \eta_{EL}}{\eta_{EL} \cdot \frac{\omega_{comp}}{LHV_{H2}} + 1} \cdot \frac{\omega_{comp}}{LHV_{H2}} \tag{49}$$

The compressor CAPEX is estimated to be 1600 EUR/KW_e, as reported in [35]. Additionally, the OPEX is assumed to be 1 % of the CAPEX, based on findings presented in the same source [35].

The compressor's lifetime is expected to be 25 years, as indicated in [35].

The compressor energy consumption is 3.8 MJ/Kg_{H2}, as reported in [52]. The compressor is designed to handle an input pressure of 3 MPa, as specified in [125], which is compatible with the pressure output of the electrolyzer. Furthermore, it is capable of delivering hydrogen at an output pressure of up to 35 MPa, as mentioned in the same source [125].

The compressor capacity factor is assumed to be up to 90% of its capacity.

Table 29: Compressor parameters and assumptions.

Parameter	Value	Unit	Source
Compressor capacity	75	KW	*assumption*
Compressor CAPEX	1 600	EUR/KW_e	[35]
Compressor OPEX	1	% of CAPEX	[35]
Compressor lifetime	25	years	[35]
Compressor energy consumption	3.8	MJ/Kg_{H2}	[52]
Compressor input pressure	3	MPa	[125]
Compressor output pressure	up to 35	MPa	[125]
Compressor capacity factor	up to 90	% of capacity	*assumption*

4.3.3 Hydrogen Tank

Table 30 provides a comprehensive overview of the parameters and assumptions related to the hydrogen tank.

The tank capacity is assumed to be 20 MW/LHV_{H2}, representing the amount of hydrogen that can be stored in the tank based on its LHV.

The tank CAPEX is estimated to be 150 EUR/KWh_{LHV}, as cited in [35]. Additionally, the OPEX is assumed to be 1 % of the CAPEX, based on findings presented in [36]. These parameters contribute to the economic analysis and assessment of the tank's cost implications within the hydrogen production system.

The tank's lifetime is expected to be 25 years, as indicated in [36]. Furthermore, the tank discharge rate is assumed to be negligible, as reported in [36]. This assumption implies that any leakage or discharge from the tank is insignificant and can be disregarded for the purposes of the analysis conducted in this study.

The tank pressure is specified as 20 MPa, as mentioned in [36]. This parameter indicates the pressure level at which the hydrogen is stored within the tank.

For the analysis conducted in this thesis, the tank's initial state of charge (SOC) is assumed to be up to 90 % of its capacity. Additionally, the minimum SOC is assumed to be 0 %, indicating that the tank can

be completely discharged if necessary.

Table 30: Hydrogen tank parameters and assumptions.

Parameter	Value	Unit	Source
Tank capacity	20	$MWh_{LHV\ H2}$	*assumption*
Tank CAPEX	15	$EUR/KWh_{LHV\ H2}$	[35]
Tank OPEX	1	% of CAPEX	[36]
Tank lifetime	25	years	[36]
Tank discharge rate	negligible leakage	-	[36]
Tank pressure	20	MPa	[36]
Tank initial SOC	up to 90	% of capacity	*assumption*
Tank minimum SOC	0	% of capacity	*assumption*

4.3.4 Fuel Cell

Table 31 presents the parameters and assumptions relevant to the PEM fuel cell, which play a crucial role in the analysis conducted in this thesis.

The fuel cell capacity is assumed to be 0.650 MW. The fuel cell CAPEX is estimated to be 3000 EUR/KW_e, as reported in [36]. Furthermore, the recurring expenditure (REPEX) and OPEX are assumed to be 21% and 2% of the CAPEX, respectively, based on findings presented in the same source [36]. These parameters contribute to the economic analysis and assessment of the fuel cell system's cost implications.

Furthermore, the fuel cell stack lifetime is reported as 25 000 hours, as indicated in [61].

Additionally, To ensure stable operation, a minimum load of 20 % of the fuel cell's capacity is assumed, as stated in [36]. This assumption guarantees that the fuel cell operates within a suitable operating range and avoids unstable or inefficient performance. The fuel cell capacity factor is assumed to be 90 % of its capacity, representing the ratio of actual power output to the maximum possible power output. This assumption is made for the analysis conducted in this thesis to account for any potential operational variations.

Besides this, the fuel cell efficiency is reported as 50 % of its capacity, as specified in [36].

The fuel cell operates at an operating pressure of 3 MPa, as mentioned in [49]. To ensure a stable pressure connection between the hydrogen tank and the fuel cell, it is imperative to incorporate a pressure-reducing valve due to the pressure disparity between the two components [126]. This valve acts as a regulatory mechanism to reduce the pressure from the tank to a level suitable for the fuel cell, thereby facilitating a stable and optimal operating condition [126].

Considering potential degradation over time, this thesis assumes a minimum degradation factor of 10% is assumed, representing a 90% decrease in the performance of the fuel cell.

Table 31 provides a comprehensive overview of the parameters and assumptions related to the PEM fuel cell, serving as a fundamental reference for the analysis and discussion presented in the thesis. The information presented in the table contributes to the evaluation and understanding of the fuel cell's role and performance within the hydrogen-based energy system under investigation.

Fig. 19 illustrates the progressive degradation of a fuel cell system over a period of 20 years, as analyzed in this study. Upon reaching the maximum degradation factor, the degradation process is reset to its initial state, denoted as 1. Moreover, the model incorporates replacement costs, referred to as REPEX costs, which account for the expenses associated with replacing the fuel cell system. Examining the Figure, it becomes evident that the fuel cell system will incur replacement costs at specific time intervals throughout the 20-year duration of the analysis. Specifically, these replacement costs occur in the following years: 3, 6, 8, 11, 13, 16, and 18.

Table 31: PEM fuel cell parameters and assumptions.

Parameter	Value	Unit	Source
Fuel cell capacity	0.650	MW	*assumption*
Fuel cell CAPEX	3 000	EUR/KW_e	[36]
Fuel cell REPEX	21	% of CAPEX	[36]
Fuel cell OPEX	2	% of CAPEX	[36]
Fuel cell stack lifetime	25 000	hours	[61]
Fuel cell minimum load	20	% of capacity	[36]
Fuel cell capacity factor	90	% of capacity	*assumption*
Fuel cell efficiency	50	% of capacity	[36]
Fuel cell operating pressure	3	MPa	[49]
Minimum degradation factor	10	% of capacity	*assumption*

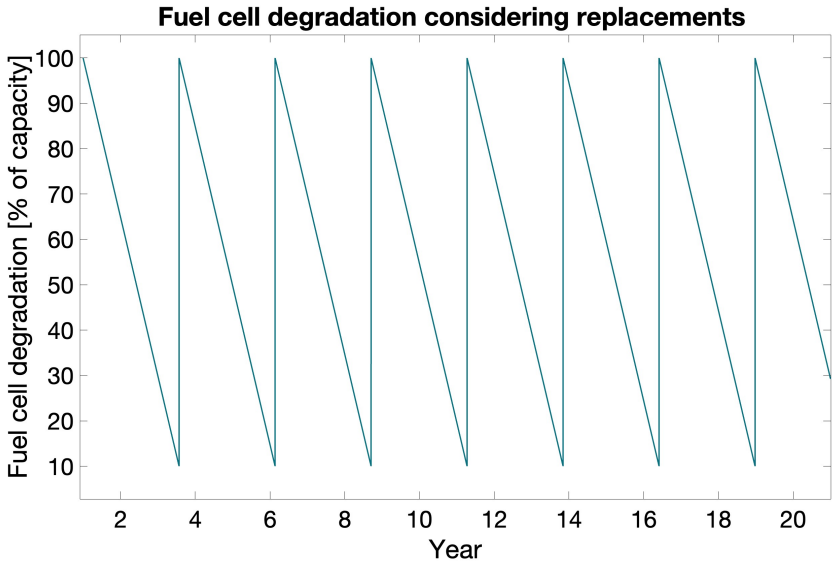

Figure 19: Fuel cell linear degradation, considering replacements and minimum degradation factor

4.4 Future Scenario Inputs

During the analysis of Future Scenarios, a consistent methodology was employed with the exception that the focus shifted to the year 2030. Noteworthy variations were observed in the costs and technical parameters of PEM fuel cell and electrolyzer, as well as market prices. Regarding market prices, it was assumed that prices from the Day-ahead SM would be considered starting from 2030 onwards, exhibiting an annual increase rate of 3.8 %. This rate corresponds to the same increase observed between 2025 and 2026. With respect to the prices of up and down FCR-D, given the expectation of price stagnation, identical values were assumed throughout the 20-year analysis period.

The optimization model is significantly influenced by certain parameters that are expected to substantially change in the future. Specifically, the CAPEX costs, lifetime, and efficiency of the electrolyzer and fuel cell, as discussed in Section 2.4.1, which are succinctly summarized in Table 32. Furthermore, the decrease in the CAPEX of the VRES was also considered, as described in Fig. 33.

Table 32: CAPEX costs, lifetime and efficiency of PEM fuel cell and electrolyzer in the Future scenarios.

	PEM electrolyzer	**PEM fuel cell**	**Source**
Efficiency [%]	76	70	[34, 97]
Lifetime [hours]	100 000	40 000	[34, 62]
CAPEX [EUR/KW_e]	823	523	[95, 34]

Table 33: CAPEX costs of solar PV and onshore wind power plants in the Future Scenario.

	Solar PV	**Oshore Wind**	**Source**
CAPEX [EUR/KW_e]	400	494	[98, 99]

5 Results and Discussion

In this Section, the main results are presented considering the Case Study and Methodology outlined in the previous Chapters. Firstly, the Present Scenarios' results are described and discussed, which includes six distinct scenarios. These scenarios comprise the integration of solar and wind energy, with an additional scenario without any renewable energy sources. Each scenario will be discussed both with and without the provision of frequency regulation services.

Following the analysis of the Present Scenarios, two Future Scenarios will be examined. One scenario involves the use of solar energy as a renewable energy source, incorporating the provision of frequency regulation services. The other scenario uses wind energy as the renewable energy source, also including frequency regulation.

Furthermore, a sensitivity analysis will be conducted to evaluate the influence of various factors such as P2P CAPEX, P2P size, market prices, and discount rates on the results.

Finally, a comprehensive discussion will be carried out based on the outcomes presented in this section.

5.1 Present Scenarios Results

The purpose of this investigation is to assess the performance and implications of various scenarios, considering the presence of renewable energy sources and participation in the Frequency Regulation Markets. By comparing and contrasting these scenarios, a comprehensive understanding of their technical and economic indicators and associated benefits can be obtained.

Table 34 provides a comparison of technical indicators for the different scenarios, as explained in Section 3.4.1, comparing the impact of participating in the Frequency Regulation Market and also the renewable energy source included.

The results show that, if wind energy is included, the shutdown occurrences for both electrolyzers and fuel cells are significantly reduced when frequency regulation is included. Similarly, the fuel cell shutdowns also decrease for all scenarios when the system provides frequency regulation. However, the electrolyzer shutdowns increase, when participating in the Frequency Regulation Markets, if solar or no renewable sources are considered. Comparing the scenarios with solar, wind, and without renewable sources, it is evident that including renewable energy sources leads to a higher number of shutdowns for both the electrolyzer and fuel cell, in all cases, this is mainly due to the variable profile of these renewable energy sources. The number of fuel cell and electrolyzer shutdowns is relevant to analyze because fewer shutdowns enhance the system stability and decrease the degradation of these components [73, 74].

The impact of participating in the Frequency Regulation Markets in the operating hours of electrolyzers and fuel cells differs depending on the renewable source considered. For example, if wind is selected or a renewable energy source is not included, both the operating hours of the electrolyzer and fuel cell decrease if the system participates in the Frequency Regulation Market. On the other hand, participating in the Frequency Regulation Market increases the operating hours of both components. Notably, the operating hours of the electrolyzer and fuel cell are highest in the scenario with solar energy, and the least hours of operation occur when renewable sources are not included.

The percentage of renewable energy injected into the grid is substantially higher in the scenarios that include frequency regulation, this is mainly due to the monetary compensation that comes with the provision of down-regulation. The results indicate that solar and wind energy sources achieve nearly 100 % energy injection in the grid, highlighting that nearly none of the renewable electricity is provided to the electrolyzer. This occurs because, by injecting electricity into the grid, the renewable energy source can participate in the Frequency Regulation Market, this way the system can leverage the potential revenue streams associated with down-regulation and electricity sales in the Day-ahead SM, which is more beneficial than charging the electrolyzer, since the model takes advantage of periods when the Day-ahead SM purchase prices are relatively inexpensive, allowing for cost-effective electrolyzer charging, maximizing

the utilization of available renewable electricity.

The bids in up-regulation and down-regulation depend on the availability of renewable energy sources, with the scenario involving wind energy allowing higher bids for regulation purposes, due to its higher energy availability.

Energy transactions in the Day-ahead Spot Market reflect the dynamics of the energy market and the impact of including frequency regulation and renewable energy sources. The scenarios with frequency regulation involve higher energy sales and purchases compared to the excluded scenarios, due to the economic benefit of having more revenue streams from the Frequency Regulation Markets. Naturally, the scenarios without renewable energy do sell as much energy in the Day-ahead SM, due to the lack of energy availability from those sources.

The total hydrogen production is consistently higher in the scenarios with renewable energy sources compared to the scenario without renewable energy. Both solar and wind energy sources contribute to increased hydrogen production, emphasizing their potential for green hydrogen generation. Notably, among the three options considered, wind energy exhibits the highest availability, followed by solar energy. Consequently, the increased availability of wind energy facilitates a greater production of hydrogen, consequently enabling the fuel cell to generate a larger quantity of electricity for injection into the grid.

Overall system efficiency remains relatively high when renewable energy sources are included. While the scenarios with frequency regulation generally exhibit slightly higher efficiencies, the difference is not substantial. This suggests that including renewable energy sources alone has an extreme impact on the overall system efficiency, and the presence of frequency regulation further enhances the system's stability without compromising efficiency.

In conclusion, the presented results highlight the technical advantages of including frequency regulation and utilizing renewable energy sources, in the studied system. The inclusion of frequency regulation promotes renewable energy integration, stimulates market activity, boosts hydrogen production, and maintains overall system efficiency.

Table 34: Technical indicators of each scenario

Frequency regulation	**Included**			**Excluded**		
Renewable source	**Solar**	**Wind**	**Without**	**Solar**	**Wind**	**Without**
Electrolyzers shutdowns [-]	9 606	4 953	3 945	8 081	6 296	3 808
Fuel cell shutdowns [-]	5 346	5 288	5 226	6 309	7 272	5 888
Electrolyzer operating hours [kh]	27.4	23.2	20.0	26.6	32.0	19.0
Fuel cell operating hours [kh]	32.2	32.0	31.7	32.0	40.1	29.3
% renewable energy injected to the grid	99.8	99.8	-	95.7	91.5	-
Bids in up-regulation [GW]	74.5	74.2	74.8	-	-	-
Bids in down-regulation [GW]	495.3	623.8	246.8	-	-	-
Sales in the Day-ahead SM[GWh]	258.0	386.2	9.60	247.5	357.0	8.7
Purchases in the Day-ahead SM[GWh]	27.9	27.5	28.0	17.4	4.71	25.3
Total H_2 produced [t]	584.2	581.5	575.1	571.3	720.57	520.2
Overall system efficiency [%]	93.2	95.4	34.2	93.0	93.5	34.2

Furthermore, Table 35 provides a comprehensive overview of the economic indicators associated with each scenario under consideration. As explained in Section 3.4.2, these economic indicators include initial investment, NPV, ROI, IRR, payback period, and LCOE.

The economic analysis conducted in this thesis employed a discount rate of 5 % to evaluate the financial viability of the considered scenarios [127]. The selection of this discount rate, lower than higher rates such as 7 % [127] or 8 % [35], was driven by the objective of obtaining positive economic indicators that

would facilitate meaningful comparisons among the scenarios [127]. The choice of a discount rate is crucial in economic analyses as it reflects the opportunity cost of capital and accounts for the time value of money. A higher discount rate corresponds to a higher level of risk associated with the investment, as it represents a higher minimum acceptable rate of return [127]. In contrast, a lower discount rate implies a relatively less risky economic environment. By utilizing a discount rate of 5 %, the analysis aimed to present more favorable economic indicators, thereby enabling effective comparison among the scenarios.

The initial investment represents the capital expenditure required for implementing each scenario. It is evident from the Table that the initial investment varies across the scenarios, ranging from 6 426 kEUR to 21 246 kEUR. These differences are attributed to the selection of the renewable source.

The NPV indicates the financial value generated over the project's lifetime, taking into account the initial investment and cash flows. Positive NPV values, observed when renewable energy sources and Frequency Regulation Markets are included, suggest favorable economic outcomes. Specifically, the best NPV is obtained when wind is included as the renewable energy source. On the other hand, the scenarios that exclude renewable sources and frequency regulation exhibit negative NPV values, indicating potential financial losses.

The ROI measures the profitability of the investment and is expressed as a percentage. In Table 35, including frequency regulation and renewable sources lead to ROI values ranging from 15.6. % to 22.4 %, indicating relatively positive returns on investment. In contrast, the other scenarios exhibit considerably negative ROI values. These results emphasize the potential financial risks associated with non-participation in frequency regulation and not including renewable sources.

The internal rate of return (IRR) provides an estimate of the project's profitability by calculating the discount rate that equates the present value of cash inflows with the present value of cash outflows. Positive IRR values indicate potential profitability, while negative values suggest potential financial losses. The included frequency regulation scenarios demonstrate positive IRR values, ranging from 0.068 to 0.076. Conversely, the scenarios that exclude frequency regulation and renewable sources show negative IRR values, further highlighting the potential financial risks associated with non-participation in frequency regulation.

The payback period represents the time required for the initial investment to be recovered through cash inflows. Notably, the Table indicates "NO" for the payback period in certain scenarios, implying that the initial investment is not fully recovered within the project's duration. The only scenarios that have a payback period within the 20 years period of analysis are the scenarios that include frequency regulation and a renewable energy source.

The LCOE provides insights into the average cost of generating each megawatt-hour (MWh) of electricity over the project's lifetime. In Table 35, the renewable sources together with frequency regulation scenarios exhibit LCOE values ranging from 106.3 EUR/MWh to 129.2 EUR/MWh, suggesting relatively competitive electricity generation costs. In contrast, the excluded scenarios display higher LCOE values, indicating increased electricity generation costs, particularly in the absence of frequency regulation.

In summary, the economic indicators presented in Table 35 describe the financial performance and viability of each scenario. The inclusion of renewable energy sources and participation in the frequency regulation scenarios demonstrate more favorable economic outcomes, as reflected by positive NPV and ROI values. Conversely, the scenarios where they are excluded, indicate potential financial losses, as evidenced by negative NPV and ROI values. Additionally, the LCOE values provide insights into the relative cost competitiveness of electricity generation across the scenarios. These findings contributed to the understanding of the economic implications and trade-offs associated with the different renewable source options and the inclusion or exclusion of frequency regulation.

Therefore, this Section will focus on the in-depth analysis of these two specific scenarios, namely the scenario incorporating solar PV and participation in the Frequency Regulation Market, and the scenario involving wind and participation in the Frequency Regulation Market. The technical and economic find-

ings of these selected scenarios are presented and visualized in Fig. 20 to 30b. These Figures offer a comprehensive depiction of the energy flows, market bids, revenue streams, and system performance. The decision to concentrate on these specific results stems from their relevance in the context of the study's objectives and research questions.

Table 35: Economic indicators of each scenario

Frequency regulation	**Included**			**Excluded**		
Renewable source	**Solar**	**Wind**	**Without**	**Solar**	**Wind**	**Without**
Initial Investment [kEUR]	16 026	21 246	6 426	16 026	21 246	6 426
NPV [kEUR]	2 506	4 751	-3 586	-11 619	-12 156	-11 763
ROI [%]	15.6	22.4	-55.8	-72.5	-57.2	-183.1
IRR [-]	0.068	0.076	-0.039	-0.070	-0.039	-0.77
Payback period [years]	18	16	NO	NO	NO	NO
LCOE [EUR/MWh]	129.2	106.3	1722.0	133.9	113.2	2 059.2

Fig. 20 provides an overview of the annual energy flows within the two analyzed scenarios. Upon closer examination, one conclusion from this analysis is that the contribution of renewable energy to the electrolyzer is minimal in both cases. This outcome can be attributed to the economic advantage of selling electricity generated from renewable sources to the grid, rather than utilizing it to charge the electrolyzer. Furthermore, it is worth noting that the Wind Scenario exhibits a greater availability of energy, resulting in a higher proportion of energy being injected into the grid from the renewable source. However, in terms of the energy flows between the fuel cell and the grid, as well as between the grid and the electrolyzer, similarities can be observed across both scenarios. These energy flows are predominantly influenced by market prices, rather than the availability of renewable resources.

In Fig. 21, the annual down-regulation bids are represented using negative values, so that it is easier to compare the participation in up and down-regulation by each component. One evident difference is that, as a consequence of the higher energy available to provide to the grid, the Wind Scenario has more energy available for down-regulation. Besides that, every year, for both scenarios, the capacity reserved for down-regulation is much higher than for up-regulation, this is a consequence of the nature of the assets and market characteristics.

In Fig. 21, the annual down-regulation bids are depicted using negative values to facilitate the comparison of participation in up and down-regulation across each component. A notable distinction is observed, wherein the Wind Scenario, due to its greater energy availability, these scenarios exhibit a higher amount of energy allocated for down-regulation. Additionally, in both scenarios, the capacity reserved for down-regulation is consistently higher than the reserved for up-regulation, on an annual basis. The prominence of down-regulation capacity allocation aligns with the nature of the assets and the market characteristics. It suggests that the system is designed to ensure a surplus of capacity available for decreasing the injected electricity into the grid, as opposed to increasing it. This characteristic of the system can be attributed to the superior availability and efficiency of the renewable energy component compared to the fuel cell and electrolyzer. The renewable energy source has greater installed capacity and operational efficiency, enabling it to generate a surplus of electricity that can be curtailed or reduced during periods of excess supply.

Fig. 22 illustrates the energy bids in the Day-ahead SM, where negative values represent purchased bids and positive values denote selling bids. Consistent with previous discussions, the down-regulation bids of the fuel cell and renewable source exhibit a direct relationship with the selling bids in the Day-ahead market. Consequently, the energy-selling bids consistently surpass the energy purchased from the grid for electrolyzer charging purposes each year. As a result, the selling bids in the market exceed the energy acquired from the grid for electrolyzer charging, emphasizing the system's inclination towards maximizing economic gains and capitalizing on surplus electricity generation from the renewable source and the fuel cell's down-regulation capabilities.

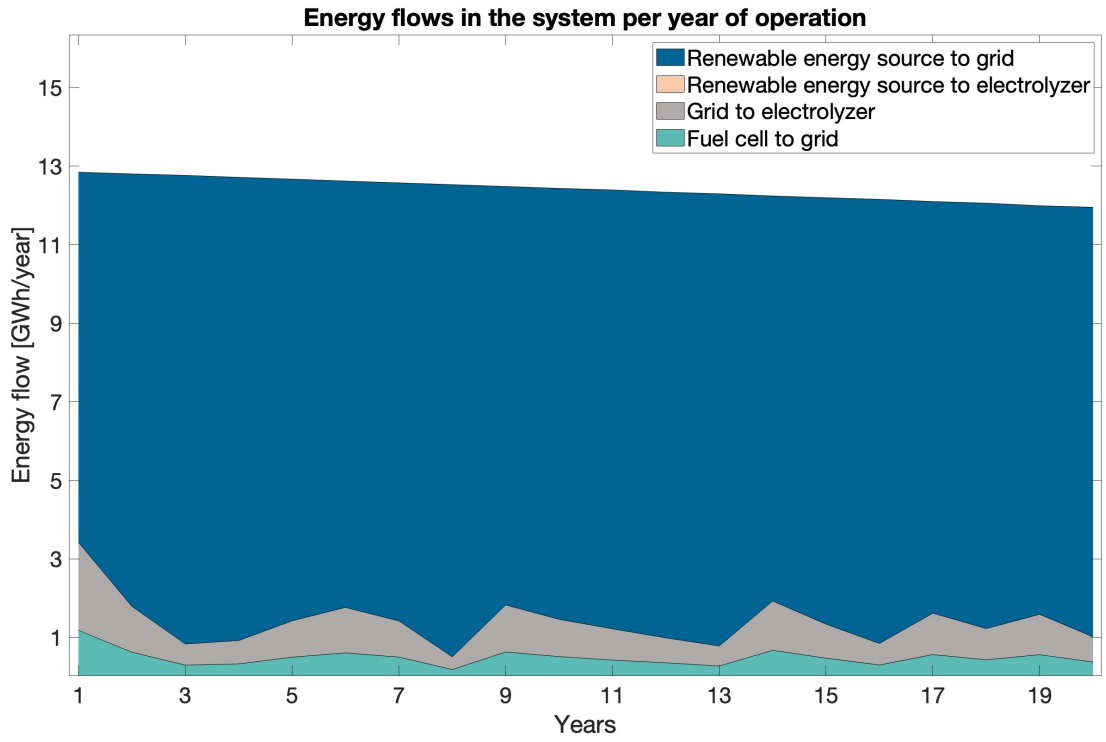

(a) Solar PV as the renewable energy source

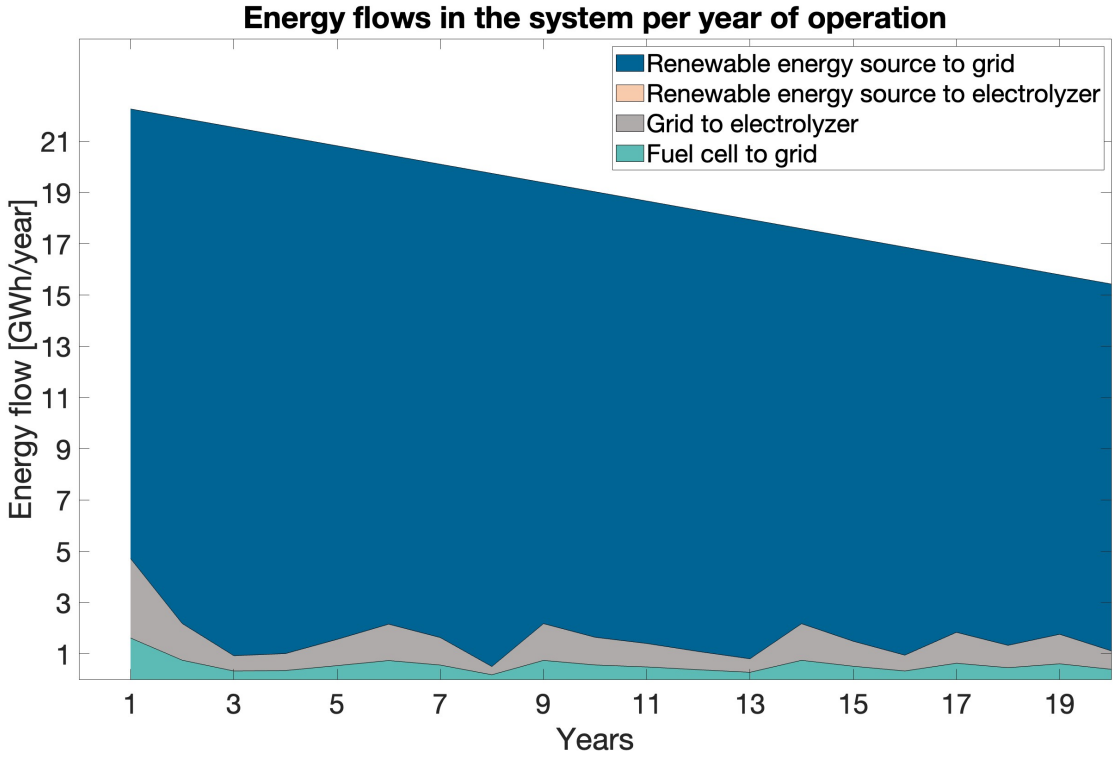

(b) Onshore Wind as the renewable energy source

Figure 20: Energy flows in the system per year, for each renewable source configuration

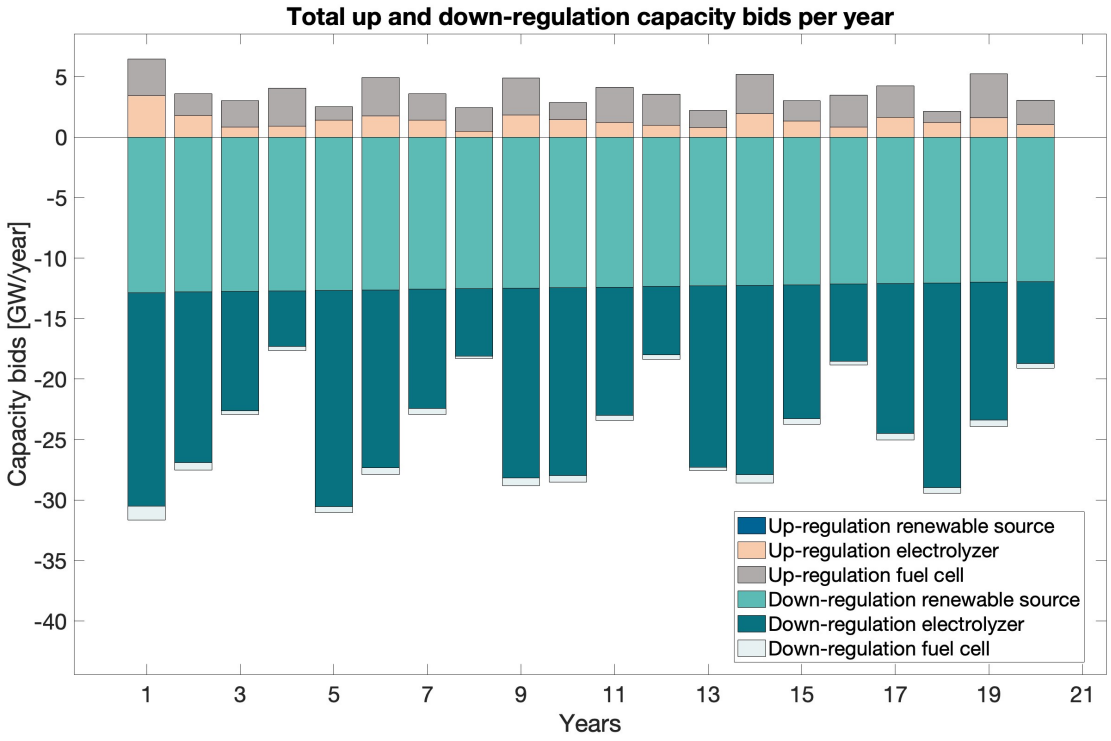

(a) Solar PV as the renewable energy source

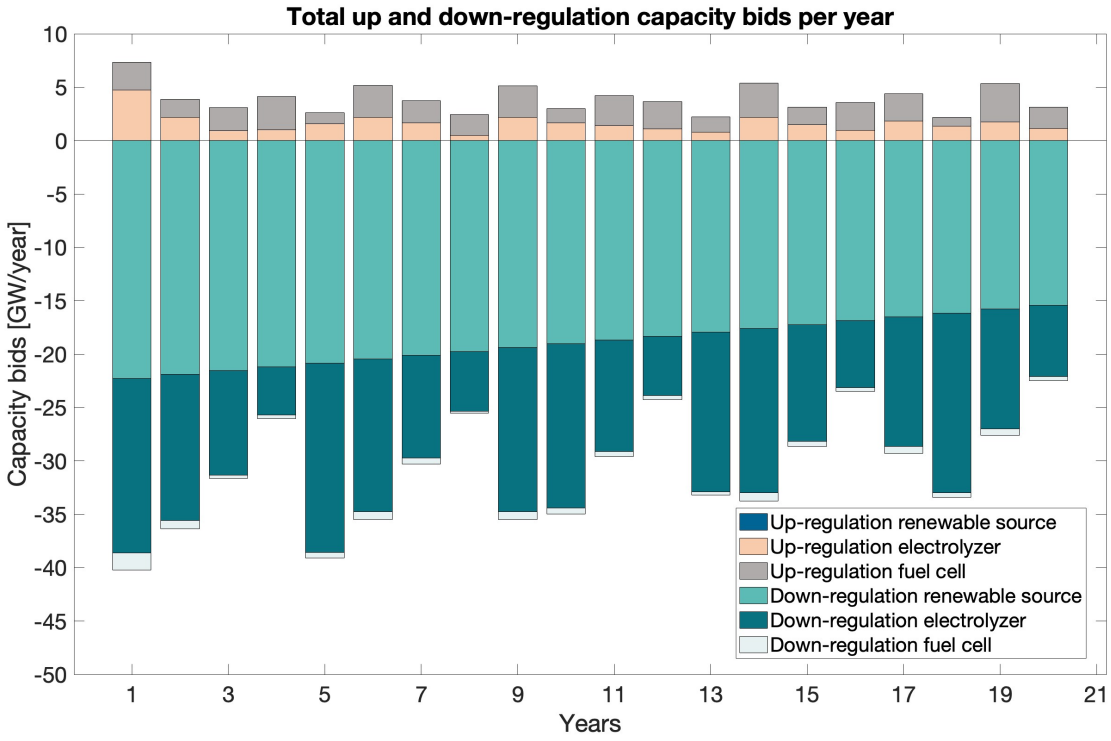

(b) Onshore Wind as the renewable energy source

Figure 21: System components' capacity bids in the up and down-regulation frequency markets, per year, for each renewable source configuration.

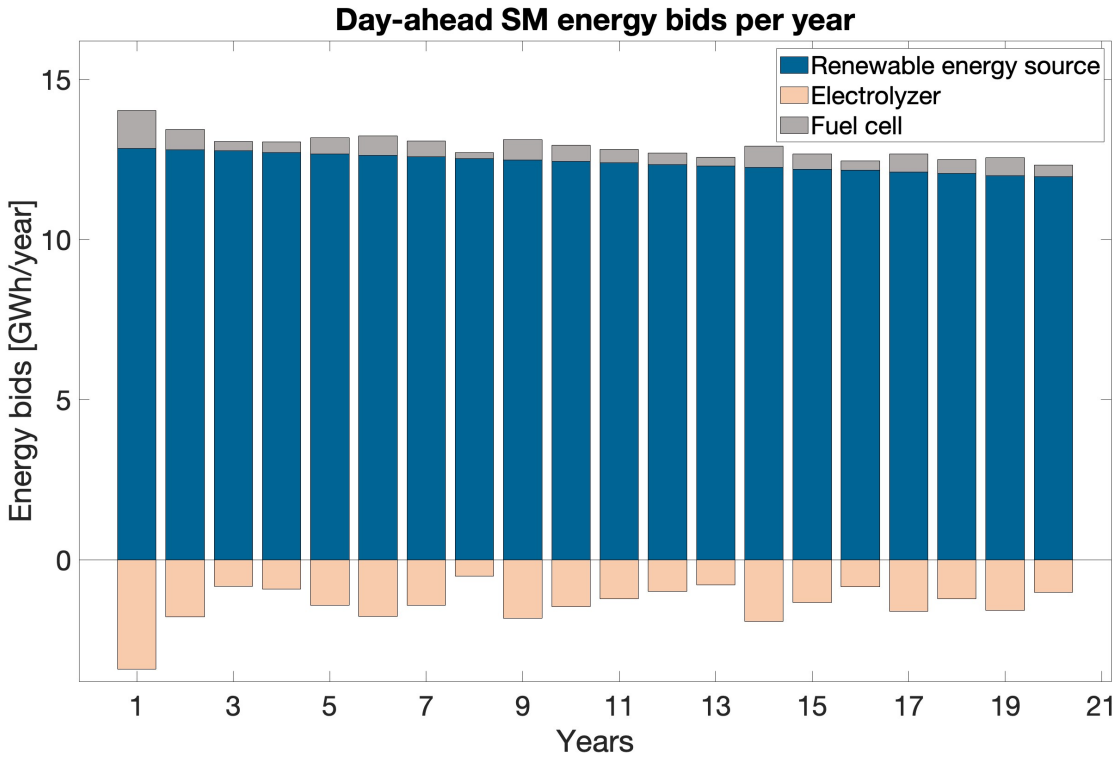

(a) Solar PV as the renewable energy source

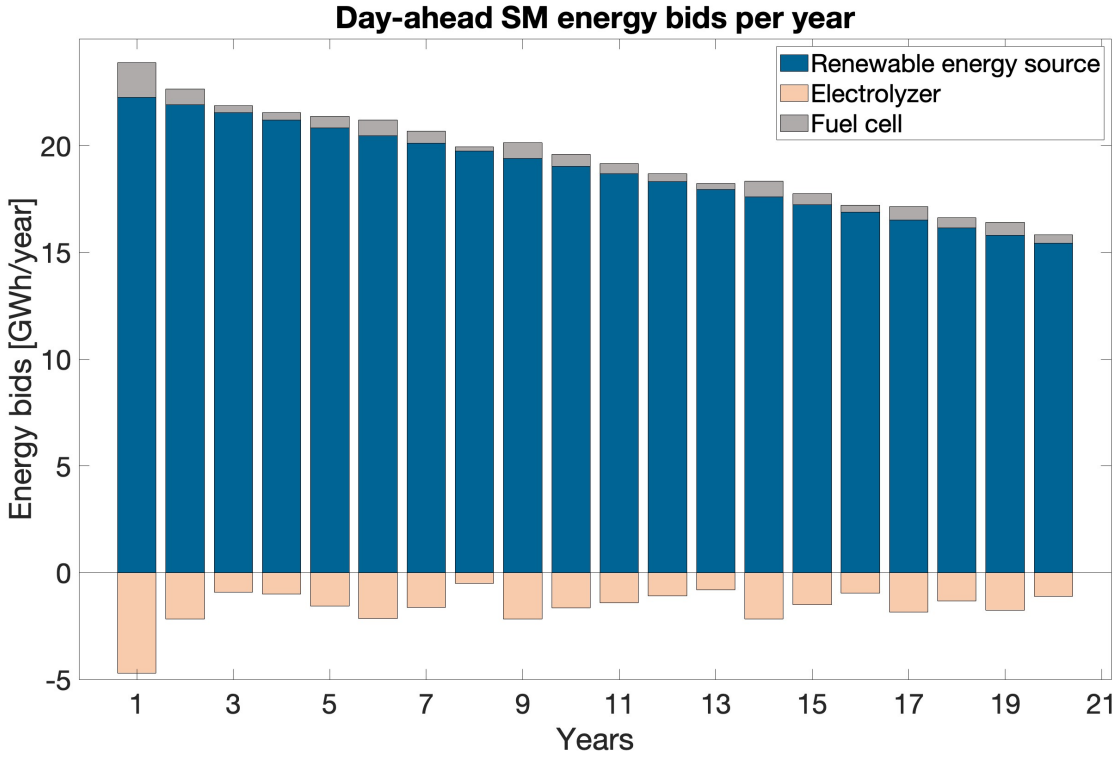

(b) Onshore Wind as the renewable energy source

Figure 22: System components' energy bids in the Day-ahead SM, per year, for each renewable source configuration.

Fig. 23 presents the annual revenues of the system, excluding the investment costs (CAPEX) that are accounted for in year 0. It should be noted that the analysis assumes the system starts operations in year 1. The OPEX costs remain constant throughout the years, while the REPEX costs occur whenever the fuel cell or the electrolyzer reaches their maximum degradation factor, and need to be replaced.

Upon analyzing the revenue distribution, it becomes evident that the majority of positive cash flows are derived from participation in the down-regulation frequency market. This is followed by revenue from the sales in the Day-ahead SM and, finally, up-regulation provision. In contrast, the costs associated with purchasing electricity from the Day-ahead SM are relatively lower compared to other cash flows, except in the first year. In the initial year, the prices in the Day-ahead SM are at their highest, resulting in higher electricity purchasing costs. However, it is important to note that the revenue from selling electricity is also higher in the first year, thereby compensating for the elevated purchasing costs.

Moreover, it is important to acknowledge that the revenue stream is influenced by various factors, such as market conditions, bid strategies, and the availability of renewable energy sources. The presented revenues come from the specific optimization model developed during this thesis, which reflects the system's ability to capitalize on favorable market prices and the efficient utilization of energy resources, further contributing to the overall economic viability of the system.

The findings shown in Fig. 24 reveal that in both scenarios, the primary source of revenue is derived from the renewable source, accompanied by participation in the down-regulation market. Conversely, the fuel cell component has the least influence on the overall revenue generation, while the up-regulation market yields the lowest revenue among the examined components.

These outcomes highlight the significance of the renewable source as a crucial revenue generator within the system. This can be attributed to its ability to produce and inject renewable electricity into the grid, allowing for substantial financial gains. Furthermore, participation in the down-regulation market enhances revenue opportunities by providing additional compensation for the system's flexibility and capacity to reduce electricity supply during periods of excess generation.

On the other hand, the fuel cell component's contribution to the overall revenue is relatively modest. This can be attributed to factors such as its low efficiency in producing hydrogen and converting it into electricity, compared to the generation of renewable energy.

Overall, these findings emphasize the economic significance of the renewable source and the down-regulation market in maximizing revenue generation within the system. By prioritizing these aspects, system operators can enhance the financial performance and overall viability of the studied scenarios.

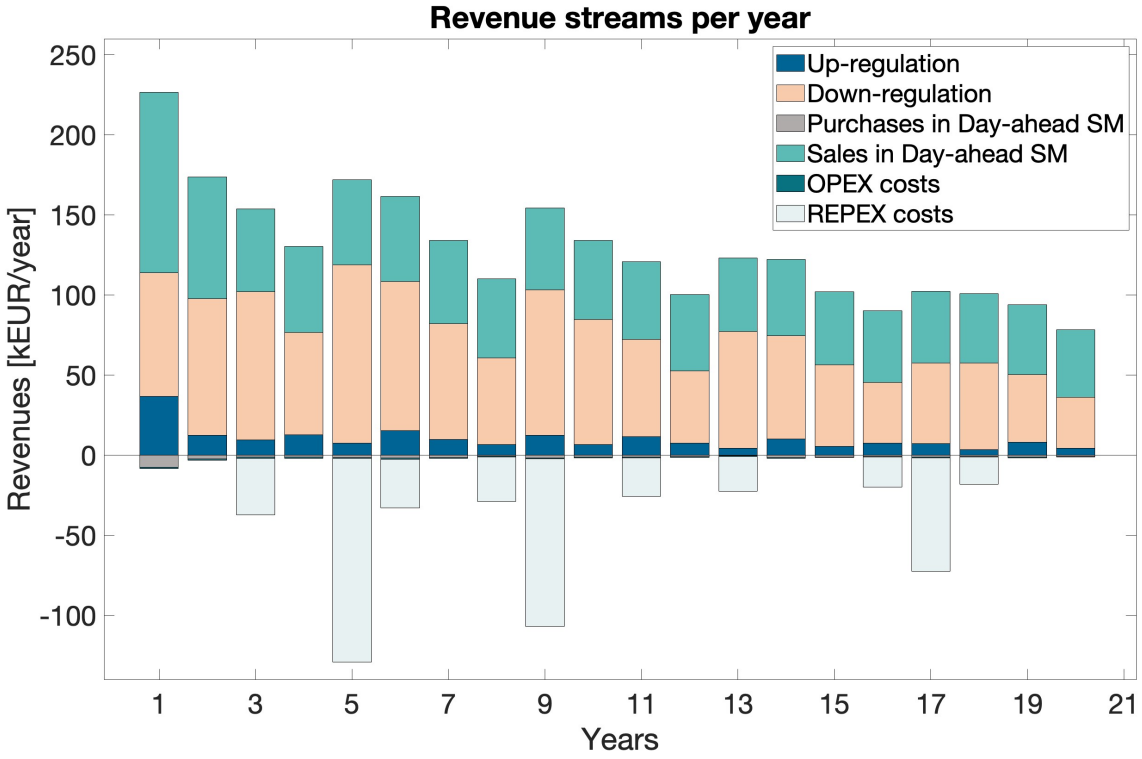

(a) Solar PV as the renewable energy source

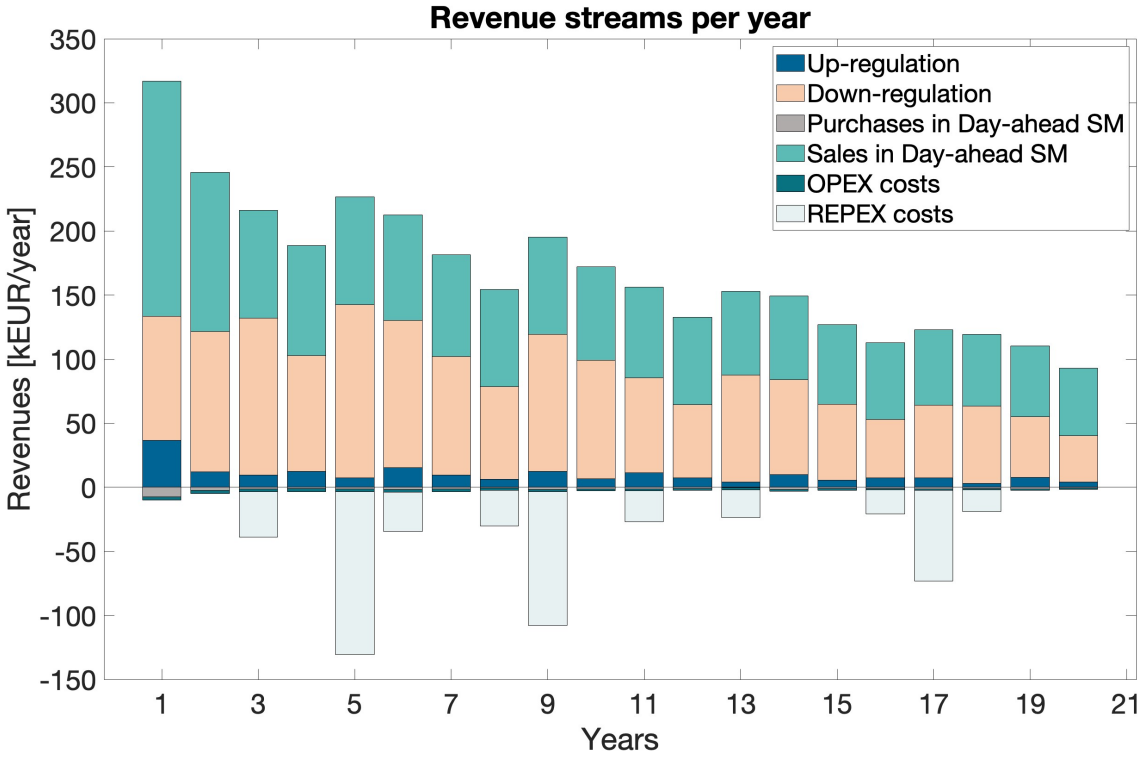

(b) Onshore Wind as the renewable energy source

Figure 23: Annual revenue streams of the system

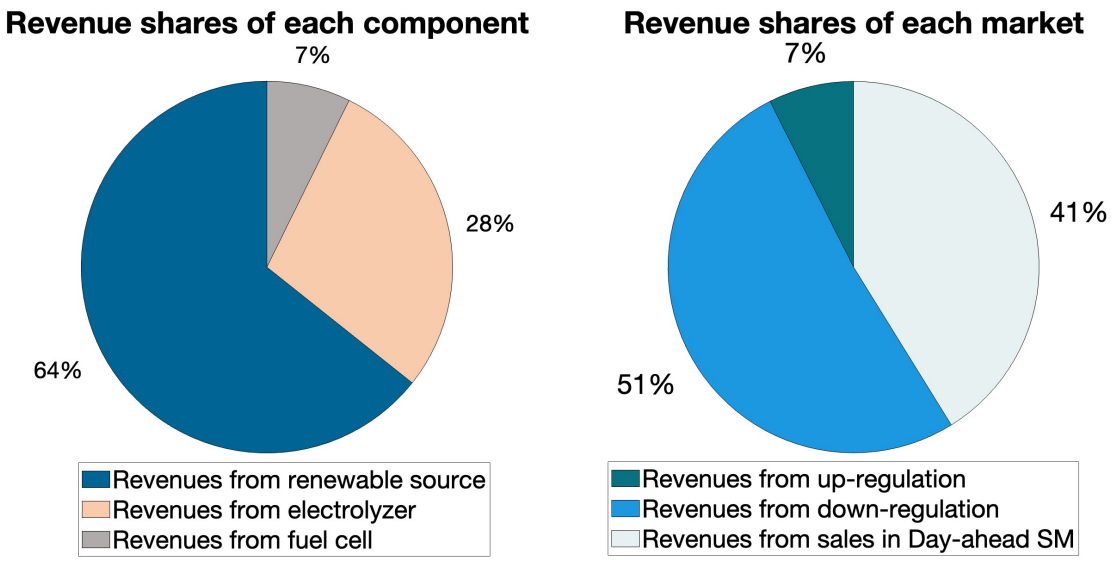

(a) Solar PV as the renewable energy source

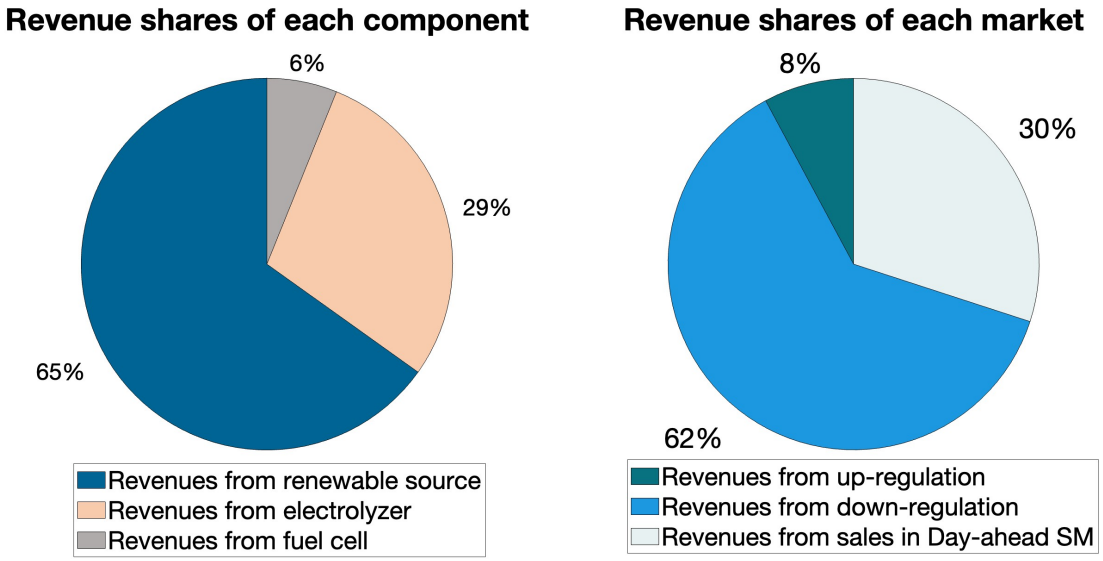

(b) Onshore Wind as the renewable energy source

Figure 24: Revenue share of each system's components and market, for both renewable energy source configuration

5.2 Future Scenarios Results

In this Section, an analysis is conducted on the Future Scenarios, as defined in Section 4.4. These scenarios involve modifications to the CAPEX of the renewable source, electrolyzer, and fuel cell, as indicated in Tables 32 and 33. Consequently, adjustments are made to the OPEX and REPEX, as these are typically represented as a percentage of the corresponding CAPEX values. Additionally, the lifetime and efficiency characteristics of the fuel cell and electrolyzer are appropriately altered, as outlined in Table 32.

Table 36 presents the technical indicators for the selected future scenarios and their variance compared to the values of the present scenarios.

The number of shutdowns for electrolyzers is observed to increase by 6.0% in the Solar Scenario and by 15% in the Wind Scenario, indicating a higher occurrence of shutdown events. Similarly, the number of fuel cell shutdowns shows a substantial increase of 24.1% in the Solar Scenario and 24.9% in the Wind Scenario compared to the present scenario, suggesting a higher frequency of shutdowns for fuel cells.

In terms of operating hours, both the solar and Wind Scenarios exhibit an increase. The Solar Scenario experiences a significant increase of 13.1% in electrolyzer operating hours and a substantial growth of 46.6% in fuel cell operating hours. The Wind Scenario demonstrates a more considerable increase in both electrolyzer and fuel cell operating hours, with growth rates of 18.1% and 49.4%, respectively.

The percentage of renewable energy injected into the grid remains relatively stable, with a marginal decrease of 0.2% in the Solar Scenario and a minor decrease of 0.1% in the Wind Scenario compared to the present scenario.

In the up-regulation market, both scenarios display a decline in bids. The Solar Scenario shows a reduction of 14.9%, while the Wind Scenario exhibits a larger decrease of 16.2%. Similarly, in the down-regulation market, there is a decrease in bids of 7.0% for the Solar Scenario and 5.6% for the Wind Scenario.

Energy transactions in the Day-ahead SM demonstrate slight variations. The Solar Scenario shows a small increase of 1.3% in energy sold, while the Wind Scenario displays a modest increase of 0.6%. Conversely, the energy purchased from the Day-ahead SM experiences a decrease of 9.7% in the Solar Scenario and a more substantial decrease of 12.4% in the Wind Scenario compared to the present scenario.

The total hydrogen (H2) produced remains relatively unchanged in both scenarios, with a minimal variation of approximately 0% in the Solar Scenario and a slight increase of 1.9% in the Wind Scenario compared to the present scenario.

In terms of overall system efficiency, both scenarios show improvements. The Solar Scenario demonstrates an increase of 2.4%, while the Wind Scenario exhibits a slightly lower increase of 1.5%.

The findings from this Table indicate that the selected future scenarios present changes in various technical indicators compared to the present scenario. These changes suggest potential shifts in system performance. For example, the fuel cell is activated more often, which contributes to an increase in the energy sold in the Day-ahead SM. Despite the fact of the electrolyzer is more activated in the future scenario, the hydrogen production does not increase significantly, meaning that the electrolyzer is not activated at full capacity, and it is being charged using electricity from a renewable source since the energy purchases in the Day-ahead SM decreased.

Table 36: Technical indicators for the selected Future Scenarios and their relative difference normalized by the Present Scenarios values.

Scenario	Solar	Difference [%]	Wind	Difference [%]
Electrolyzers shutdowns [-]	10180	6.0	5695	15
Fuel cell shutdowns [-]	6634	24.1	6607	24.9
Electrolyzer operating hours [kh]	31.0	13.1	27.4	18.1
Fuel cell operating hours [kh]	47.2	46.6	47.8	49.4
% renewable energy injected to the grid [%]	99.6	-0.2	99.7	-0.1
Bids in up-regulation [GW]	63.4	-14.9	62.2	-16.2
Bids in down-regulation [GW]	460.5	-7.0	588.8	-5.6
Energy sold in the Day-ahead SM[GWh]	261.4	1.3	388.6	0.6
Energy purchased in the Day-ahead SM[GWh]	25.2	-9.7	24.1	-12.4
Total H_2 produced [t]	584.4	0	592.6	1.9
Overall system efficiency [%]	95.4	2.4	96.8	1.5

Table 37 presents the economic indicators for the selected future scenarios and their variance compared to the values of the present scenarios.

The initial investment required for the Solar Scenario is significantly lower, showing a decrease of 49.8 % compared to the present scenario, this is due to the decreases in the CAPEX of the system components. Similarly, the Wind Scenario exhibits a substantial reduction of 56.8 % in the initial investment. These findings suggest that future scenarios offer cost advantages in terms of the upfront investment required for renewable energy sources.

The NPV shows a significant increase in both scenarios, indicating a positive economic impact. The Wind Scenario experiences a substantial growth of 440.8 % in NPV, while the Solar Scenario shows an even larger increase of 614.6 %. These results suggest that the future scenarios yield higher economic returns compared to the present scenario.

The ROI demonstrates remarkable improvements in both scenarios. The Solar Scenario exhibits a ROI of 222.7 %, which is substantially higher than in the Present Scenario. While the Wind Scenario shows a similarly impressive ROI of 260.1 %. These findings indicate that the future scenarios offer higher profitability compared to the present scenario.

The IRR also displays substantial enhancements. The Solar Scenario demonstrates a notable increase of 288.1 % in IRR, while the Wind Scenario exhibits an even more significant growth of 307.9 %. These results suggest that the future scenarios provide higher rates of return on investment.

The payback period shows a considerable decrease in both scenarios, indicating a shorter time required to recover the initial investment. The Solar Scenario experiences a reduction of 66.7 % in the payback period, while the Wind Scenario also shows a substantial decrease of 64.0 %.

The LCOE demonstrates cost improvements in both scenarios. The Solar Scenario exhibits a decrease of 60.4% in LCOE, while the Wind Scenario shows an even larger reduction of 64.0 %. These findings suggest that the future scenarios offer lower costs per unit of electricity generated compared to the present scenario.

Fig. 25 reveals a notable difference between the Future scenarios and the Present scenarios, primarily observed in the REPEX costs. In the Future scenarios, these costs exhibit a peak during year 12, coinciding with the replacement of the electrolyzer. Lower REPEX costs result from the extended lifetimes of both the electrolyzer and fuel cell.

The results from Table 37 and Fig. 25 indicate that the selected future scenarios present notable improvements in various economic indicators compared to the present scenario. These improvements include

lower initial investment, higher net present value, increased return on investment, improved internal rate of return, shorter payback period (Fig. 27), and lower levelized cost of electricity (Fig. 26).

These findings highlight the economic benefits associated with the future scenarios and suggest their potential viability and attractiveness from an economic standpoint.

Table 37: Economic indicators for the selected Future Scenarios and their relative difference normalized by the Present Scenarios values.

Scenario	Solar	Difference [%]	Wind	Difference [%]
Initial Investment [kEUR]	8 043	-49.8	9 171	-56.8
NPV [kEUR]	17 193	614.6	25 692	440.8
ROI [%]	222.7	1 327.5	260.1	1 063.3
IRR [-]	0.26	288.1	0.31	307.9
Payback period [years]	6	-66.7	5	-68.8
LCOE [EUR/MWh]	51.2	-60.4	38.25	-64.0

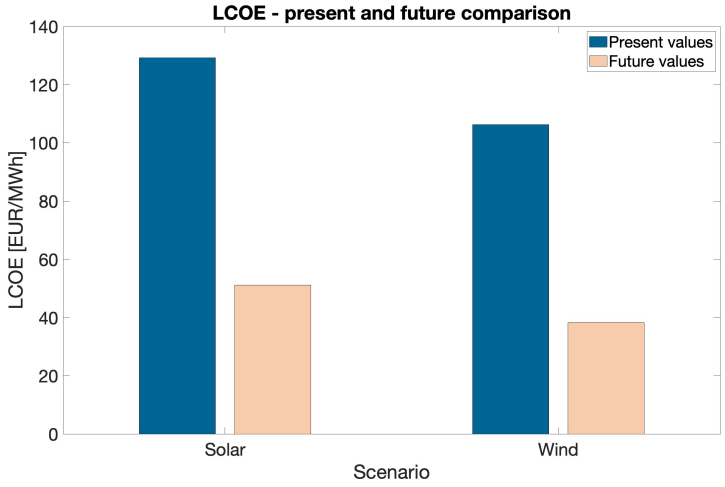

Figure 26: LCOE comparison between solar and wind Scenarios with present and future values

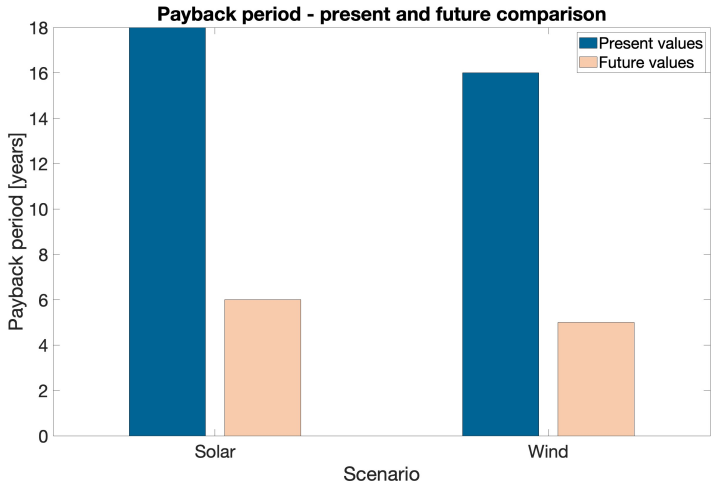

Figure 27: Payback period comparison between solar and wind Scenarios with present and future values

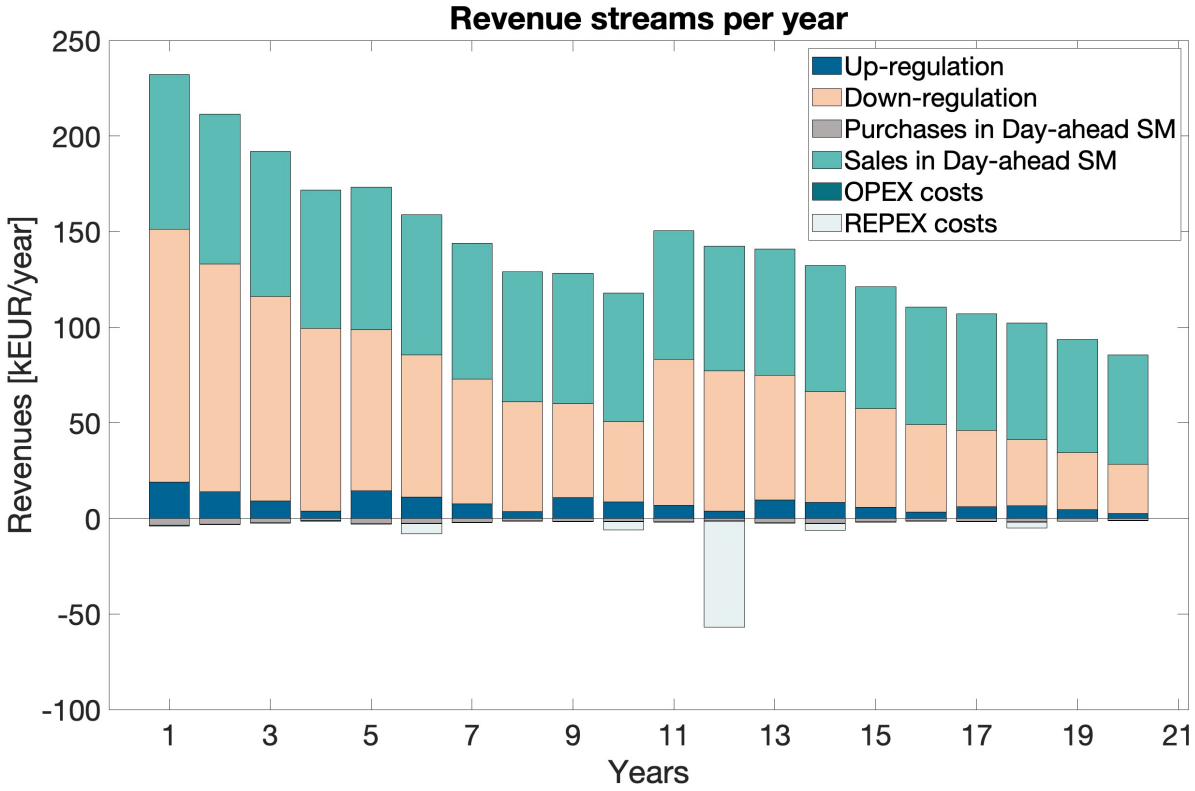

(a) Solar PV as the renewable energy source

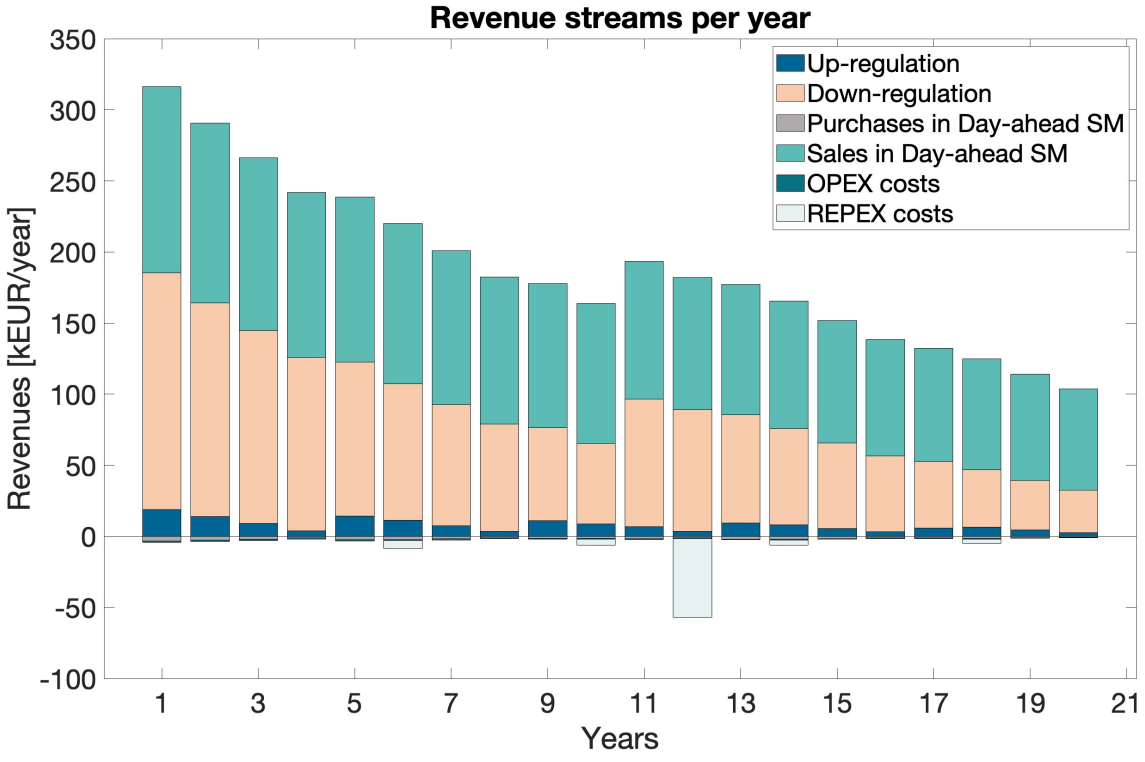

(b) Onshore Wind as the renewable energy source

Figure 25: Annual revenue streams of the system for the Future Scenarios

5.3 Sensitivity Analysis

The results presented in the last Sections are based on multiple parameters that are subject to uncertainty and are derived from the available literature. These parameters often rely on assumptions about the future or represent generalized averages within a given range. In order to better understand the effects of these uncertainties, a sensitivity analysis is conducted.

The sensitivity analysis explores the impact of four specific parameters that are considered uncertain. These parameters include (i) the size of the P2P system, which includes the electrolyzer, compressor, tank, and fuel cell. This parameter is predetermined and not a result of the optimization process; (ii) the prices associated with frequency regulation over the project's lifespan, as these prices are uncertain and subject to forecast inaccuracies; (iii) the day-ahead SM prices, also subject to uncertain forecasts; and (iv) the CAPEX of the P2P system, which can vary based on different values found in the literature.

Each of these sensitivity variables is adjusted within a range of -10% to +10% of their original values, and these adjusted values are incorporated as input variables into the optimization process. The optimization is performed considering these adjusted input parameters while assuming specific system boundary conditions for two scenarios: one involving participation in frequency regulation with solar as the renewable energy source, and the other involving participation in frequency regulation with wind as the renewable energy source. Therefore, the variation of the sensitivity variables affects all parameters and the operation of the system.

To assess the impact on the economic feasibility of the project, this Section examines the influence of the variability in these parameters on three key indicators: the LCOE, NPV, and payback period of the project. These indicators provide insights into the project's financial viability considering the fluctuation in the examined parameters.

As illustrated in Fig. 28, the analysis of both the Wind and Solar Scenarios reveals that the most influential sensitivity variable affecting the LCOE is the CAPEX of the P2P system. This outcome can be attributed to the fact that the CAPEX has a direct impact on both the OPEX and REPEX since these expenses are determined as percentages of the CAPEX. Consequently, any variations in the CAPEX are expected to have a significant influence on the economic indicators.

Furthermore, the size of the P2P system also affects the LCOE since investment costs are dependent on the chosen system size. It is evident that the additional electricity that can be generated by the fuel cell does not compensate for the subsequent increase in investment costs.

When examining the influence of market price changes on economic indicators, it is evident that their impact is relatively modest. The analysis indicates that an increase in frequency regulation prices leads to a slight decrease in the LCOE. According to Equation 48, this reduction signifies an increase in the electricity delivered to the grid, since the system costs are maintained. Conversely, an increase in the Day-ahead SM prices results in a higher LCOE, meaning that slightly less electricity delivered is delivered to the grid under such circumstances.

With regard to the payback period, as described in Fig. 30, the analysis identifies two sensitivity variables that have the most significant influence in both scenarios: the P2P system CAPEX system and the frequency regulation price. These variables have a substantial impact on the duration required to recover the initial investment.

For the Solar Scenario, an increase of 10% in the frequency regulation prices results in a noteworthy reduction of the payback period, decreasing it from 18 to 16 years. Conversely, a decrease of 10% in the prices extends the payback period to 20 years.

The payback period decreases from 16 to 15 years, in the Wind Scenario, when the frequency regulation prices increase by 10 %. On the other hand, if the prices decrease by 10 % the payback period reaches 18 years.

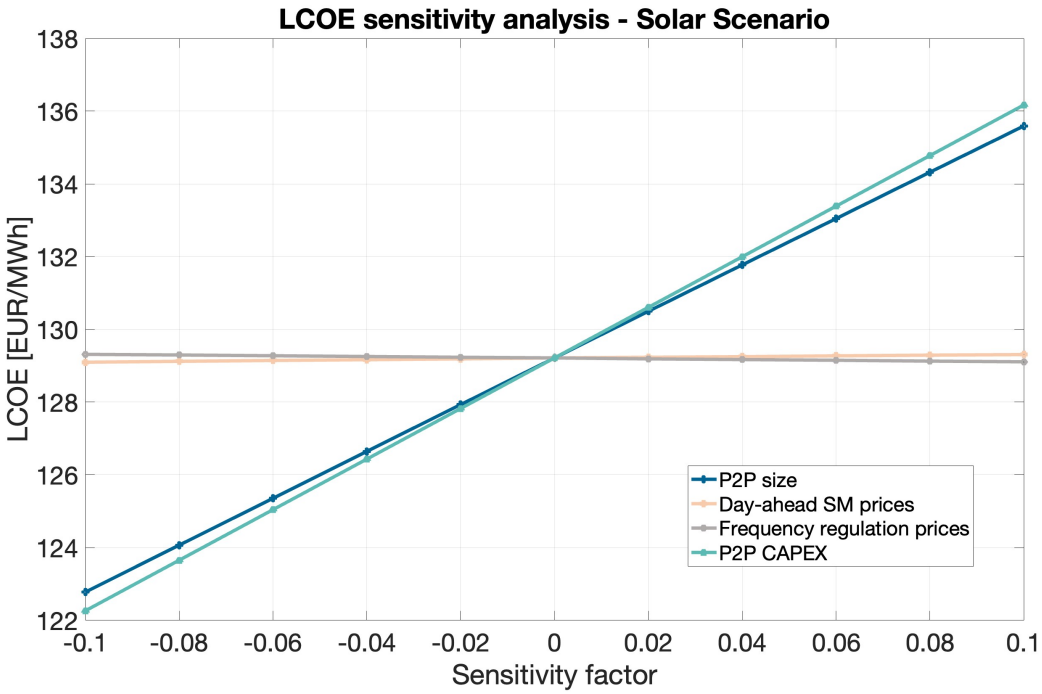

(a) Solar PV as the renewable energy source

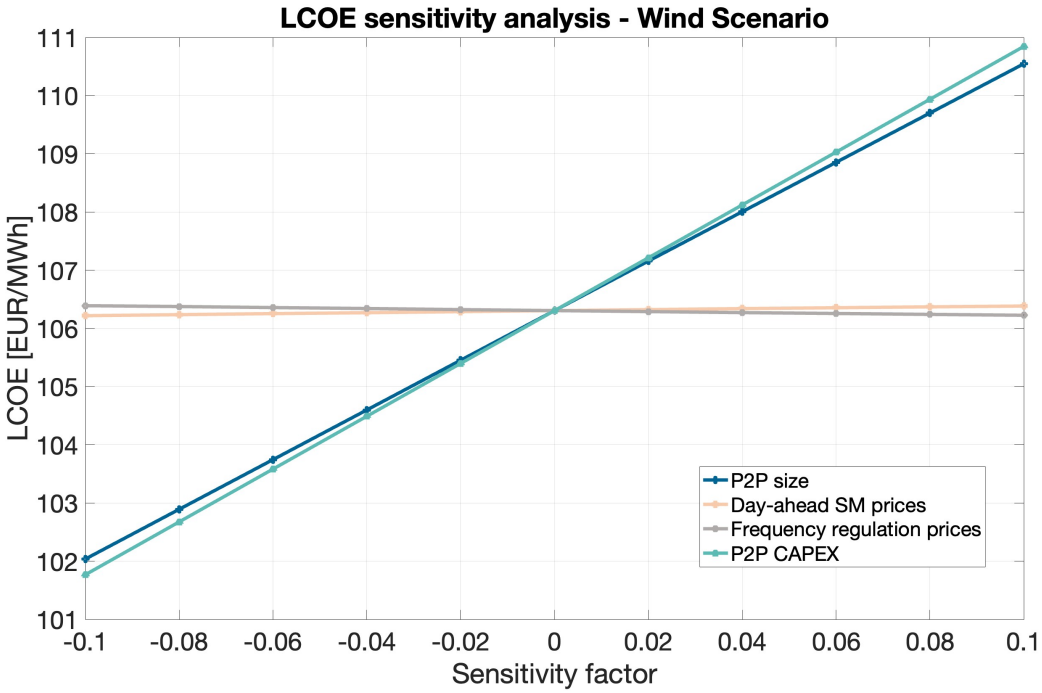

(b) Onshore Wind as the renewable energy source

Figure 28: LCOE sensitivity analysis as a factor of the sensitivity variables

Similarly, alterations in the P2P CAPEX significantly impact the payback period. In this analysis, the P2P size causes the payback period to range from 16 to 10 years in the Solar Scenario and 15 to 18 years in the Wind Scenario. The P2P system size contributes to the variations in the payback period due to its relationship with investment costs. However, in the Wind Scenario, the variance in P2P system size is not enough to change the payback period, which is kept at 16 years.

Furthermore, the Day-ahead Spot Market (SM) prices also have an impact on the payback period. In the Solar Scenario, a decrease of 10% in these prices leads to a payback period of 20 years, while an increase of 10% reduces it to 17 years. Additionally, a rise of 10 % in the Wind Scenario results in a payback period of 15 years, and a decrease of 15 % leads to a payback period of 18 years.

In relation to the NPV, analogous to the findings on the payback period, the analysis identifies the P2P CAPEX and the frequency regulation price are two sensitivity variables that have the most significant influence in the Solar Scenario, as presented in Fig. 30. In the Wind Scenario, frequency regulation price and Day-ahead SM price are the two parameters that impact the NPV the most. Since the Wind Scenario has more renewable energy available, that can be sold in the Day-ahead SM, any variance in the prices of this market has a more significant impact in this scenario than in the Solar Scenario.

An increase in the frequency regulation and Day-ahead SM prices results in higher and more positive cash flows, thereby positively impacting the NPV. A price increase in these markets enhances the overall financial performance of the project by generating greater revenue streams.

Conversely, the increase in the P2P system size and CAPEX contributes to higher system costs. These cost escalations have a negative impact on the NPV, as they decrease the overall profitability of the project.

In addition, the assessment of the discount rate's impact on the economic feasibility of the project was conducted by calculating the NPV, payback period, and LCOE for different discount rate values. Specifically, the discount rates of 7% and 8% were selected for analysis, as the previous results were based on a discount rate of 5%. This choice allows for a comprehensive comparison of the different scenarios under varying discount rate conditions.

The findings, as presented in Table 38, reveal the effect of varying interest rates on the project's economic viability. It is observed that discount rates of 7 % and 8 % render the project economically unfeasible for the Solar Scenarios, as evidenced by negative NPV values, the absence of a payback period, and non-competitive LCOEs in comparison to other technologies. The same occurs for the Wind Scenario when the discount rate of 8%.

Table 38: Discount rate impact on economic indicators for the wind and Solar Scenario including the participation in the Frequency Regulation Markets.

Discount rate	**7%**		**8%**	
Renewable source	**Solar**	**Wind**	**Solar**	**Wind**
NPV [kEUR]	-276.0	985	-1 423.2	-576.0
Payback period [years]	NO	20	NO	NO
LCOE [EUR/MWh]	146.0	119.9	154.8	127.0

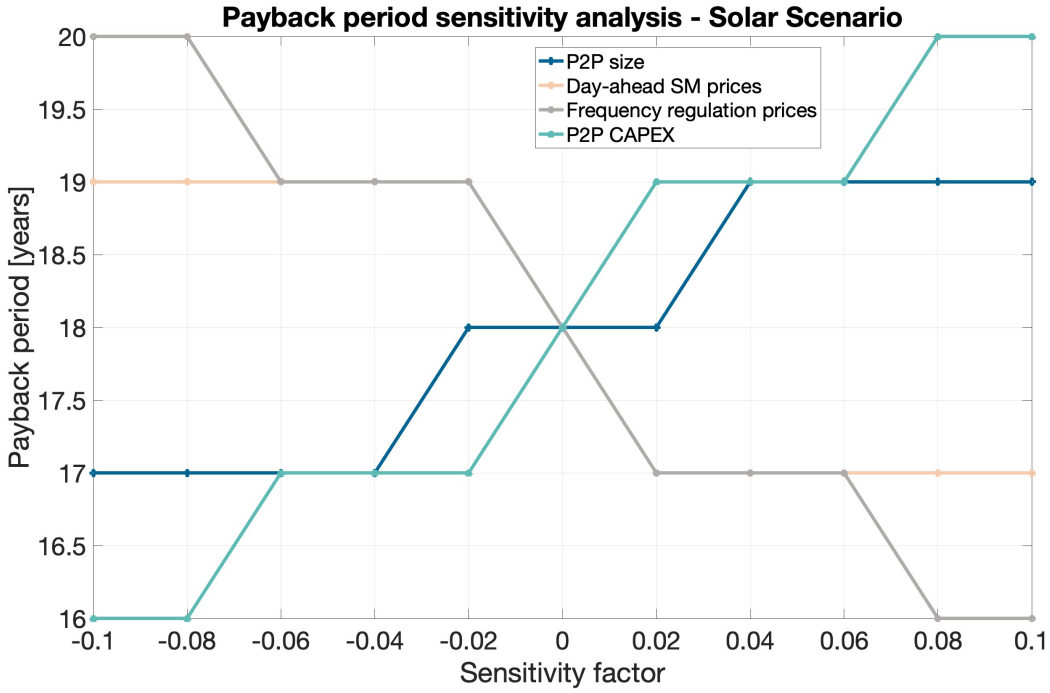

(a) Solar PV as the renewable energy source

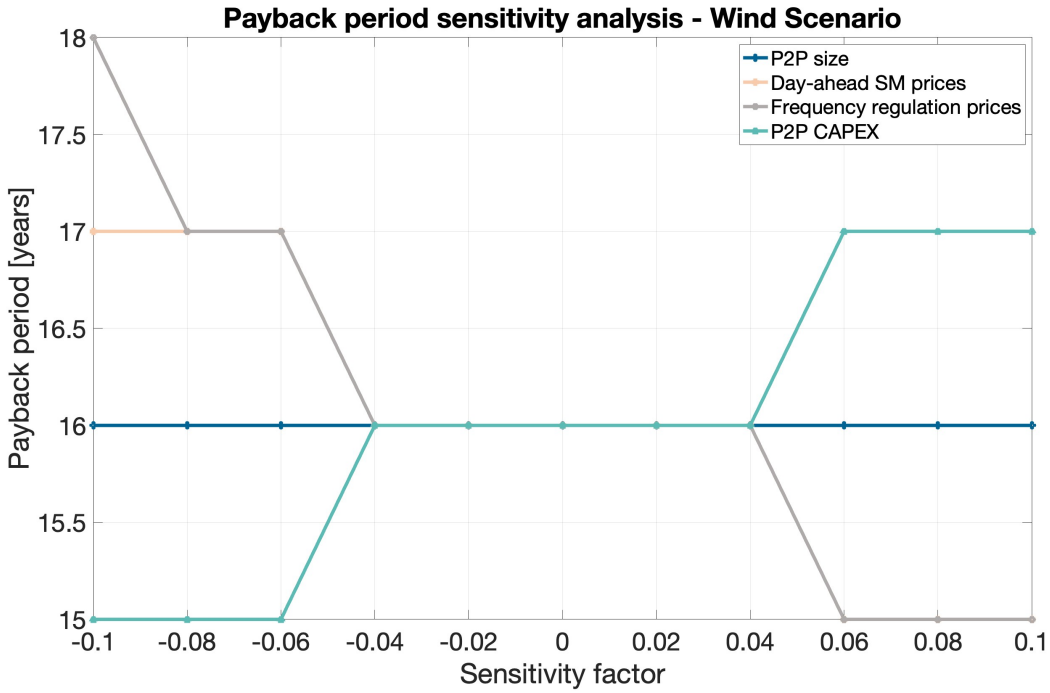

(b) Onshore Wind as the renewable energy source

Figure 29: Payback period sensitivity analysis as a factor of the sensitivity variables

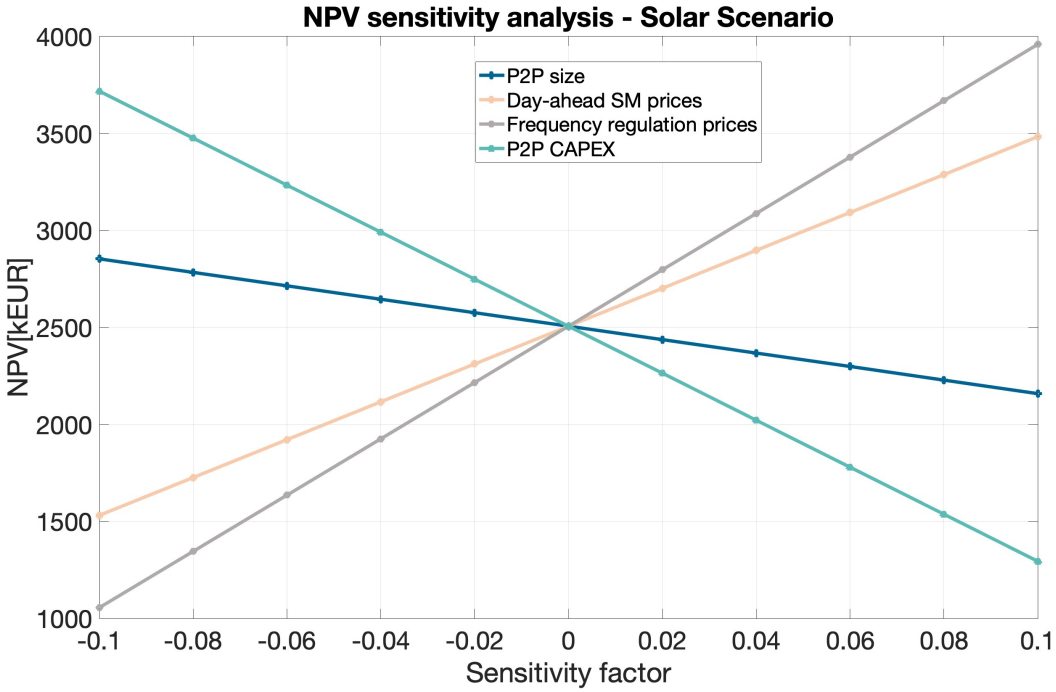

(a) Solar PV as the renewable energy source

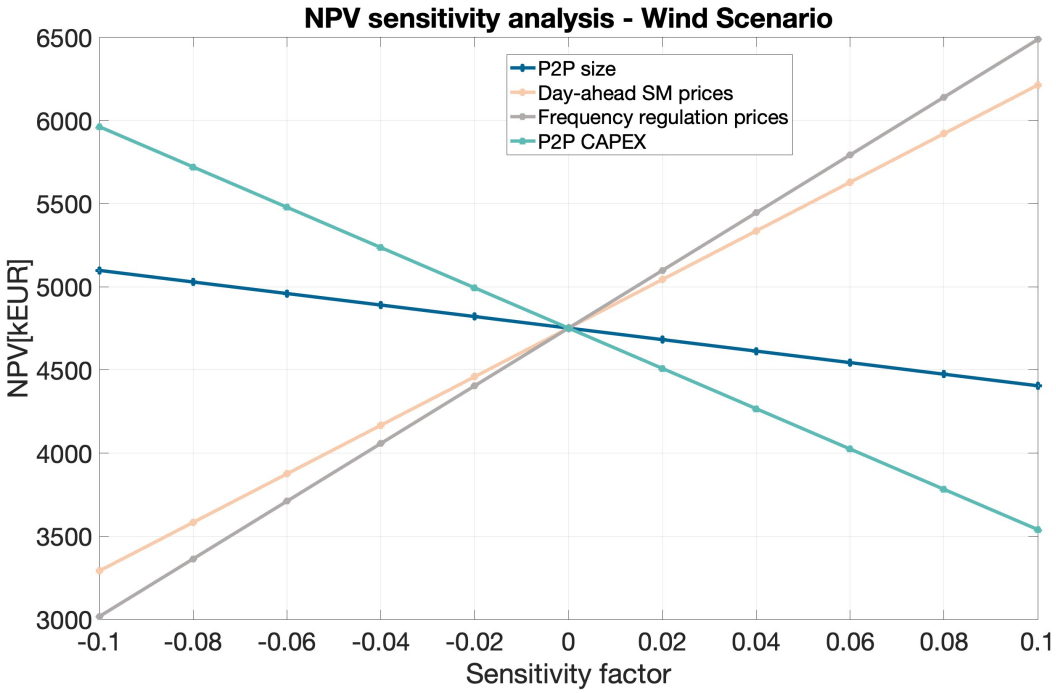

(b) Onshore Wind as the renewable energy source

Figure 30: Payback period sensitivity analysis as a factor of the sensitivity variables

5.4 Final Discussion

Energy storage systems have emerged as a viable solution to address the challenges associated with the increasing share of VRES in the power sector. Among the various options studied and considered for this purpose, batteries, hydro pumps, and hydrogen have gained recognition as possible solutions [128]. Batteries, in particular, are anticipated to experience significant growth and are envisioned to be utilized alongside VRES to mitigate grid stability concerns arising from their inherent variability [129]. According to existing literature, the Levelized Cost of Electricity (LCOE) for integrating battery energy systems with wind or solar power plants typically ranges between 140–280 EUR/MWh [130].

Hence, the solution investigated in this thesis presents a competitive alternative to battery-based systems. However, it is important to note that the obtained results are based on certain assumptions, including a discount rate of 5 % and the utilization of a "perfect-sight" bid strategy. Consequently, the real-world LCOE may potentially exceed the values presented in this thesis. In light of these considerations, Section 9 will describe the limitations of the study and suggest future research. By addressing these limitations and conducting further investigations, more reliable and conclusive results can be attained to confirm the economic and technical feasibility of the analyzed energy system.

In the context of the final discussion on the results, it is evident that the provision of frequency regulation services, coupled with the integration of a renewable energy source, plays a critical role in determining the economic viability of the project. Comparative analysis between the wind and Solar Scenarios concludes the superior performance of wind technologies owing to their higher availability. Moreover, the revenue primarily originates from the renewable energy component, while the fuel cell component contributes the least revenue. Additionally, the up-regulation market demonstrates the lowest contribution to overall revenue, while the down-regulation market contributes to the majority of the revenue. Furthermore, the findings indicate that with the expansion of the P2P size, there is a notable decline in the overall economic performance of the system. Consequently, it can be inferred that the P2P configuration may not be optimal for this particular application.

On the other hand, considering future scenarios, the outlook appears promising due to anticipated advancements in the efficiency and lifetime of electrolyzers and fuel cells. Furthermore, the reduction in CAPEX associated with system components and improvements in Day-ahead Spot Market prices contribute to the optimistic outlook.

Finally, the sensitivity analysis conducted reveals the significant impact of variations in sensitivity variables on project profitability, potentially rendering the project economically unfeasible. Thus, careful consideration of these variables is crucial to ensure the viability and success of the project.

6 Environmental Impact

The environmental impact of this thesis lies in its focus on renewable energy sources, specifically solar and wind power plants, coupled with a hydrogen storage system. The adoption and integration of these renewable energy technologies contribute to the decarbonization of the power sector, aiming to reduce greenhouse gas emissions and mitigate the effects of climate change [19].

By utilizing clean and sustainable energy alternatives to fossil fuels, this thesis aligns with the goal of achieving NZE and supports the transition towards a more environmentally friendly energy system [19]. Additionally, the study explores the potential of hydrogen storage systems to improve the stability and reliability of the power grid, thereby addressing the challenges posed by the intermittent nature of renewable energy sources [30].

According to the IEA, the carbon intensity of final energy in Sweden was 24.3 gCO2eq/MJ in the year 2020 [131]. Table 39 provides an overview of the total renewable energy generation and the corresponding carbon emissions reduction achieved for each scenario analyzed in the study. In the solar scenario, the adoption of renewable energy results in the avoidance of approximately 6 049 tonnes of CO2eq emissions over a period of 20 years. This signifies a substantial reduction in greenhouse gas emissions compared to conventional energy sources. Similarly, in the wind scenario, the implementation of wind power plants leads to the avoidance of approximately 33 024 tonnes of CO2 emissions over the same 20-year timeframe. These emission reductions highlight the significant environmental benefits associated with the utilization of renewable energy sources, contributing to the overall mitigation of climate change.

Table 39: CO_2 emissions avoided in each scenario, during the 20 years period analyzed.

Scenario	**Renewable energy generated [GWh]**	$CO_{2_{eq}}$ **emissions avoided [t]**
Solar PV	248.8	6 049
Onshore Wind	377.2	33 024

Overall, the thesis contributes to a more sustainable and environmentally conscious energy landscape by promoting the utilization of renewable energy and exploring the role of hydrogen in facilitating the integration of renewable into the power sector.

7 Social and Gender Impact

This thesis mainly focuses on the technical and economic specifications associated with the integration of hydrogen-based energy storage systems and renewable power plants within the frequency regulation market. Nonetheless, it is important to acknowledge that the social and gender impact of this thesis emerges indirectly through the broader implications of renewable energy and the transition towards sustainable energy sources [132].

Renewable energy endeavors and the decarbonization of the power sector yield social advantages by diminishing greenhouse gas emissions, enhancing air quality, and mitigating the repercussions of climate change [132]. These advantages can contribute to the cultivation of a more sustainable and inclusive society, potentially benefiting diverse social groups, including women who may experience increased prospects for employment and engagement in renewable energy industries [133, 134].

Moreover, the implementation of renewable energy projects should consider gender inclusivity and address any potential gender disparities prevalent within the energy sector. Facilitating equal access to education, training, and employment opportunities in the realm of renewable energy can help rectify existing gender gaps. For instance, throughout the development of this thesis, 66.7% of the individuals involved were women (the master's student and Flower's supervisor). According to Fig. 31, the renewable energy sector exhibits a relatively higher degree of gender inclusivity compared to the conventional energy sector, as women tend to be more attracted to the diverse and multidisciplinary aspects of renewable energy in comparison to the traditional energy sector as a whole [12]. Nevertheless, it is important to note that the energy sector continues to be predominantly perceived as a male-dominated domain. Therefore, ensuring the representation and empowerment of women in decision-making processes, research, and developmental initiatives pertaining to renewable energy is of utmost importance.

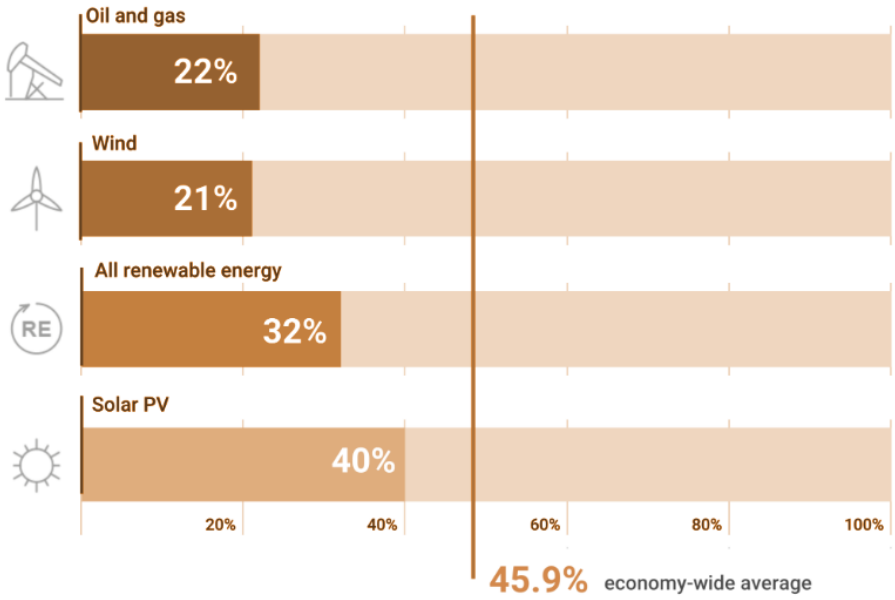

Figure 31: Women in oil and gas, renewable overall, wind, solar PV, and economy-wide average [12]

8 Project Budget and Planning

The timeline of this project is outlined in Fig. 32. Phase one includes the collaborative development of a proposal with Flower, aimed at defining the scope of the master's thesis. Simultaneously, a comprehensive literature review was conducted to ensure well-informed decisions regarding the thesis's future trajectory. Phase two involved the development of the optimization algorithm and subsequent analysis of the model's results. In phase three, the author conducted a sensitivity analysis and performed a comparative assessment of the various scenarios under analyzed. Lastly, phase four was dedicated to finalizing the thesis report and preparing for the presentation.

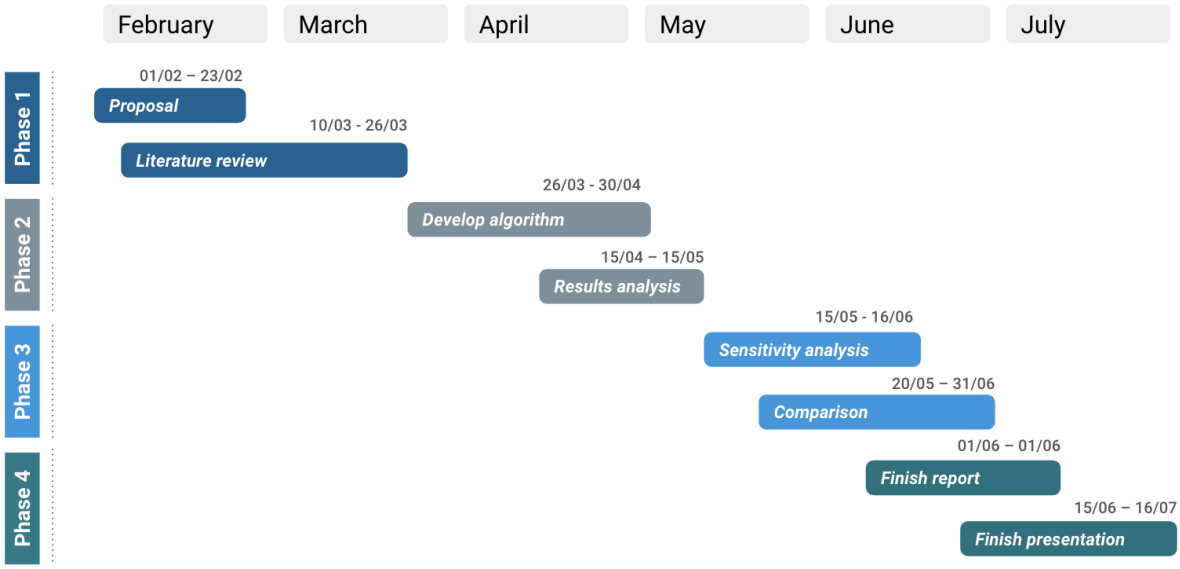

Figure 32: Project timeline (project planning)

This project includes two distinct categories of costs, namely project development costs and project implementation costs. The costs associated with project development are the labor expenses and the acquisition of software, specifically the optimization solver Gurobi. The breakdown of the project development costs is presented in Table 40. Throughout the course of this thesis, the Gurobi solver was utilized under a complementary academic license. However, it is important to note that for future endeavors, if Flower seeks to reuse the optimization model, the acquisition of the Gurobi solver would be required. The estimated cost of purchasing the Gurobi solver license is anticipated to be 8000 euros.

Table 40: Project budget expressed in euros.

	Hours	**Cost/hour**	**Total cost**
Master Student Labor (Intern)	960	17	16320
Gurobi solver	-	-	8 000
Total costs	-	-	24320

With respect to project implementation, a comprehensive cost analysis cannot be provided at this time. Furthermore, it is important to note that the evaluation of the implementation of the model's outcomes was beyond the scope of the project, leaving this aspect for future research.

9 Future Research and Limitations

This chapter explores potential directions for future research and identifies limitations encountered during the investigation of solar PV and wind power plants with hydrogen energy storage systems as frequency regulation providers, in the context of the Swedish grid. The findings emphasize the limitations and need for further research to enhance the understanding and implementation of this project.

Regarding the pre-qualification requirements, using hydrogen technologies as frequency regulation providers, is relatively new in the existing Swedish grid. Therefore, the pre-qualification process might be complex due to their emerging nature. Complying with pre-qualification requirements, particularly the full activation time, can pose significant difficulties. Thus, further research is needed to ensure compatibility with grid standards and the approval from the TSO.

Furthermore, in this study, the electrolyzer and fuel cell degradation was assumed to follow a linear pattern. However, given the dynamic nature of the operation and the unique utilization of these assets as frequency regulation providers, additional research is essential to understand the impact of such dynamic operation on the degradation of these assets. Investigating the complex connection between operational dynamics and degradation processes will contribute to the development of accurate degradation models, enabling more precise asset management strategies.

Additionally, accurate long-term prediction of market prices, including Say-ahead SM prices and frequency regulation prices, remains as an important challenge. The difficulty in forecasting these prices introduces limitations to the economic analysis and optimization conducted in this project. Future research should focus on refining forecasting techniques to account for the inherent uncertainties associated with market dynamics, renewable energy availability, and regulatory changes. Advancements in this area will support decision-making processes for market participants. In addition to the ´uncertainty associated with market prices, it is important to recognize that frequency market regulations, particularly in European countries and specifically in Sweden, are subject to change. For instance, specific regulations of FCR-N, FCR-D up and FCR-D down, are expected to undergo alterations in the upcoming year [93]. These regulatory changes will introduce new requirements and guidelines for the provision of FCR services. These regulatory modifications can significantly impact the operation and financial outcomes of power generation projects.

Since the findings indicate that with the expansion of the P2P size, there is a notable decline in the overall economic performance of the system, another potential future research involves exploring other system configurations. One possibility is to investigate configurations that exclude the fuel cell component, given its relatively minor contribution to revenue. Instead, the hydrogen produced by the electrolyzer could be utilized for alternative purposes, such as selling it in the hydrogen market or supplying it to specific loads. Additionally, incorporating an electric load into the system configuration could be considered as a means to further enhance system efficiency and optimize revenue generation. Such investigations would provide valuable insights into the feasibility and economic viability of different system configurations.

Besides this, this thesis employed a bid strategy based on "perfect foresight," assuming access to real-time market and environmental data for the entire analysis period. However, in real-world scenarios, market participants must rely on predictive methods to forecast wind and solar availability, as well as market prices. Therefore, the bid strategy employed in this thesis represents a limitation. Future research should aim to develop bid strategies that incorporate realistic predictive models, considering the uncertainties inherent in renewable energy generation and market dynamics.

Finally, this work primarily focused on the market participation of solar PV and wind power plants with hydrogen energy storage systems, excluding considerations related to the integration of supporting power electronics such as converters, inverters, and transformers. Future research should explore the technical requirements and implications of integrating these power electronics components, assessing their impact on overall system performance, efficiency and costs. Such investigations will facilitate the development of comprehensive solutions for the successful grid integration of these assets.

This chapter has outlined areas that require further investigation and understanding within the scope of the thesis. Addressing the challenges associated with pre-qualification requirements, degradation modeling, long-term market price prediction, bid strategy, and the integration of supporting power electronics will contribute to advancing knowledge and fostering practical solutions. Through continued research and refinement, the potential of this approach can be realized, supporting the transition to a sustainable and resilient energy system.

10 Conclusions

This thesis undertook a comprehensive techno-economic analysis of a solar and wind power plant integrated with a hydrogen storage system, focusing on their role as providers of frequency regulation services. The primary objective of this study was to develop an optimization model utilizing the Gurobi solver to evaluate the profitability of participating in the Day-ahead SM and offering frequency regulation services using the aforementioned assets. A case study based in Sweden was employed to simulate and analyze the results obtained from the optimization model.

Renewable energy sources such as solar and wind have gained significant importance in the energy transition towards decarbonization and achieving net-zero emissions. This thesis recognizes their potential as clean and sustainable alternatives to fossil fuels, contributing to the reduction of greenhouse gas emissions and combating climate change. The rapid growth of renewable energy, driven by technological advancements and policy incentives, has made it a cost-effective and viable option for meeting our energy needs.

With the objective of addressing the challenges associated with the integration of renewable energy sources and ensuring grid stability, the study explores the utilization of hydrogen as an energy carrier and storage system. By analyzing the techno-economic feasibility of integrating hydrogen with solar and wind power plants, the thesis highlights the potential benefits of hydrogen in providing frequency regulation services and balancing the grid.

The research outcomes contribute to decision-making processes by offering valuable insights into various factors influencing the profitability of renewable energy projects. The optimization model developed in this study provides a framework for determining the optimal operation of the integrated energy system, maximizing profits while considering market prices, asset specifications, and discount rates.

The findings reveal that revenues from frequency regulation services play a crucial role in enhancing the overall profitability of the project. Wind scenarios outperform solar scenarios due to their higher availability, compensating for initial investment costs. Future scenarios indicate that market landscapes and technological advancements will significantly improve economic indicators, making renewable energy projects more attractive.

Moreover, the sensitivity analysis conducted in this study identifies the key variables influencing the NPV in different scenarios. Frequency regulation prices and Day-ahead SM prices are found to be primary factors in wind scenarios, while frequency regulation prices and P2P CAPEX influence NPV in solar scenarios. Additionally, the study highlights that discount rates of 5% and 7% compromise the economic feasibility of the project.

In conclusion, this thesis successfully develops an optimization model for determining the optimal operation of an integrated energy system and investigates the impact of frequency regulation provision on project profitability. Based on the case study and methodology employed in this thesis, it is concluded that the integration of PV and wind power plants with hydrogen energy storage systems is both technically and economically viable. Besides this, by exploring future scenarios, the research provides valuable insights into the potential effects of market adaptations and technological developments on profitability. The findings emphasize the importance of considering factors such as market prices, system size, cost of the components, and discount rates in the techno-economic analysis of renewable energy projects. Concluding, this thesis contributes to the growing body of knowledge in the field and offers guidance for stakeholders involved in the planning and implementation of renewable energy systems.

References

[1] B. Qin, M. Wang, G. Zhang, and Z. Zhang, "Impact of renewable energy penetration rate on power system frequency stability," *Energy Reports*, vol. 8, pp. 997–1003, 2022.

[2] Svenska Kraftnät, "Långsiktig marknadsanalys 2021," Tech. Rep., 2021. [Online]. Available: https://www.svk.se/siteassets/om-oss/rapporter/2021/langsiktig-marknadsanalys-2021.pdf

[3] M. Carmo, D. L. Fritz, J. Mergel, and D. Stolten, "A comprehensive review on pem water electrolysis," *International journal of hydrogen energy*, vol. 38, no. 12, pp. 4901–4934, 2013.

[4] I. Hassan, H. S. Ramadan, M. A. Saleh, and D. Hissel, "Hydrogen storage technologies for stationary and mobile applications: Review, analysis and perspectives," *Renewable and Sustainable Energy Reviews*, vol. 149, p. 111311, 2021.

[5] S. Mekhilef, R. Saidur, and A. Safari, "Comparative study of different fuel cell technologies," *Renewable and Sustainable Energy Reviews*, vol. 16, no. 1, pp. 981–989, 2012.

[6] W. Li and D. M. Becker, "Day-ahead electricity price prediction applying hybrid models of lstm-based deep learning methods and feature selection algorithms under consideration of market coupling," *Energy*, vol. 237, p. 121543, 2021.

[7] Svenska kraftnät, "Information on different ancillary services," 2023. [Online]. Available: https://www.svk.se/en/stakeholders-portal/electricity-market/provision-of-ancillary-services/information-on-different-ancillary-services/

[8] IEA - International Energy Agency, "World energy outlook 2022," 2022.

[9] Svenska Kraftnät, "Kortsiktig marknadsanalys 2021," 2022. [Online]. Available: https://www.svk.se/siteassets/om-oss/rapporter/2022/kortsiktig-marknadsanalys-2021.pdf

[10] Mimer, "Fcr," In Mimer [Website], 2023. [Online]. Available: hhttps://mimer.svk.se/PrimaryRegulation/PrimaryRegulationIndex

[11] Nord Pool, "Day-ahead prices," In Nord Pool [Website], 2023. [Online]. Available: https://www.nordpoolgroup.com/en/Market-data1/#/nordic/table

[12] IRENA - International Renewable Energy Agency, "Gender - overview," Tech. Rep., 2023. [Online]. Available: https://www.irena.org/Energy-Transition/Socio-economic-impact/Gender

[13] Office of Energy Efficiency and Renewable Energy, USA Energy Department, "Comparison of fuel cell technologies," Tech. Rep. [Online]. Available: https://www.energy.gov/eere/fuelcells/comparison-fuel-cell-technologies

[14] IRENA - International Renewable Energy Agency, "Energy profile sweden," 2022. [Online]. Available: https://www.irena.org/-/media/Files/IRENA/Agency/Statistics/Statistical_Profiles/Europe/Sweden_Europe_RE_SP.pdf

[15] Energimyndighetens, "Underlagsrapport - förslag till nationell strategi för vätgas, elektrobränslen och ammoniak," 2021. [Online]. Available: https://www.energimyndigheten.se/nyhetsarkiv/2021/forslag-till-nationell-strategi-for-fossilfri-vatgas/

[16] ENTSO-E, "Picasso," 2022. [Online]. Available: https://www.entsoe.eu/network_codes/eb/picasso/

[17] ENTSO-E, "Manually activated reserves initiative," Tech. Rep., 2022. [Online]. Available:

https://www.entsoe.eu/network_codes/eb/mari/

[18] Fingrid, "Datasets," 2023. [Online]. Available: https://data.fingrid.fi/open-data-forms/search/en/index.html?selected_datasets=177

[19] IEA - International Energy Agency, "Net zero by 2050 - a roadmap for the global energy sector," Tech. Rep., 2021. [Online]. Available: www.iea.org/t&c/

[20] R. Kothari, V. V. Tyagi, and A. Pathak, "Waste-to-energy: A way from renewable energy sources to sustainable development," *Renewable and Sustainable Energy Reviews*, vol. 14, no. 9, pp. 3164–3170, 2010.

[21] IRENA - International Renewable Energy Agency, "Renewable power generation costs in 2021," Tech. Rep., 2022. [Online]. Available: https://www.irena.org/publications/2022/Jul/-/media/Files/IRENA/Agency/Publication/2022/Jul/IRENA_Power_Generation_Costs_2021_Summary.pdf?la=en&hash=C0C810E72185BB4132AC5EA07FA26C669D3AFBFC

[22] IEA - International Energy Agency, "Renewable electricity," Tech. Rep., 2022. [Online]. Available: https://www.irena.org/publications/2022/Jul/Renewable-Power-Generation-Costs-in-2021

[23] McKinsey Company, "Hydrogen for net-zero," Tech. Rep., 2021. [Online]. Available: www.hydrogencouncil.com

[24] "Hybrid wind and solar photovoltaic generation with energy storage systems: A systematic literature review and contributions to technical and economic regulations," *Energies*, vol. 14, 10 2021.

[25] K. Mazloomi and C. Gomes, "Hydrogen as an energy carrier: Prospects and challenges," *Renewable and Sustainable Energy Reviews*, vol. 16, no. 5, pp. 3024–3033, 2012.

[26] IRENA - International Renewable Energy Agency, "Renewable capacity statistics 2022," Tech. Rep., 2022. [Online]. Available: https://www.irena.org/-/media/Files/IRENA/Agency/Publication/2022/Apr/IRENA_RE_Capacity_Statistics_2022.pdf

[27] L. Hirth and I. Ziegenhagen, "Balancing power and variable renewables: Three links," *Renewable and Sustainable Energy Reviews*, vol. 50, pp. 1035–1051, 2015.

[28] A. D. Papalexopoulos and P. E. Andrianesis, "Performance-based pricing of frequency regulation in electricity markets," *IEEE Transactions on Power systems*, vol. 29, no. 1, pp. 441–449, 2012.

[29] J. Riesz, J. Gilmore, and I. MacGill, "Frequency control ancillary service market design: Insights from the australian national electricity market," *The Electricity Journal*, vol. 28, no. 3, pp. 86–99, 2015.

[30] A. Banshwar, N. K. Sharma, Y. R. Sood, and R. Shrivastava, "Renewable energy sources as a new participant in ancillary service markets," *Energy strategy reviews*, vol. 18, pp. 106–120, 2017.

[31] F. Kahrl, H. Kim, A. D. Mills, R. H. Wiser, C. Crespo Montañés, and W. Gorman, "Variable renewable energy participation in us ancillary services markets: economic evaluation and key issues," 2021.

[32] H.-I. Su and A. El Gamal, "Modeling and analysis of the role of energy storage for renewable integration: Power balancing," *IEEE Transactions on Power Systems*, vol. 28, no. 4, pp. 4109–4117, 2013.

[33] IRENA - International Renewable Energy Agency, "Battery storage for renewables: Market status and technology outlook," Tech. Rep., 2015. [Online]. Available: https://www.irena.org/-/media/

Files/IRENA/Agency/Publication/2022/Apr/IRENA_RE_Capacity_Statistics_2022.pdf

[34] IEA - International Energy Agency, "The future of hydrogen," 2019. [Online]. Available: https://www.hydrogenexpo.com/media/9370/the_future_of_hydrogen_iea.pdf

[35] E. Crespi, P. Colbertaldo, G. Guandalini, and S. Campanari, "Energy storage with power-to-power systems relying on photovoltaic and hydrogen: modelling the operation with secondary reserve provision," *Journal of Energy Storage*, vol. 55, p. 105613, 2022.

[36] ——, "Design of hybrid power-to-power systems for continuous clean pv-based energy supply," *International Journal of Hydrogen Energy*, vol. 46, pp. 13 691–13 708, 4 2021.

[37] IEA - International Energy Agency, "Sweden," Tech. Rep., 2021. [Online]. Available: https://www.iea.org/countries/sweden

[38] Strategy for fossil free competitiveness, "Fossil free sweden," Tech. Rep., 2021. [Online]. Available: https://fossilfrittsverige.se/wp-content/uploads/2021/01/Hydrogen_strategy_for-_fossil_free_competitiveness_ENG.pdf

[39] C. Mikovits, E. Wetterlund, S. Wehrle, J. Baumgartner, and J. Schmidt, "Stronger together: Multi-annual variability of hydrogen production supported by wind power in sweden," *Applied Energy*, vol. 282, p. 116082, 2021.

[40] Office of Energy Efficiency and Renewable Energy, USA Energy Department, "Fuel cells," Office of Energy Efficiency and Renewable Energy, USA Energy Department, Tech. Rep. [Online]. Available: https://www.energy.gov/eere/fuelcells/fuel-cells

[41] G. Cipriani, V. Di Dio, F. Genduso, D. La Cascia, R. Liga, R. Miceli, and G. R. Galluzzo, "Perspective on hydrogen energy carrier and its automotive applications," *International Journal of Hydrogen Energy*, vol. 39, no. 16, pp. 8482–8494, 2014.

[42] N. Stetson, S. McWhorter, and C. Ahn, *Introduction to hydrogen storage*. Elsevier, 2016.

[43] D. Bessarabov, H. Wang, H. Li, and N. Zhao, *PEM electrolysis for hydrogen production: principles and applications*. CRC press, 2016.

[44] P. Patel and K. Ayers, "Electrolysis for hydrogen production," vol. 44. Cambridge University Press, 9 2019, pp. 684–685.

[45] C. Hora, F. C. Dan, N. Rancov, G. E. Badea, and C. Secui, "Main trends and research directions in hydrogen generation using low temperature electrolysis: A systematic literature review," vol. 15. MDPI, 8 2022.

[46] O. Schmidt, A. Gambhir, I. Staffell, A. Hawkes, J. Nelson, and S. Few, "Future cost and performance of water electrolysis: An expert elicitation study," *International journal of hydrogen energy*, vol. 42, no. 52, pp. 30 470–30 492, 2017.

[47] E. Taibi, R. Miranda, M. Carmo, and H. Blanco, "Green hydrogen cost reduction," 2020.

[48] A. Buttler and H. Spliethoff, "Current status of water electrolysis for energy storage, grid balancing and sector coupling via power-to-gas and power-to-liquids: A review," *Renewable and Sustainable Energy Reviews*, vol. 82, pp. 2440–2454, 2018.

[49] R. Hancke, T. Holm, and Ø. Ulleberg, "The case for high-pressure pem water electrolysis," *Energy Conversion and Management*, vol. 261, p. 115642, 2022.

[50] Ö. F. Selamet, F. Becerikli, M. D. Mat, and Y. Kaplan, "Development and testing of a highly efficient proton exchange membrane (pem) electrolyzer stack," *International Journal of hydrogen energy*, vol. 36, no. 17, pp. 11 480–11 487, 2011.

[51] S. M. Saba, M. Müller, M. Robinius, and D. Stolten, "The investment costs of electrolysis–a comparison of cost studies from the past 30 years," *International journal of hydrogen energy*, vol. 43, no. 3, pp. 1209–1223, 2018.

[52] Office of Energy Efficiency and Renewable Energy, USA Energy Department, "Doe hydrogen and fuel cells program record," Tech. Rep., 2009. [Online]. Available: https://www.hydrogen.energy.gov/pdfs/9013_energy_requirements_for_hydrogen_gas_compression.pdf

[53] H. Barthélémy, M. Weber, and F. Barbier, "Hydrogen storage: Recent improvements and industrial perspectives," *International Journal of Hydrogen Energy*, vol. 42, no. 11, pp. 7254–7262, 2017.

[54] E. Rivard, M. Trudeau, and K. Zaghib, "Hydrogen storage for mobility: a review," *Materials*, vol. 12, no. 12, p. 1973, 2019.

[55] R. Kurz, B. Winkelmann, S. Freund, M. McBain, M. Keith, D. Zhang, S. Cich, P. Renzi, and J. Schmitt, "Chapter 6 - transport and storage," in *Machinery and Energy Systems for the Hydrogen Economy*, K. Brun and T. Allison, Eds. Elsevier, 2022, pp. 215–249. [Online]. Available: https://www.sciencedirect.com/science/article/pii/B9780323903943000035

[56] R. Chahine and T. Bose, "Low-pressure adsorption storage of hydrogen," *International Journal of Hydrogen Energy*, vol. 19, no. 2, pp. 161–164, 1994.

[57] T. Egeland-Eriksen, A. Hajizadeh, and S. Sartori, "Hydrogen-based systems for integration of renewable energy in power systems: Achievements and perspectives," *international journal of hydrogen energy*, vol. 46, no. 63, pp. 31 963–31 983, 2021.

[58] R. O'hayre, S.-W. Cha, W. Colella, and F. B. Prinz, *Fuel cell fundamentals*. John Wiley & Sons, 2016.

[59] J.-H. Jo and S.-C. Yi, "A computational simulation of an alkaline fuel cell," *Journal of Power Sources*, vol. 84, no. 1, pp. 87–106, 1999.

[60] J. Hoeflinger and P. Hofmann, "Air mass flow and pressure optimisation of a pem fuel cell range extender system," *international journal of hydrogen energy*, vol. 45, no. 53, pp. 29 246–29 258, 2020.

[61] I. Staffell, "A review of small stationary fuel cell performance," *Fuel*, 2009.

[62] J. Coolegem, Tech. Rep.

[63] N. Sammes, *Fuel cell technology: reaching towards commercialization*. Springer Science & Business Media, 2006.

[64] E. Gülzow, "Alkaline fuel cells," *Fuel cells*, vol. 4, no. 4, pp. 251–255, 2004.

[65] R. Bhattacharyya, A. Misra, and K. Sandeep, "Photovoltaic solar energy conversion for hydrogen production by alkaline water electrolysis: conceptual design and analysis," *Energy Conversion and management*, vol. 133, pp. 1–13, 2017.

[66] M. Nasser, T. F. Megahed, S. Ookawara, and H. Hassan, "A review of water electrolysis–based systems for hydrogen production using hybrid/solar/wind energy systems," *Environmental Science and Pollution Research*, pp. 1–25, 2022.

[67] M. Nasser, T. MEGAHED, S. Ookawara, and H. Hassan, "Techno-economic assessment of green

hydrogen production using different configurations of wind turbines and pv panels," *Journal of Energy Systems*, vol. 6, no. 4, pp. 560–572, 2022.

[68] ——, "Techno-economic assessment of green hydrogen production using different configurations of wind turbines and pv panels," *Journal of Energy Systems*, vol. 6, no. 4, pp. 560–572, 2022.

[69] M. Korpås and A. T. Holen, "Operation planning of hydrogen storage connected to wind power operating in a power market," *IEEE Transactions on Energy Conversion*, vol. 21, pp. 742–749, 9 2006.

[70] F. Alshehri, V. G. Suárez, J. L. R. Torres, A. Perilla, and M. van der Meijden, "Modelling and evaluation of pem hydrogen technologies for frequency ancillary services in future multi-energy sustainable power systems," *Heliyon*, vol. 5, no. 4, p. e01396, 2019.

[71] A. Dadkhah, D. Bozalakov, J. D. De Kooning, and L. Vandevelde, "Techno-economic analysis and optimal operation of a hydrogen refueling station providing frequency ancillary services," *IEEE Transactions on Industry Applications*, vol. 58, no. 4, pp. 5171–5183, 2022.

[72] M. Koleva, O. J. Guerra, J. Eichman, B. M. Hodge, and J. Kurtz, "Optimal design of solar-driven electrolytic hydrogen production systems within electricity markets," *Journal of Power Sources*, vol. 483, 1 2021.

[73] A. Weiß, A. Siebel, M. Bernt, T.-H. Shen, V. Tileli, and H. Gasteiger, "Impact of intermittent operation on lifetime and performance of a pem water electrolyzer," *Journal of the electrochemical society*, vol. 166, no. 8, p. F487, 2019.

[74] A. Liponi, A. Baccioli, L. Ferrari, and U. Desideri, "Techno-economic analysis of hydrogen production from pv plants," in *E3S Web of Conferences*, vol. 334. EDP Sciences, 2022, p. 01001.

[75] B. Guinot, F. Montignac, B. Champel, and D. Vannucci, "Profitability of an electrolysis based hydrogen production plant providing grid balancing services," *International Journal of Hydrogen Energy*, vol. 40, no. 29, pp. 8778–8787, 2015.

[76] R. Loisel, L. Baranger, N. Chemouri, S. Spinu, and S. Pardo, "Economic evaluation of hybrid offshore wind power and hydrogen storage system," *International Journal of Hydrogen Energy*, vol. 40, pp. 6727–6739, 6 2015.

[77] A. H. Schrotenboer, A. A. Veenstra, M. A. uit het Broek, and E. Ursavas, "A irenan hydrogen cost reductionn hydrogen cost reductionn hydrogen energy system: Optimal control strategies for integrated hydrogen storage and power generation with wind energy," *Renewable and Sustainable Energy Reviews*, vol. 168, 10 2022.

[78] A. Liponi, A. Baccioli, L. Ferrari, and U. Desideri, "Techno-economic analysis of hydrogen production from pv plants," vol. 334. EDP Sciences, 1 2022.

[79] I. Pavić, N. Čović, and H. Pandžić, "Pv–battery-hydrogen plant: Cutting irenan hydrogen cost reductionn hydrogen cost reductionn hydrogen costs through multi-market positioning," *Applied Energy*, vol. 328, p. 120103, 2022.

[80] O. Borne, K. Korte, Y. Perez, M. Petit, and A. Purkus, "Barriers to entry in frequency-regulation services markets: Review of the status quo and options for improvements," *Renewable and Sustainable Energy Reviews*, vol. 81, pp. 605–614, 2018.

[81] M. Dreidy, H. Mokhlis, and S. Mekhilef, "Inertia response and frequency control techniques for renewable energy sources: A review," *Renewable and sustainable energy reviews*, vol. 69, pp. 144–155, 2017.

[82] P. Tielens and D. Van Hertem, "The relevance of inertia in power systems," *Renewable and Sustainable Energy Reviews*, vol. 55, pp. 999–1009, 2016.

[83] A. Khodadadi, L. Herre, P. Shinde, R. Eriksson, L. Söder, and M. Amelin, "Nordic balancing markets: Overview of market rules," in *2020 17th International Conference on the European Energy Market (EEM)*. IEEE, 2020, pp. 1–6.

[84] D. Gan, D. Feng, and J. Xie, *Electricity markets and power system economics*. CRC Press, 2013.

[85] A. W. Dowling and V. M. Zavala, "Economic opportunities for industrial systems from frequency regulation markets," *Computers & Chemical Engineering*, vol. 114, pp. 254–264, 2018.

[86] Svenska kraftnät, "Operations and electricity markets," 2021. [Online]. Available: https://www.svk.se/en/national-grid/operations-and-electricity-markets/#:~:text=Sweden%20is%20divided%20into%20four,transmission%20capacity%20between%20bidding%20areas.

[87] R. Liikamaa, "Electric power distribution in sweden," 2019.

[88] ENERGINET, FINGRID, Statnett, Svenska kraftnät, "The way forward - solutions for a changing nordic power system," 2018. [Online]. Available: https://www.svk.se/siteassets/om-oss/rapporter/2018/the-way-forward---solutions-for-a-changing-nordic-power-system.pdf

[89] Nord Pool AS, "Product specifications nordic/ baltic market areas," 2021. [Online]. Available: https://www.nordpoolgroup.com/49649b/globalassets/download-center/rules-and-regulations/product-specifications-nordic-and-baltic-market-05.04.21.pdf

[90] Svenska Kraftnät, "Electricity trade," 2023. [Online]. Available: https://www.svk.se/en/national-grid/operations-and-electricity-markets/electricity-trade/

[91] Nordic Balancing Model, "Roadmap and projects," 2023. [Online]. Available: https://nordicbalancingmodel.net

[92] N. Hjalmar Pihl, "Swedish fcr prices–an analysis of the data," 2019.

[93] Svenska Kraftnät, "Workshop for new requirements for fcr in the nordics," 2022. [Online]. Available: https://www.svk.se/en/about-us/meet-svenska-kraftnat/event/2022/workshop-for-new-requirements-for-fcr-in-the-nordics/

[94] Energiforsk , "Sektorkoppling fÖr ett mer effektivt energisystem," 2021. [Online]. Available: https://energiforsk.se/media/29722/sektorkoppling-for-ett-mer-effektivt-energisystem-energiforskrapport-2021-764.pdf

[95] Bruce S, Temminghoff M, Hayward J, Schmidt E, Munnings C, Palfreyman D, Hartley P, "National hydrogen roadmap," 2018. [Online]. Available: https://static1.squarespace.com/static/58e8f58d20099ea6eb9ab918/t/5e965cdbf01cf06d99b46750/1586912484503/18-00314_EN_NationalHydrogenRoadmap_WEB_180823.pdf

[96] A. Bharti and R. Natarajan, "Proton exchange membrane testing and diagnostics," in *PEM Fuel Cells*. Elsevier, 2022, pp. 137–171.

[97] Horizon Educational, "The future of fuel cells," Tech. Rep., 2023. [Online]. Available: https://www.horizoneducational.com/the-future-of-fuel-cells/t1426

[98] L. Sens, U. Neuling, and M. Kaltschmitt, "Capital expenditure and levelized cost of electricity of photovoltaic plants and wind turbines–development by 2050," *Renewable Energy*, vol. 185, pp. 525–537, 2022.

[99] R. Wiser, J. Rand, J. Seel, P. Beiter, E. Baker, E. Lantz, and P. Gilman, "Expert elicitation survey predicts 37% to 49% declines in wind energy costs by 2050," *Nature Energy*, vol. 6, no. 5, pp. 555–565, 2021.

[100] European Comission, "Proposal for a regulation of the european parliament and of the council," 2023. [Online]. Available: https://eur-lex.europa.eu/legal-content/EN/TXT/PDF/?uri=CELEX:52023PC0147&from=EN

[101] Y.-h. Li, "Competitiveness in power systemfrequency regulation markets," Master's thesis, Universitat Politècnica de Catalunya, 2021.

[102] G. Zang, P. Sun, A. A. Elgowainy, A. Bafana, and M. Wang, "Performance and cost analysis of liquid fuel production from h2 and co2 based on the fischer-tropsch process," *Journal of CO2 Utilization*, vol. 46, p. 101459, 2021.

[103] Office of Energy Efficiency and Renewable Energy, USA Energy Department, "Technical targets for liquid alkaline electrolysis." [Online]. Available: https://www.energy.gov/eere/fuelcells/technical-targets-liquid-alkaline-electrolysis

[104] ——, "Technical targets for proton exchange membrane electrolysis." [Online]. Available: https://www.energy.gov/eere/fuelcells/technical-targets-liquid-alkaline-electrolysis

[105] L. Vidas and R. Castro, "Recent developments on hydrogen production technologies: state-of-the-art review with a focus on green-electrolysis," *Applied Sciences*, vol. 11, no. 23, p. 11363, 2021.

[106] Y. Yu, H. Li, H. Wang, X.-Z. Yuan, G. Wang, and M. Pan, "A review on performance degradation of proton exchange membrane fuel cells during startup and shutdown processes: Causes, consequences, and mitigation strategies," *Journal of Power Sources*, vol. 205, pp. 10–23, 2012.

[107] C. Rakousky, U. Reimer, K. Wippermann, S. Kuhri, M. Carmo, W. Lueke, and D. Stolten, "Polymer electrolyte membrane water electrolysis: Restraining degradation in the presence of fluctuating power," *Journal of Power Sources*, vol. 342, pp. 38–47, 2017.

[108] P. Wu and R. Bucknall, "Hybrid fuel cell and battery propulsion system modelling and multi-objective optimisation for a coastal ferry," *International journal of hydrogen energy*, vol. 45, no. 4, pp. 3193–3208, 2020.

[109] GlobalData Power Intelligence Center, "Power plant profile: Swedbank solar pv park, sweden," Tech. Rep., 2023. [Online]. Available: https://www.power-technology.com/marketdata/power-plant-profile-swedbank-solar-pv-park-sweden/

[110] European Commission, Tech. Rep.

[111] E. Despotou, "1.10 - vision for photovoltaics in the future," in *Comprehensive Renewable Energy*, A. Sayigh, Ed. Oxford: Elsevier, 2012, pp. 179–198. [Online]. Available: https://www.sciencedirect.com/science/article/pii/B9780080878720001098

[112] S. Bari, "Optimum orientation of domestic solar water heaters for the low latitude countries," *Energy conversion and management*, vol. 42, no. 10, pp. 1205–1214, 2001.

[113] M. Friman, "Techno-economic analysis of solar powered hydrogen production in vicinity of swedish steel industries," 2020.

[114] A. Westén, "On the profitability of large-scale pv plants in sweden: Site selection, grid connection and design," 2019.

[115] The Wind Energy Market Intelligence, "Hedbodberget (sweden)," 2023. [Online]. Available: https://www.thewindpower.net/windfarm_en_1034_hedbodberget.php

[116] S. Pawson, "Modern-era retrospective analysis for research and applications, version 2," 2022. [Online]. Available: https://gmao.gsfc.nasa.gov/reanalysis/MERRA-2/

[117] Vestas, "V90-2.0 MW™," 2022. [Online]. Available: https://www.vestas.com/en/products/2-mw-platform/V90-2-0-MW

[118] Technical University of Denmark (DTU Wind Energy) and World Bank Group, "Global wind atlas," In Global Wind Atlas [Website], 2023. [Online]. Available: https://globalwindatlas.info/

[119] A. Schröder, F. Kunz, J. Meiss, R. Mendelevitch, and C. Von Hirschhausen, "Current and prospective costs of electricity generation until 2050," 2013.

[120] M. Ram, M. Child, A. Aghahosseini, D. Bogdanov, A. Lohrmann, and C. Breyer, "A comparative analysis of electricity generation costs from renewable, fossil fuel and nuclear sources in g20 countries for the period 2015-2030," *Journal of Cleaner Production*, vol. 199, pp. 687–704, 2018.

[121] I. Staffell and R. Green, "How does wind farm performance decline with age?" *Renewable energy*, vol. 66, pp. 775–786, 2014.

[122] J. W. R. I. S. Erik Thornström, Sampo Seppänen, "Nordic tax report 2022," Tech. Rep., 2022. [Online]. Available: https://www.energiforetagen.se/globalassets/dokument/nordenergi/sk-21-nordenergi-tax-2022.pdf

[123] North European Power Perspectives, "Twenty statements on the electricity demand in sweden," Tech. Rep., 2016. [Online]. Available: https://www.nepp.se/etapp1/pdf/Electricity_demand_Sweden.pdf

[124] M. Rezaei, A. Akimov, and E. M. Gray, "Economics of solar-based hydrogen production: Sensitivity to financial and technical factors," *International Journal of Hydrogen Energy*, vol. 47, no. 65, pp. 27 930–27 943, 2022.

[125] K. O. Obodo, C. N. M. Ouma, and D. Bessarabov, "Low-temperature water electrolysis," in *Power to Fuel*. Elsevier, 2021, pp. 17–50.

[126] Y. Shen, H. Lv, Y. Hu, J. Li, H. Lan, and C. Zhang, "Preliminary hazard identification for qualitative risk assessment on onboard hydrogen storage and supply systems of hydrogen fuel cell vehicles," *Renewable Energy*, 2023.

[127] S. Lorenczik, S. Kim, B. Wanner, J. M. Bermudez Menendez, U. Remme, T. Hasegawa, J. H. Keppler, L. Mir, G. Sousa, M. Berthelemy *et al.*, "Projected costs of generating electricity-2020 edition," 2020.

[128] N. Kittner, F. Lill, and D. M. Kammen, "Energy storage deployment and innovation for the clean energy transition," *Nature Energy*, vol. 2, no. 9, pp. 1–6, 2017.

[129] IEA - International Energy Agency, "Trends in batteries," Tech. Rep., 2022. [Online]. Available: https://www.iea.org/reports/global-ev-outlook-2023/trends-in-batteries

[130] A. Boretti, "Integration of solar thermal and photovoltaic, wind, and battery energy storage through ai in neom city," *Energy and AI*, vol. 3, p. 100038, 2021.

[131] IEA - International Energy Agency, "Sweden - key energy statistics, 2020." Tech. Rep., 2021. [Online]. Available: https://www.iea.org/countries/sweden

[132] M. Farghali, A. I. Osman, Z. Chen, A. Abdelhaleem, I. Ihara, I. M. Mohamed, P.-S. Yap, and D. W. Rooney, "Social, environmental, and economic consequences of integrating renewable energies in the electricity sector: a review," *Environmental Chemistry Letters*, pp. 1–38, 2023.

[133] IRENA - International Renewable Energy Agency, "Solar pv: A gender perspective," Tech. Rep., 2022. [Online]. Available: https://www.irena.org/Publications/2020/Jan/Wind-energy-A-gender-perspective

[134] ——, "Wind energy: A gender perspective," Tech. Rep., 2020. [Online]. Available: https://www.irena.org/Publications/2020/Jan/Wind-energy-A-gender-perspective

[135] C. Almeida, "Master's thesis repository," 2023. [Online]. Available: https://github.com/catarinaAlmeida9930/MasterThesisCatarinaAlmeida_OptimizationModel

Appendix A: Optimization Model Python Code

The optimization model files containing the Python code pertaining to each of the analyzed scenarios and the input Excel files can be accessed in the GitHub repository [135]. The code snippet provided in this appendix specifically corresponds to the scenario where frequency regulation and integration of renewable energy sources are considered.

```

# #  Master's Thesis - Optimization model - Catarina Almeida - 20Y Analysis with Linear Degradation - With Frequency Regulation

# ## Base-case Scenario

# ### Import Libraries

import numpy as np
import numpy_financial as npf
import matplotlib.pyplot as plt
import pandas as pd
import gurobipy as gp
from gurobipy import GRB
import openpyxl
import gurobipy_pandas as gppd
print(gp.gurobi.version())
import csv


#### 1. Create new model


m=gp.Model('MIP1')


#### 2. Variables and Constants

### Constants

##Sensitivity Analysis


# CHANGE NUMBER OF YEARS HERE
years = 20


## hours in an year

gra = np.arange(0, 100, 1)
n = np.arange(0, 8760*years, 1)
M=10e6

###
# Read the Excel file with a specific sheet
df_down = pd.read_excel('prices_FCR_D.xlsx', sheet_name='FCR-D_down')
df_up = pd.read_excel('prices_FCR_D.xlsx', sheet_name='FCR-D_up')
df_DA = pd.read_excel('prices_FCR_D.xlsx', sheet_name='Day-ahead')

# Create an empty array to store the combined values
combined_array_down = np.empty((0,))
combined_array_up = np.empty((0,))
combined_array_DA = np.empty((0,))

```

```
## DA, FCR-D up and down prices from D-2 in 2022
for year_column in df_down.columns[:years]:
    year_values_down = df_down[year_column].values
    combined_array_down = np.concatenate((combined_array_down,
        year_values_down))

    year_values_up = df_up[year_column].values
    combined_array_up = np.concatenate((combined_array_up, year_values_up))

    year_values_DA = df_DA[year_column].values
    combined_array_DA = np.concatenate((combined_array_DA, year_values_DA))

down_prices = combined_array_down
up_prices = combined_array_up
SM_prices_sell = combined_array_DA*0.75
SM_prices_pur = combined_array_DA*1.25

## solar and wind availability
df_av = pd.read_excel('Availability.xlsx')
PV_av = df_av['PV KW/KWcap']
PV_av=PV_av.astype(float)
PV_av = pd.concat([PV_av] * years, axis=0, ignore_index=True)
wind_av = df_av['Wind KW/KWcap']
wind_av = pd.concat([wind_av] * years, axis=0, ignore_index=True)

## system size
PV_cap = 12 #MW
wind_cap = 12 #MW
rene_cap = 12
EL_cap = 3#MW
comp_cap = 0.075 #MW
tank_cap = 20 #MWhlvh
FC_cap = 0.650 # MW

## costs
# CAPEX
PV_capex = 800 #kEUR/MW
wind_capex = 1235 #kEUR/MW
rene_capex = wind_capex
EL_capex = 1352 #kEUR/MW
comp_capex = 1600 #kEUR/MW
tank_capex = 15 #kEUR/MWh
FC_capex = 3000 #kEUR/MW

# OPEX
PV_opex = 0.01 #%CAPEX
wind_opex = 0.03 #%CAPEX
rene_opex = wind_opex
EL_opex = 0.01 #%CAPEX
comp_opex = 0.01 #%CAPEX
tank_opex = 0.025 #%CAPEX
FC_opex = 0.02 #%CAPEX

# REPEX
EL_repex = 0.40 # % CAPEX
FC_repex = 0.21 # % CAPEX

## Renewable power production
E_PV = PV_cap*PV_av
E_wind = wind_cap*wind_av
E_rene = E_wind
```

```
114
115 ## Technical specifications
116 EL_eff = 0.70 # EL efficiency [%]
117 FC_eff = 0.50 #FC efficiency [%]
118 wcomp = 3.8 # MJ/KgH2 compressor consumption
119 LHVh2 = 120 # MJ/Kg LHV of H2
120 etank = 0.00 # self-discahrge of the tank
121 eEL = 0.010 # minimum load of EL
122 eFC = 0.010 # minimum load of FC
123 cfEL = 0.9 # capacity factor EL
124 cfFC = 0.9 # capacity factor FC
125 ltEL= 40000 # lifetime electrolyzer [h]
126 ltFC= 25000 # lifetime fuel cell [h]
127
128 ## Index
129 i = pd.RangeIndex(8760*years, name ="i")
130
131 ## CHOOSE RENEWABLE SOURCE
132 E_rene=pd.Series(E_rene, index=i)
133
134 Inv_costs = (rene_capex*rene_cap*(1+rene_opex) +
        FC_capex*FC_cap*(1+FC_opex)+7*FC_repex*FC_cap +
        EL_capex*EL_cap*(EL_opex+1)+4*EL_repex*EL_cap +
        comp_capex*comp_cap*(comp_opex+1) + tank_capex*tank_cap*(1+tank_opex))*1000
135 Inv_costs
136
137
138
139 ### Degradation
140
141 deg_PV_year = 0.0036  # %/year
142 deg_PV = np.empty(8760*years)
143 deg_PV[0] =1
144 deg_wind_year = 0.016  # %/year
145 deg_wind = np.empty(8760*years)
146 deg_wind[0] =1
147 deg_EL = np.empty(8760*years)
148 deg_FC = np.empty(8760*years)
149 deg_EL[0]=1
150 deg_FC[0]=1
151
152 deg_rene=deg_PV
153
154 for h in range(len(n)-1):
155
156     if deg_EL[h] >= 0.1:
157         deg_EL[h+1]=deg_EL[h]-(1/ltEL)
158     else:
159         deg_EL[h+1]=1
160         print("EL",h/8760+1)
161
162     if deg_FC[h] >= 0.1:
163         deg_FC[h+1]=deg_FC[h]-(1/ltFC)
164     else:
165         deg_FC[h+1]=1
166         print("FC",h/8760+1)
167
168     deg_PV[h+1]=deg_PV[h]- deg_PV_year/8760
169     deg_wind[h+1]=deg_wind[h]-(deg_wind_year/8760)
170
171 ## Renewable power production after degradation
```

```
E_PV = E_PV*deg_PV
E_wind = E_wind*deg_wind
E_rene=E_wind


### Variables

E_H2_prod= gppd.add_vars(m, i, name="E_H2_prod", vtype=GRB.CONTINUOUS)
    #hydrogen prodcution
E_rene_to_EL= gppd.add_vars(m, i, name="E_rene_to_EL", vtype=GRB.CONTINUOUS)
    #electricity from rene to EL
E_rene_to_grid= gppd.add_vars(m, i, name="E_rene_to_grid",
    vtype=GRB.CONTINUOUS) #electricity from rene to grid
E_grid_to_EL= gppd.add_vars(m, i, name="E_grid_to_EL", vtype=GRB.CONTINUOUS)
    #electricity from grid to EL
E_comp= gppd.add_vars(m, i, name="E_comp", vtype=GRB.CONTINUOUS) #electricity
    consumption from compressor
E_FC_to_grid= gppd.add_vars(m, i, name="E_FC_to_grid", vtype=GRB.CONTINUOUS)
    #electricity from FC to grid
E_H2_cons= gppd.add_vars(m, i, name="E_H2_cons", vtype=GRB.CONTINUOUS)
    #hydrogen consumption
E_tank= gppd.add_vars(m, i, name="E_tank", vtype=GRB.CONTINUOUS) #tank content
A_EL = gppd.add_vars(m, i, name="A_EL", vtype=GRB.BINARY) #EL activation
A_FC = gppd.add_vars(m, i, name="A_FC", vtype=GRB.BINARY) #FC activation

A_rene_sm = gppd.add_vars(m, i, name="A_rene_sm", vtype=GRB.BINARY)
    #participation
A_FC_sm = gppd.add_vars(m, i, name="A_FC_sm", vtype=GRB.BINARY) #participation
A_EL_sm = gppd.add_vars(m, i, name="A_EL_sm", vtype=GRB.BINARY) #participation


A_FC_up = gppd.add_vars(m, i, name="A_FC_up", vtype=GRB.BINARY) #participation
A_EL_up = gppd.add_vars(m, i, name="A_EL_up", vtype=GRB.BINARY) #participation
A_rene_up= gppd.add_vars(m, i,lb=0, name="A_rene_up", vtype=GRB.CONTINUOUS) #FC
    to grid spot market

A_FC_down = gppd.add_vars(m, i, name="A_FC_down", vtype=GRB.BINARY)
    #participation
A_EL_down= gppd.add_vars(m, i, name="A_EL_down", vtype=GRB.BINARY)
    #participation
A_rene_down= gppd.add_vars(m, i,lb=0, name="A_rene_down", vtype=GRB.CONTINUOUS)
    #FC to grid spot market

E_FC_sm= gppd.add_vars(m, i,lb=0, name="E_FC_sm", vtype=GRB.CONTINUOUS) #FC to
    grid spot market
E_EL_sm= gppd.add_vars(m, i, lb=0, name="E_EL_sm", vtype=GRB.CONTINUOUS) # EL
    to grid spot market
E_rene_sm= gppd.add_vars(m, i, lb=0, name="E_rene_sm", vtype=GRB.CONTINUOUS)
    #RENE to grid spot market
E_FC_up= gppd.add_vars(m, i, name="E_FC_up", vtype=GRB.CONTINUOUS) #FC to grid
    up
E_EL_up= gppd.add_vars(m, i, name="E_EL_up", vtype=GRB.CONTINUOUS) # EL to grid
    up
E_rene_up= gppd.add_vars(m, i, name="E_rene_up", vtype=GRB.CONTINUOUS) #RENE to
    grid up
E_FC_down= gppd.add_vars(m, i, name="E_FC_down", vtype=GRB.CONTINUOUS) #FC to
    grid down
E_EL_down= gppd.add_vars(m, i, name="E_EL_down", vtype=GRB.CONTINUOUS) # EL to
    grid down
E_rene_down= gppd.add_vars(m, i, name="E_rene_down", vtype=GRB.CONTINUOUS)
    #RENE to grid down
```

```
P_up= gppd.add_vars(m, i, name="P_up", vtype=GRB.CONTINUOUS) # Up reg provided to the grid
P_down= gppd.add_vars(m, i, name="P_down", vtype=GRB.CONTINUOUS) # Down provided to the grid
E_SM_sell= gppd.add_vars(m, i, name="E_SM_sell", vtype=GRB.CONTINUOUS) # Energy sold to the grid
E_SM_pur= gppd.add_vars(m, i, name="E_SM_pur", vtype=GRB.CONTINUOUS) # Energy purchased from the grid
E_SM_pur= gppd.add_vars(m, i, name="E_SM_pur", vtype=GRB.CONTINUOUS) # Energy purchased from the grid


# ### 3. Constraints

### Energy Balances
const = gppd.add_constrs(m,E_rene_to_EL + E_rene_to_grid, GRB.EQUAL, E_rene , name="rene_prod") # Rene production
m.update()
const1 = gppd.add_constrs(m,E_H2_prod, GRB.EQUAL, (E_rene_to_EL + E_grid_to_EL - E_comp)*EL_eff, name="H2_prod") # Hydrogen production
m.update()
const2 = gppd.add_constrs(m,E_FC_to_grid, GRB.EQUAL, E_H2_cons*FC_eff, name="H2_cons") # Hydrogen consumption
m.update()
constr3 = gppd.add_constrs(m,E_H2_cons, GRB.LESS_EQUAL, E_tank, name="H2_cons_max") # Hydrogen consumption max
m.update()
const4 = gppd.add_constrs(m,E_comp, GRB.EQUAL, (E_H2_prod/LHVh2)*wcomp, name="Comp_con") # Hydrogen consumption
m.update()

m.addConstr(E_tank[0] == 0.9*tank_cap) # Initial tank content
m.update()

print ("energy balance check")

### Activation Constraints
const5 = gppd.add_constrs(m,A_EL*eEL*EL_cap, GRB.LESS_EQUAL, E_grid_to_EL + E_rene_to_EL - E_comp, name="min_EL_load") # Minimum EL load
m.update()
const6 = gppd.add_constrs(m,E_grid_to_EL + E_rene_to_EL - E_comp, GRB.LESS_EQUAL, A_EL*EL_cap*cfEL*deg_EL , name="max_EL_load") # Maximum EL load
m.update()
const7 = gppd.add_constrs(m,A_FC*eFC*FC_cap, GRB.LESS_EQUAL, E_FC_to_grid, name="min_FC_load") # Minimum FC load
m.update()
const8 = gppd.add_constrs(m,E_FC_to_grid, GRB.LESS_EQUAL, A_FC*FC_cap*cfFC*deg_FC , name="max_FC_load") # Maximum FC load
m.update()
const9 = gppd.add_constrs(m,E_tank, GRB.LESS_EQUAL, tank_cap , name="tank_max") # Maximum tank content
m.update()
print ("activation check")

### Services to the grid
const10 = gppd.add_constrs(m,E_FC_to_grid, GRB.EQUAL, E_FC_sm , name="FC_to_Grid") # FC grid services
m.update()
const11 = gppd.add_constrs(m,E_rene_to_grid, GRB.EQUAL, E_rene_sm  , name="RENE_to_Grid") # RENE grid services
```

```
m.update()
const12 = gppd.add_constrs(m,E_grid_to_EL, GRB.EQUAL, E_EL_sm,
    name="Grid_to_EL") # FC grid services
m.update()
print ("services check")

### Minimum bid
const13 = gppd.add_constrs(m,E_EL_down, GRB.GREATER_EQUAL, 0.1*A_EL_down,
    name="Grid_to_EL") # Minimum bid
m.update()

const14 = gppd.add_constrs(m,E_EL_down, GRB.LESS_EQUAL, M*A_EL_down,
    name="Grid_to_EL") # Minimum bid
m.update()

const15 = gppd.add_constrs(m,E_FC_down, GRB.GREATER_EQUAL, 0.1*A_FC_down,
    name="Grid_to_EL") # Minimum bid
m.update()
const16 = gppd.add_constrs(m,E_FC_down, GRB.LESS_EQUAL, M*A_FC_down,
    name="Grid_to_EL") # Minimum bid
m.update()
const17 = gppd.add_constrs(m,E_rene_down, GRB.GREATER_EQUAL, 0.1*A_rene_down,
    name="Grid_to_EL") # Minimum bid
m.update()
const18 = gppd.add_constrs(m,E_rene_down, GRB.LESS_EQUAL, M*A_rene_down,
    name="Grid_to_EL") # Minimum bid
m.update()

const19 = gppd.add_constrs(m,E_EL_up, GRB.GREATER_EQUAL, 0.1*A_EL_up,
    name="Grid_to_EL") # Minimum bid
m.update()
const20 = gppd.add_constrs(m,E_EL_up, GRB.LESS_EQUAL, M*A_EL_up,
    name="Grid_to_EL") # Minimum bid
m.update()

const21 = gppd.add_constrs(m,E_FC_up, GRB.GREATER_EQUAL, 0.1*A_FC_up,
    name="Grid_to_EL") # Minimum bid
m.update()
const22 = gppd.add_constrs(m,E_FC_up, GRB.LESS_EQUAL, M*A_FC_up,
    name="Grid_to_EL") # Minimum bid
m.update()

const23 = gppd.add_constrs(m,E_rene_up, GRB.GREATER_EQUAL, 0.1*A_rene_up,
    name="Grid_to_EL") # Minimum bid
m.update()
const24 = gppd.add_constrs(m,E_rene_up, GRB.LESS_EQUAL, M*A_rene_up,
    name="Grid_to_EL") # Minimum bid
m.update()

const25 = gppd.add_constrs(m,E_EL_sm, GRB.GREATER_EQUAL, 0.1*A_EL_sm,
    name="Grid_to_EL") # Minimum bid
m.update()
const26 = gppd.add_constrs(m,E_EL_sm, GRB.LESS_EQUAL, M*A_EL_sm,
    name="Grid_to_EL") # Minimum bid
m.update()

const27 = gppd.add_constrs(m,E_FC_sm, GRB.GREATER_EQUAL, 0.1*A_FC_sm,
    name="Grid_to_EL") # Minimum bid
m.update()
const28 = gppd.add_constrs(m,E_FC_sm, GRB.LESS_EQUAL, M*A_FC_sm,
    name="Grid_to_EL") # Minimum bid
```

```
299 m.update()
300
301 const29 = gppd.add_constrs(m,E_rene_sm, GRB.GREATER_EQUAL, 0.1*A_rene_sm,
        name="Grid_to_EL") # Minimum bid
302 m.update()
303 const30 = gppd.add_constrs(m,E_rene_sm, GRB.LESS_EQUAL, M*A_rene_sm,
        name="Grid_to_EL") # Minimum bid
304 m.update()
305
306 print ("minimum␣bid␣check")
307
308 ### Power availability
309 const31 = gppd.add_constrs(m,P_up, GRB.EQUAL, E_EL_up + E_FC_up + E_rene_up ,
        name="up_reg") # up grid services
310 m.update()
311
312 const32 = gppd.add_constrs(m,P_down, GRB.EQUAL, E_EL_down + E_FC_down +
        E_rene_down , name="up_reg") # up grid services
313 m.update()
314
315 const33 = gppd.add_constrs(m,E_FC_down, GRB.LESS_EQUAL, E_FC_sm,
        name="FC_down_max") #Max FC down reg
316 m.update()
317
318 const34 = gppd.add_constrs(m,E_FC_up, GRB.LESS_EQUAL,
        FC_cap*cfFC*deg_FC-E_FC_sm, name="FC_up_max") # Max FC up reg
319 m.update()
320
321 const35 = gppd.add_constrs(m,E_EL_up, GRB.LESS_EQUAL, E_EL_sm,
        name="EL_up_max") #Max EL up reg
322 m.update()
323
324 const36 = gppd.add_constrs(m,E_EL_down, GRB.LESS_EQUAL,
        EL_cap*cfEL*deg_EL-E_EL_sm, name="EL_down_max") # Max EL down reg
325 m.update()
326
327 const37 = gppd.add_constrs(m,E_rene_down, GRB.LESS_EQUAL,E_rene_sm,
        name="rene_down_max") #Max rene down reg
328 m.update()
329
330 const38 = gppd.add_constrs(m,E_rene_up, GRB.LESS_EQUAL,
        E_rene-E_rene_to_EL-E_rene_sm, name="rene_up_max") # Max rene up reg
331 m.update()
332
333 print ("power␣availability␣check")
334
335 ### Spot Market
336 const39 = gppd.add_constrs(m,E_SM_sell, GRB.EQUAL,E_FC_sm+ E_rene_sm ,
        name="SM_sell") # Energy sold in the sport market
337 m.update()
338
339 const40 = gppd.add_constrs(m,E_SM_pur, GRB.EQUAL,E_EL_sm , name="SM_pur") #
        energy purchased in the spot market
340 m.update()
341
342 print ("spot␣market␣check")
343
344
345 ### Hydrogen content in the tank
346 indices = list(range(len(n) - 1))
347
```

```
348 # Create a list of expressions for the constraint
349 [m.addConstr(E_tank[j+1] == E_tank[j]*(1-etank) + E_H2_prod[j] - E_H2_cons[j])
        for j in indices]
350 m.update()
351
352 print ("hydrogen content check")
353
354
355 # ### 4. Objective function
356
357
358 revenue = gp.LinExpr()
359
360 revenue = -1*Inv_costs
361
362 for k in i:
363     revenue+= 0.9*P_up[k]*up_prices[k] + 0.9*P_down[k]*down_prices[k] +
            E_SM_sell[k]*SM_prices_sell[k] - E_SM_pur[k]*SM_prices_pur[k]
364
365 m.setObjective(revenue, GRB.MAXIMIZE)
366
367 # ### 5. Optimize model
368
369 m.optimize()
```